Abstract

Title of Dissertation: Polymer Capsules Exhibiting Emergent Properties Due to Internal Chemical Reactions

Kerry C. DeMella, Doctor of Philosophy, 2018

Dissertation Directed By: Professor Srinivasa R. Raghavan
Department of Chemical and Biomolecular Engineering

Life is an "emergent" property – i.e., one exhibited by living systems due to interactions between their parts, but not shown by any of the parts on their own. Such emergent behavior is seen at various length scales, down to that of a single cell. In a single eukaryotic cell, there exist internal compartments called organelles, such as the nucleus and mitochondria. While the organelles each have distinct functions, it is the overall cell that has the property of life – i.e., the whole is greater than the sum of the parts. Inspired by these attributes of living cells, this dissertation attempts to create millimeter-scale polymer capsules that exhibit emergent properties. To achieve these properties, we use the lumen of the capsule as the site for a chemical reaction, which in turn bestows a specific behavior to the overall capsule. Three studies are described in this vein in this dissertation.

First, in Chapter 3, we design capsules that rapidly inflate and then burst, ejecting their core contents. These capsules have a core of catalytic silver (Ag) particles and a crosslinked polymer shell. When a fuel (hydrogen peroxide, H_2O_2) is added to water, a catalytic reaction generates gas (O_2) in the capsule. The gas causes the capsule to inflate

over time until the shell finally ruptures. The inflation extent and duration, as well as the rupture intensity can be tuned by altering the core and shell composition. Also, instead of a catalytic reaction, capsule inflation can be achieved by combining reactants, one in the capsule and the other in the solution, that together generate a different gas (e.g., CO_2).

In Chapter 4, we describe a second emergent property of capsules having a design similar to those in Chapter 3. The capsules here contain both the catalytic Ag particles as well as a solute (dye). We monitor the release of dye in the presence of the O_2-generating reaction ("active release") or by diffusion alone ("passive release"). Active dye release is shown to be much faster than passive release, i.e., the dye is "pumped" out due to the reaction. More interestingly, when the dye is Rhodamine 6G (R6G), it gets released in a series of *pulses,* i.e., dye releases for a few seconds, then it stops, and then resumes. The number and duration of the pulses can be tuned. The reason for pulsed release is attributed to the binding interaction of R6G to Ag particles.

Finally, in Chapter 5, we show the use of an external trigger (temperature) to induce emergent behavior in capsules. For this, we first coat individual capsules with an impermeable shell made of wax. This is done by briefly immersing a cold capsule in molten wax so that a wax layer solidifies around the capsule. This layer is impermeable when the capsule is placed in water, but when heated, the wax melts and the contents can diffuse out. We construct multicompartment capsules (MCCs) that have one or two wax-coated inner compartments. The MCCs are used to conduct cascade reactions such as the iodine clock reaction. Also, an MCC with H_2O_2 in a compartment and Ag particles in the lumen is used to demonstrate thermally triggered capsule inflation.

Polymer Capsules Exhibiting Emergent Properties Due to Internal Chemical Reactions

By

Kerry C. DeMella

Dissertation submitted to the Faculty of the Graduate School of the
University of Maryland, College Park, in partial fulfillment of
the requirements for the degree of
Doctor of Philosophy
2018

Advisory Committee:

Prof. Srinivasa Raghavan, Chair, Department of Chemical & Biomolecular Engineering, Advisor

Professor Jeffery Davis, Department of Chemistry & Biochemistry

Professor Philip DeShong, Department of Chemistry & Biochemistry

Professor Daniel Falvey, Department of Chemistry & Biochemistry

Professor Robert Briber, Department of Material Science & Engineering, Dean's Representative

Acknowledgements

First and foremost, I would like to thank my advisor, Professor Raghavan. Dr. Raghavan has placed his trust in me from the very beginning and has fully supported me during my time in his lab. He has encouraged me to explore my own ideas and has guided me to become an excellent storyteller and presenter. I have been fully challenged in his lab to self-motivate, investigate unknown research areas, and approach various projects from several different angles. He has also given me the opportunity to lead small groups of undergraduate researchers and become a figurehead in the lab. Dr. Raghavan truly cares about his students and encourages them to pursue areas of research that will help them attain their goals. I could not be more appreciative of my time in this lab. For all this, I am truly grateful.

I would also like to thank my committee: Professor Robert Briber, Professor Jeffery Davis, Professor Philip DeShong, and Professor Daniel Falvey for their advice and suggestions. I am appreciative to the following undergraduate students for their help with experiments and for giving me some of my first lab management experience: Claire Tomaszewski, David Hessler, Sulin Wu, Karan Patel, Greg Jarnutowski, Shanshan Jin, Austin Hughes. Additionally, I need to thank Hema Choudhary for volunteering to help me with additional experiments during the last couple of weeks in lab and Ben Calvin for improving Chapter 5 with programming and encouraging me to step outside of my comfort zone and learn to code.

Next, I would like to thank my colleagues and friends. I am so grateful for all of the support you all have given me. Specifically, I want to extend my thanks to Dr. Brady

Zarket, Dr. Gail Blakley, Dr. Ankit Gargava, Niti Agrawal, and Kim Brady for your guidance and friendship during my time here. I would also like to thank Dr. Jasmin Athas, So Hyun Ahn, Trip Fernandes, Leah Borden, Hema Choudhary, Nikhil Subraveti, and all of the Complex Fluids and Nanomaterials lab group members. I also need to thank my fitness family at Recwell UMD. You all have kept me sane and happy during my time here.

Finally, I would like to acknowledge my family for all their support and love throughout this process. Specifically, thank you to my parents, Fred and Colleen DeMella. You have always been there to encourage me and remind me to keep things in perspective. I could not have made it here without you and I am so thankful to have such an amazing family.

Table of Contents

List of Figures

Chapter 1

Introduction and Overview

1.1 Problem Description and Motivation

Many systems in nature exhibit "emergent" behaviors, i.e. behaviors that rely on individual parts working together to produce an overall effect.[1-8] The ultimate emergent behavior is life itself – i.e., living systems ranging from multicellular organisms to single cells are composed of numerous parts, but those parts on their own are not living entities.[9, 10] For example, a single eukaryotic cell has several internal compartments (called organelles) including the nucleus, mitochondria, and lysosomes.[11] Each of these organelles is a distinct entity, surrounded by its own membrane, and has unique internal contents that give it a distinct role within the cell. The ability of the cell to continuously function and reproduce depends on the cross-talk and interaction between various organelles. However, if the organelles are removed from the cell, they would cease to have their characteristic role, and would be no different from a container full of molecules. In other words, the whole (cell) is greater than the sum of the parts (organelles).[9, 10]

A long-standing goal for scientists has been to mimic the complex behaviors seen in nature. Thus, at the scale of a living cell, the goal is to create an abiotic container that can exhibit some of the features of a cell. In this context, recent interest has centered around *capsules*, which are spherical containers having a shell made of polymers or lipids

and a core composed of an aqueous solution or gel. Scientists have found ways to create multicompartment capsules (MCCs) with multiple inner compartments, mimicking the structure in a eukaryotic cell.[12-17] The next challenge is to induce the internal compartments of an MCC to interact with each other, i.e., for a change in one compartment to trigger a response in the adjacent one.[18-33] One concept that has been studied in this regard in an MCC is a cascade reaction using enzymes entrapped in individual compartments.[34] Thus, the ability of an MCC to generate a product from such a cascade is one example of an emergent response.

Other attempts have also been made to endow capsules with a unique emergent response, such as the property of autonomous motion or self-propulsion. Capsules that can self-propel, called "micromotors", have been designed.[35-39] They contain a catalyst in their core, and when exposed to a chemical fuel, generate gas through a catalytic reaction. The expulsion of the gas through one end of the capsule results in their propulsion in the opposite direction through the liquid medium. This continues until the fuel added to the medium is consumed. Thus, the emergent response of micromotors is their propulsion; this is not exhibited by any of the components in the micromotor but arises due to a chemical reaction involving the internal components.

1.2 Proposed Approach

In this dissertation, we describe the synthesis of capsules showing emergent properties that are above and beyond the properties of their internal contents or

components. Taking a cue from the studies previously done with micromotors, we will seek to induce the desired response by exploiting a chemical reaction that will involve the core contents of the capsule. We have designed and created three different types of capsules with emergent behavior, which are briefly described here.

1.2.1 Capsules Exhibiting Inflation and Core Ejection

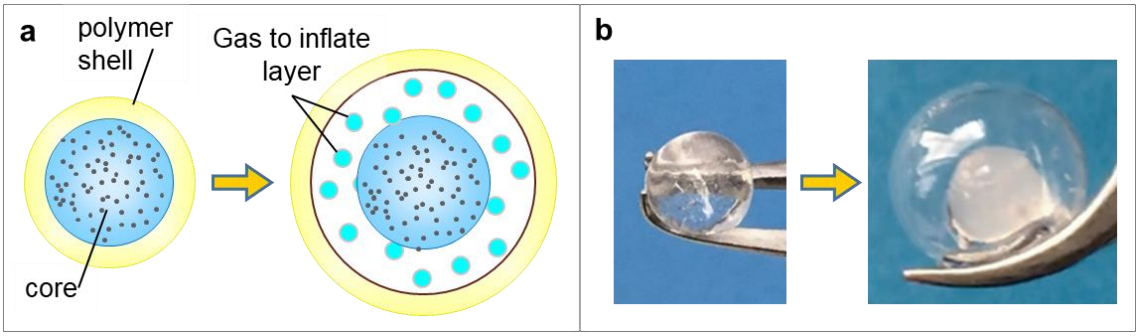

Figure 1.1. Capsules exhibiting inflation and core ejection. The capsules have an aqueous gelled core containing catalytic particles and a crosslinked polymer shell. When placed in a chemical fuel, the particles catalyze a reaction that produces gas. The gas causes the polymer shell to inflate around the core, until, ultimately, the shell ruptures. The rupture can be abrupt and violent in some cases, which induces the core to be ejected outward. Schematics of the inflation are shown on the left (a) and photos of the same are shown on the right (b).

In Chapter 3, we design capsules that rapidly inflate and then burst, ejecting their core contents. These capsules have a core of catalytic silver (Ag) particles and a crosslinked polymer shell. When a fuel (hydrogen peroxide, H_2O_2) is added to water, a catalytic reaction generates oxygen (O_2) gas in the capsule. The gas causes the capsule to inflate to about double their original size over time (Figure 1.1) until the shell finally ruptures. The inflation extent and duration, as well as the rupture intensity can be tuned

by altering the core and shell composition. In some cases, the rupture can be abrupt and violent, causing the core to be ejected out of the capsule. Interestingly, the capsule inflation is reminiscent of the inflation seen in nature by creatures like the pufferfish, which swell up to deter predators. Likewise, the violent ejection of core content is reminiscent of the jellyfish, which shoots needles out of cells called nematocysts when predators approach.

1.2.2 Capsules Exhibiting Pulsed-Release of Solute

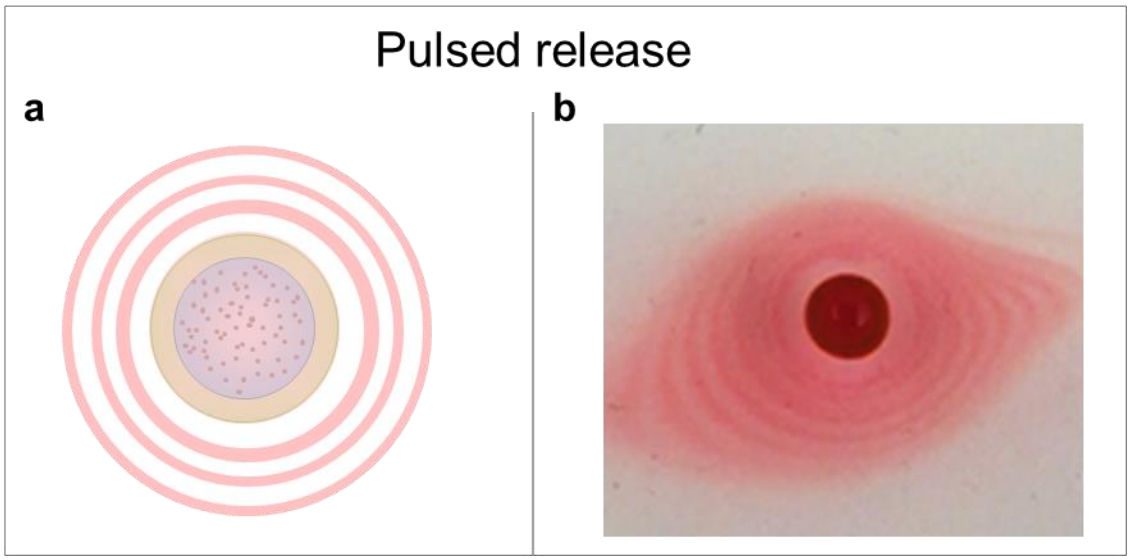

Figure 1.2. Capsules exhibiting pulsed release of Rhodamine 6G (R6G) dye. The capsules have an aqueous gelled core that contains catalytic silver (Ag) particles and a crosslinked polymer shell. The capsules are additionally loaded with R6G and then exposed to the chemical fuel, which produces O_2 gas. The dye is observed to get released rapidly from the capsule in a series of pulses, which emanate outward as concentric rings from the capsule. A schematic of the pulsing is shown on the left (a) and a photo of the same is shown on the right (b).

In Chapter 4, we describe another emergent property of capsules having a design similar to those in Chapter 3. The capsules here contain both the catalytic Ag particles as well as a solute (dye) in their core. We monitor the release of dye in the presence of the O_2-generating reaction ("active release") or by diffusion alone ("passive release"). Active dye release is shown to be much faster than passive release, i.e., the dye gets "pumped" out due to the evolution of gas. More interestingly, when the dye is Rhodamine 6G (R6G), it gets released in a series of *pulses* (Figure 1.2), i.e., the dye gets released for a few seconds, then the release stops, and then the release resumes. This manifests as a series of concentric rings of dye around the capsule. To our knowledge, such pulsed release has never been reported in the literature. Both the number and duration of the pulses can be tuned based on the Ag concentration and the shell properties. The reason for this pulsed release is attributed to the binding interaction of R6G to Ag particles.

1.2.3 Thermally Triggered Emergent Behavior of Capsules

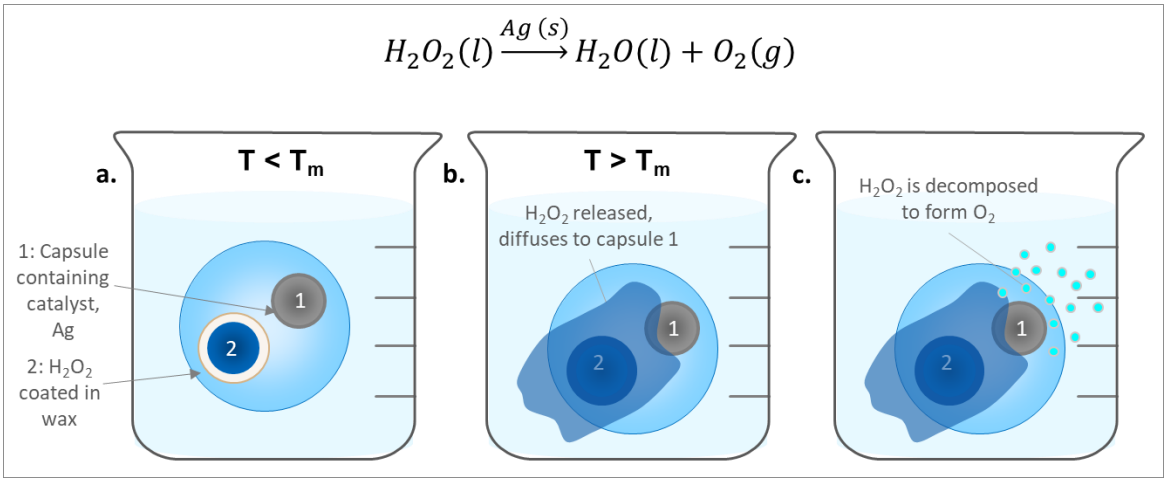

Figure 1.3. Thermally triggered solute release from wax-shelled capsules and its application in implementing cascade reactions. (a) A multicompartment capsule (MCC) is shown in which the two inner capsules have an aqueous core and a wax shell. The shell is impermeable at room temperature, but when the system is heated above the melting temperature of the wax shell, (b) the contents in the capsule cores are released. (c) This allows the reagents in the adjacent capsules to contact and undergo a reaction. Schematics of the MCC, before and after triggering.

Finally, in Chapter 5, we show the use of an external trigger (temperature) to induce emergent behavior in capsules. For this, we first coat individual capsules with an impermeable shell made of wax. This is done by briefly immersing a cold capsule in molten wax so that a wax shell solidifies around the capsule. This shell is impermeable when the capsule is placed in water, but when heated, the wax melts and the contents can diffuse out. We construct multicompartment capsules (MCCs) that have one or two wax-shelled inner compartments (Figure 1.3). The MCCs are used to conduct cascade reactions such as the iodine clock reaction, with the reagents stored in the compartments and induced to interact only when the shells melt under heat. Also, an MCC with the

chemical fuel (H_2O_2) in a compartment and Ag particles in the lumen is used to demonstrate thermally triggered capsule inflation.

1.3 Significance of This Work

We believe this work is significant in two respects. First, in our work, we have devised several unique kinds of capsules (such as capsules that are impermeable to gas or to aqueous solutes) with new ways to synthesize these capsules. Our designs and techniques are simple and inexpensive, allowing researchers to replicate this work easily. The second, more important, aspect is the successful demonstration of emergent properties by exploiting chemical reactions. To our knowledge, reports of capsule exhibiting inflation, core ejection, and pulsed-release of solute are rare or non-existent in the literature. The thermal triggering of reactions between compartmentalized solutes is also novel. These ideas could prove useful in various contexts, including the delivery of therapeutic molecules in the body, the controlled delivery of agrochemicals, or in the implementation of assays using hazardous reagents.

Chapter 2

Background

2.1 Emergent Behavior in Living Systems

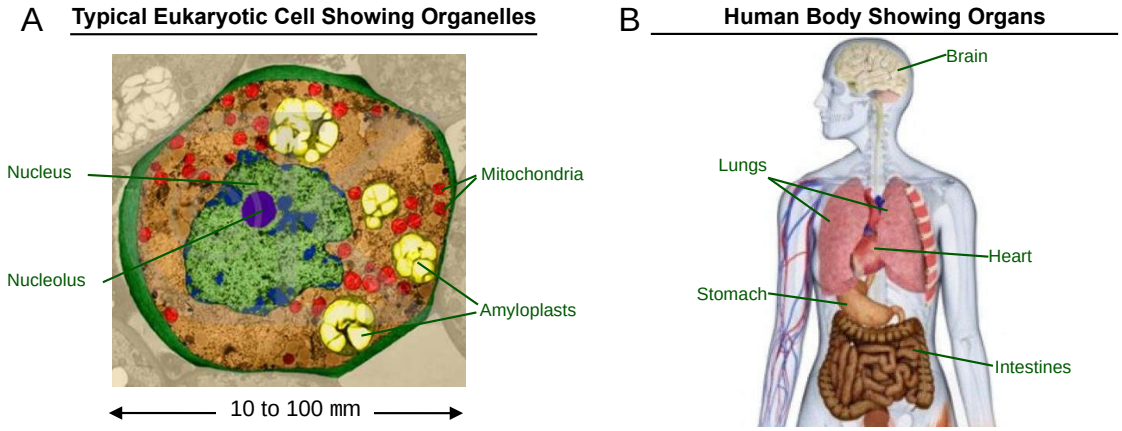

Figure 2.1 Life as an emergent behavior of living systems. The overall system shows a response or behavior that is not exhibited by its constituent parts. This is seen at both (a) the level of an individual cell; and (b) the level of an organism or animal. The schematic in (a) shows the cross-section of a parenchymal cell from a lily plant with false-color rendering to indicate the different organelles. The schematic in (b) shows a sketch of the human body showing some vital organs. (http://www.imaia.co.uk/human-body-diagram-no-labels.html)

The terms “emergence” and “emergent properties” have a long history dating back to Aristotle and the Greeks.[8] The terms are used to imply that a whole system is greater than the sum of its parts, i.e., that the system has properties that its constituent parts do not possess.[1-7] The ultimate emergent behavior is life itself – i.e., living systems are composed of numerous parts, but those parts on their own do not exhibit life. For example, a single eukaryotic cell, as shown in Figure 2.1a, has several internal

compartments (called organelles), each bounded by a lipid membrane.[9-11] The cell is able to synthesize proteins and lipids, store and harvest energy, store and retrieve genetic information, and recycle used or defective substances. Each of these tasks is accomplished in a different organelle, and accordingly each organelle has different internal contents. For example, lysosomes are the "recycling centers" in a cell, where proteins are degraded, and to enable recycling, they have specific enzymes as well as a low (acidic) pH to facilitate degradation. However, the acid and the enzymes remain confined in the lysosome and do not pass through into the surrounding cytoplasm.

Shifting from the micro-scale to the macro-scale, the human body in another example of emergent behavior. The body (Figure 2.1b) is composed of several organs, each separate and distinct, serving individual functions.[40] Humans breathe air through their lungs, which bring oxygen into the bloodstream and remove carbon dioxide. The oxygenated blood is then pumped through the body by the heart, which supplies tissues with oxygen and nutrients. The liver then maintains the blood's contents by degrading fats, producing urea, and filtering out toxins. Each organ plays a critical role in keeping the body alive and functioning. The organs cease to function when removed from the body, and indeed, it is only the body as a whole that can be said to be a living thing.

2.2 Emergent Behavior in Abiotic Systems

Emergent behaviors are ubiquitous in the context of living systems, but there are non-living (abiotic) systems that also exhibit emergent behavior. Examples of emergent

patterns include the fractal shapes of snowflakes, the rippled patterns of sand dunes, etc.[1-4, 6-8] In the context of chemistry, the self-assembly of structures in solution by certain molecules, e.g., of surfactants into a micelle, could also be considered as emergent behavior.[41, 42] One emergent property that we will focus on here is autonomous motion or self-propulsion. Over the past two decades, researchers have created a number of microscale or nanoscale structures that can self-propel in water. [35-39, 43] An example is a class of structures called "micromotors", which were developed in our lab.[35] Micromotors are anisotropic capsules (~ 200 μm in diameter) that contain a localized patch of iron-platinum (Fe-Pt) nanoparticles on one end (Figure 2.2).[44] The nanoparticles are both catalytic, due to the Pt, and magnetic, because of the Fe. When placed in a solution containing the chemical fuel, hydrogen peroxide (H_2O_2), the catalytic property of Pt allows for the decomposition of H_2O_2 to oxygen (O_2) gas. The gas is ejected out of the patchy end of the micromotor in the form of bubbles, and this propels the micromotor in the opposite direction (Figure 2.2). The motion can also be directed by the use of a magnet. On the whole, the emergent property of self-propulsion is exhibited by the micromotor, which in turn is due to a chemical reaction in the structure.

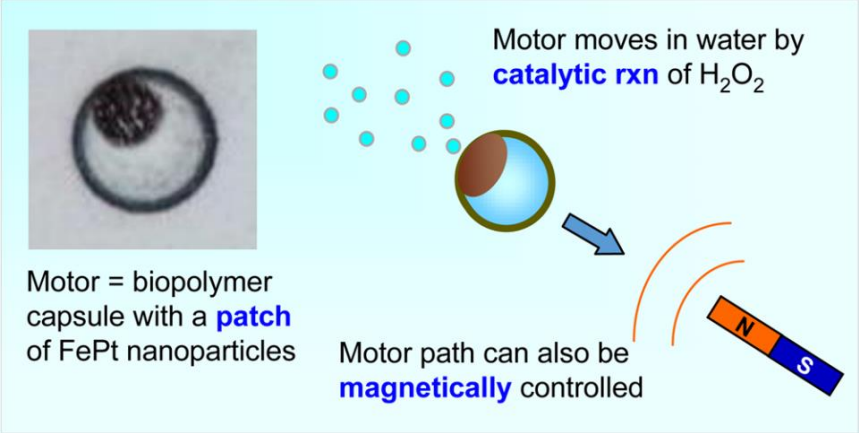

Figure 2.2. Self-propulsion of micromotors in H_2O_2 solution.[35] Schematic of the propulsion mechanism. The motor has a patch of FePt nanoparticles. The Pt in the nanoparticles catalyzes the decomposition of H_2O_2 to generate O_2 gas in the form of bubbles. The bubbles are ejected from the side with the nanoparticle patch, which propels the motor in the opposite direction. The direction of movement can be manipulated through use of a magnet due to the magnetic Fe particles.

2.3 Capsules with Polymeric Layers

The term capsule refers to a solid, spherical object that has a shell or outer layer that is distinct in composition (and properties) from the inner core. The preferred way to create capsules in our lab is by the use of polyelectrolytes, i.e., charged polymers, such as alginate (an anionic polysaccharide) and chitosan (a cationic polysaccharide). For example, when a 2 wt% alginate solution is added dropwise into a solution of divalent cations (such as 0.5 M $CaCl_2$), the alginate chains become crosslinked by the Ca^{2+} ions, and thereby the liquid drops are converted into gel-like beads (see schematic of gel structure in Figure 2.3a).[45-48] If in addition to Ca^{2+}, the receiving solution also contains chitosan, the electrostatic complexation between the oppositely charged alginate and chitosan chains at the droplet surface will lead to a shell that is distinct from the gel core, i.e., to a capsule.[45, 46, 49-53] During the formation process, any payload included with the

alginate solution will become encapsulated in the bead/capsule. These structures generally allow small molecules to permeate but macromolecules and nanoparticles will remain encapsulated.[35, 51, 54] Note that the size of the above capsules is dictated by the sizes of the (alginate) droplets. This can be varied over a diameter of 2 to 10 mm by controlling the nozzle diameter using transfer pipettes or syringes. For making smaller capsules with diameters between 100 and 1000 μm, we resort to a microfluidic setup that uses capillary tubes with inner diameters around 50 μm.[26, 55]

Recently, our lab has developed a technique by which a shell of crosslinked polymer can be grown around an alginate gel core.[56] This technique is shown in Figure 2.3 and will be used extensively in this dissertation. First, the alginate gel core is loaded with a free-radical initiator like ammonium persulfate (APS). This is subsequently transferred to a solution of a first monomer such as N-isopropylacrylamide (NIPA), with the solution also containing a chemical crosslinker, an accelerant, and a viscosity-enhancing additive (xanthan gum). The APS diffuses out of the core into the monomer solution, initiating free-radical polymerization of NIPA around the core into a distinct layer. At this point, we have a 1-layer capsule with a crosslinked NIPA shell. Thereafter, this capsule used as the core for the second step using a different monomer such as N,N′-dimethylacrylamide (DMAA). This will ultimately yield a 2-layer capsule with an inner layer of NIPA and an outer layer of DMAA. Additional layers can be subsequently added as desired.

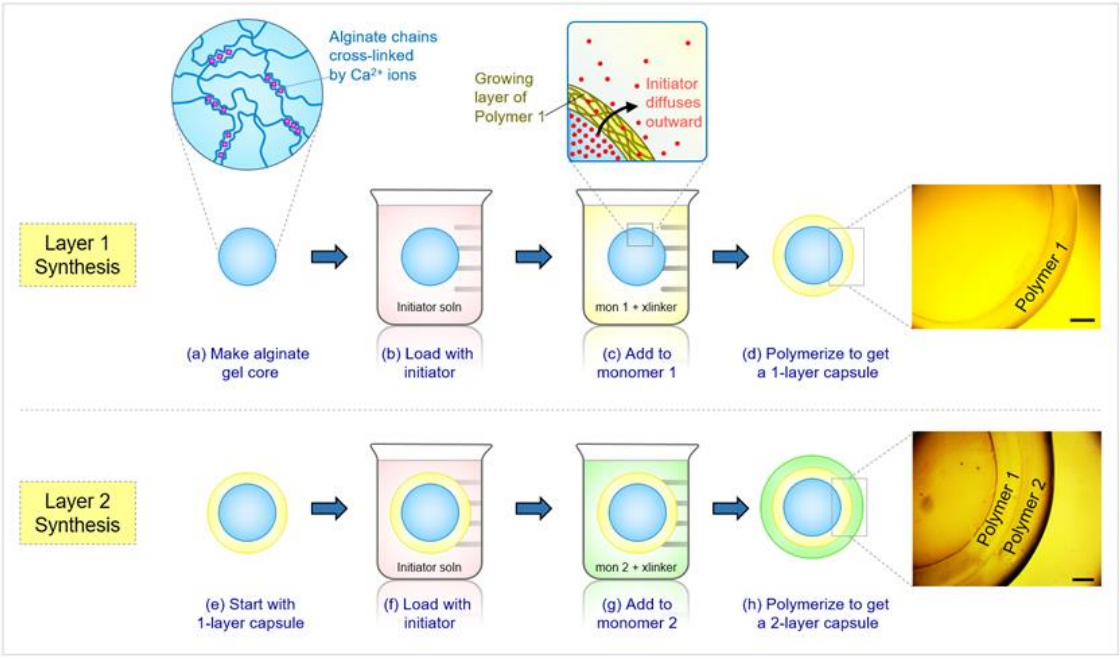

Figure 2.3. Synthesis of capsules with multiple polymeric layers.[56] First, an alginate gel core is made (a) and loaded with free-radical initiator (b). The gel is introduced into a monomer 1 solution (along with crosslinker and accelerant) (c). Upon polymerization, a layer of polymer 1 is formed around the gel core (d). The inset in c shows that this layer is formed by diffusion of initiator outward from the core into the monomer 1 solution. This process is then repeated with the one-layer capsule (e), which is loaded with initiator (f) and then contacted with monomer 2 (g). Upon polymerization, a second layer of polymer 2 is formed (h). Scale bars are 500 μm.

2.4 Capsules with a Wax Shell

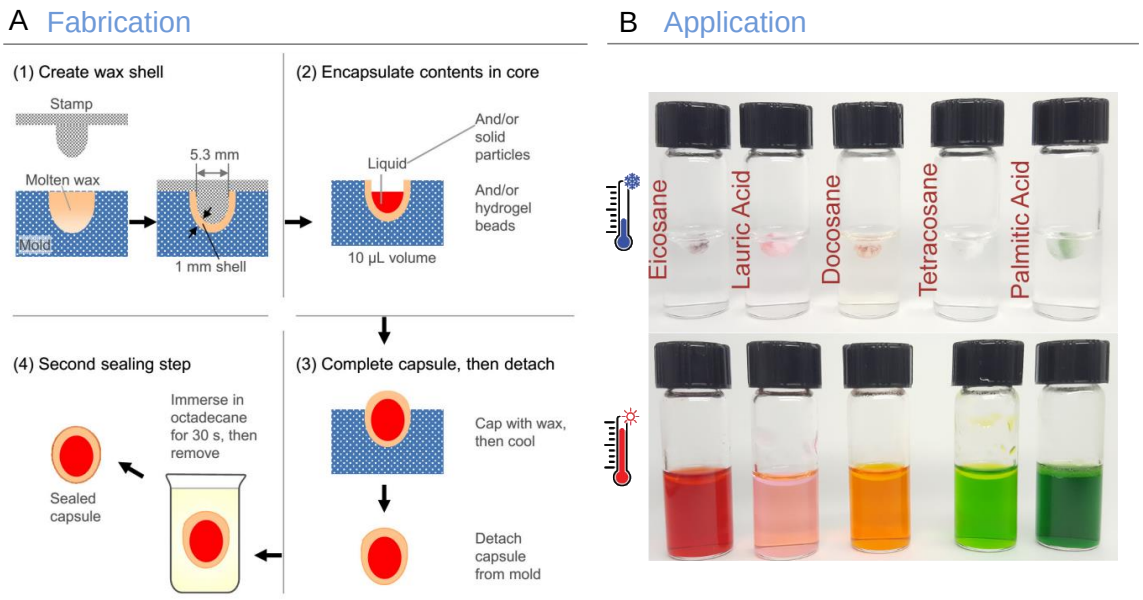

Figure 2.4. Fabrication and application of capsules with a wax shell. A) Fabrication involves: (1) pouring molten wax into molds and inserting a stamp to create hollow cavities. On cooling, a wax shell of 1 or 0.5 mm is formed. (2) Contents (liquid, solid, or gel) can then be loaded into the cavity. (3) Additional wax is used to cap the cavity, and upon cooling, the capsules can be detached. (4) Finally, a second sealing step is performed by immersing the capsules into octadecane for 30 s. **B)** Capsules can be fabricated from a variety of waxy materials. In each case, the capsule is able to hermetically seal its payload (different colored food dyes) when placed in water at room temperature. However, when the system is heated above the melting temperature of the wax shell, the shell melts and this allows the dye to diffuse into the water.

The capsules discussed in the previous section, including those with a shell of crosslinked polymer (e.g., NIPA or DMAA) are all permeable to small molecules. For example, if the capsule is loaded with a dye and then placed in water, the dye will leak out into the water within a few hours. For many applications, it would be useful to have a hermetic seal around the core to prevent the passage of any materials into or out of the capsules. In recent collaborative work, we have shown that such a hermetic seal can be

achieved using wax. Figure 2.4A shows the technique used to fabricate wax-shelled capsules. Molten wax is poured into a 3-D printed mold and then a stamp is applied to make a hemispherical shell of the wax. The wax shell is filled with the desired material and sealed by pouring more molten wax onto the surface and smoothing the tops. The shells are then separated from one another by hand before sealing the capsules with octadecane. Several waxy materials having a range of melting temperatures can be used to make the shell, as shown in Figure 2.4B. In all cases, the wax shells ensure that the payloads (different colored food dyes) remain hermetically sealed when the capsules are placed in water at room temperature. No release of dye is observed over several weeks. However, when the samples are heated above the melting temperature of the respective waxes, the shells melt, allowing the encapsulated dye to diffuse into the water. In addition to dyes, the wax-shelled capsules have been shown to safely encapsulate even hazardous reagents such as concentrated sulfuric acid.

2.5 Capsules with Multiple Internal Compartments

As noted in Section 2.1, eukaryotic cells have multiple inner compartments called organelles.[11] In an effort to mimic this structure, many research groups have reported the creation of microscale containers that have smaller inner containers. These include liposome-in-liposome structures (where the precursors are lipids),[13, 42, 57-59] polymersome-in-polymersome structures (where amphiphilic block copolymers serve as the precursors),[27, 32, 34, 60, 61] and capsule-in-capsule structures.[19, 26, 62] Our lab has focused on the latter, and our overall structures are referred to as “multicompartment capsules”

(MCCs).[26] The inner compartments are alginate/Ca^{2+}/chitosan capsules, created by electrostatic complexation, as described in Section 2.3. To create MCCs, these are suspended in a second alginate solution. Drops of this solution, containing one or more of the inner compartments, are passed through a larger nozzle into a chitosan/Ca^{2+} receiving solution (Figure 2.5), thereby forming MCCs. The payload in each inner compartment within an overall MCC can be independently controlled. We have encapsulated nanoparticles, macromolecules (e.g., enzymes), and even biological cells within individual compartments of an MCC. The MCC architecture is suitable for studying cascade reactions or processes, such as those involving enzymes or cells.

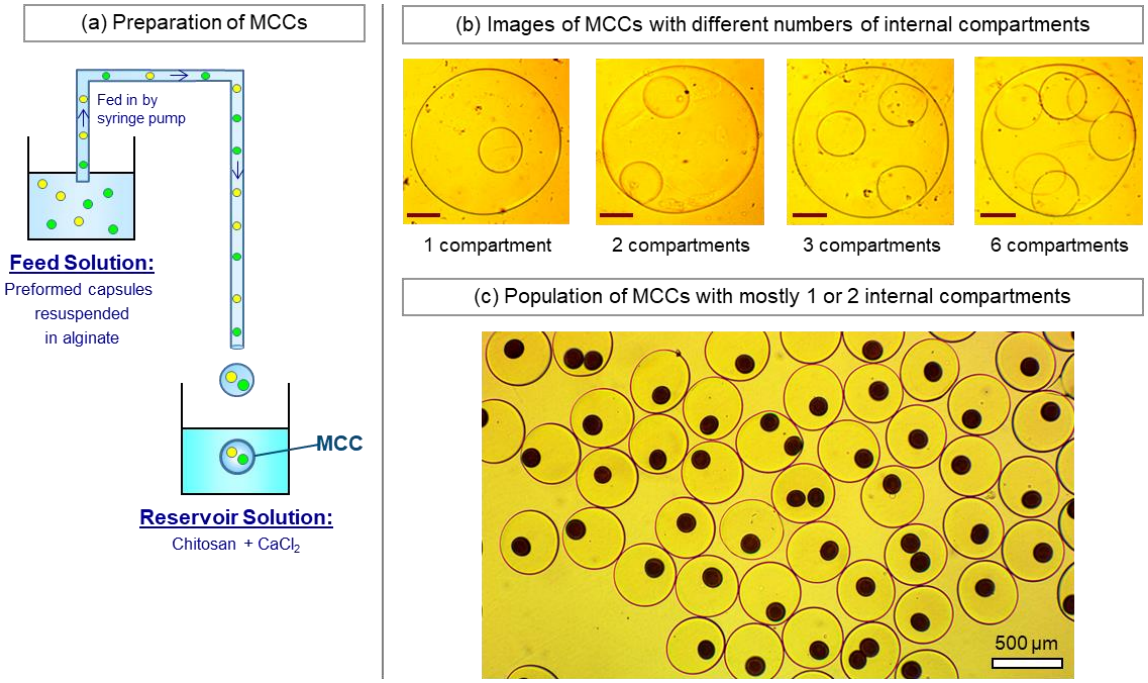

Figure 2.5. Preparation and typical images of multicompartment capsules (MCCs).[26] (a) Preparation of MCCs, using a suspension of preformed capsules in an alginate solution as the feed through a tube. Droplets at the exit of this tube are introduced into a reservoir solution containing chitosan and Ca^{2+}. The droplets are thereby converted into MCCs. (b) Optical micrographs of individual MCCs with different numbers of (identical) internal compartments. The scale bars in the images are 100 µm. (c) Optical micrographs of a population of MCCs having either one or two (identical) internal compartments. The compartments have a brown color because they contain magnetic Fe_3O_4 nanoparticles.

Chapter 3

Capsules Exhibiting Inflation and Core Ejection

3.1 Introduction

The focus of this work is on aqueous capsules. The term 'capsule' refers to structures with an inner core surrounded by a shell, with the core and the shell having different composition and properties. In the present context, the cores of the capsules are physical gels of the biopolymer, alginate. These are formed by dropwise addition of an alginate solution into a solution of divalent cations like calcium (Ca^{2+}).[46, 48, 63] We then create a layer of chemically-crosslinked polymer gel (from the acrylamide family) around the alginate gel core using a technique recently developed in our lab.[56] This involves soaking the gel core in an initiator solution and subsequently transferring to a monomer solution. The initiator diffuses outward and forms a shell of crosslinked polyacrylamide around the core. Both the core and the shell are permeable to small molecules and ions, but impermeable to macromolecules or insoluble particles. In the work done here, we have included silver (Ag) microparticles in the capsule core during synthesis; Ag was chosen for its ability to catalyze the decomposition of chemicals like hydrogen peroxide (H_2O_2).[35]

In this Chapter, we will show that our capsules exhibit the unusual phenomena of inflation and explosion (bursting). The inflation or swelling is caused by the evolution of a gas in the capsule core as a result of a catalyzed reaction; thus, this phenomenon is

somewhat like the gas-induced expansion of a balloon, albeit one that is initially filled with water. During inflation, the capsule shell (crosslinked polyacrylamide) gets stretched due to the internal pressure, until it reaches its breaking point, whereupon it finally ruptures. The rupture can be gentle or violent; in the latter case, the explosion is powerful enough to eject the core contents with force. To our knowledge, these phenomena of capsule inflation and core expulsion have not been reported previously in the literature on capsules. There have been a couple of recent examples of capsules that spontaneously rupture after some time when placed in water, e.g., due to the action of an enzyme inside or outside the capsule.[54] However, the rupture was not violent in these cases, and the core contents were released gently into solution.

Other examples have demonstrated capsule "explosion" due to an increase in osmotic pressure inside of the capsules.[64-72] Dextran-hydroxyethyl methacrylate capsules were synthesized with the incorporation of carbonate esters linking the methacrylate groups and dextran chains. Oppositely charged polymers were added layer-by-layer to the surface of the capsule to create an outer shell. In alkaline solutions, the ester groups are hydrolyzed causing degradation of the internal capsule and increasing the osmotic pressure inside of the shell. The increased osmotic pressure leads to capsule rupture within seconds. In physiological conditions, the capsule degradation and rupture takes weeks. This slow rupture in ambient condition shows a need for improvement in this system.

It is interesting to note that there are examples in nature of aquatic creatures that, when perturbed, either inflate or eject a payload with force. The former is exhibited by the family *tetraodontidae*, which include species like the pufferfish and balloonfish.[73] These fish have a highly elastic stomach, which they can fill with water or even air, causing the creature to inflate to a larger size. The inflation is a defense mechanism for several reasons. First, predators that swallow the fish before inflation may die from choking. Secondly, in their inflated, almost spherical form, the fish expose pointed spines that ward off the predator. In the context of payload ejection, aquatic creatures from the phylum *cnidaria*, such as jellyfish or sea anemones, are able to inject sub-micron needles into its predators.[74-83] Indeed, the jellyfish 'sting' experienced by swimmers in the ocean is due to the entry of a needle through their skin. Needle injection is accomplished by cells on the jellyfish tentacles called nematocysts (Figure 3.1A). Initially, the barbed needle (tubule) is coiled up in the cell, but when the cell is perturbed, an osmotic gradient (up to 150 bars) rapidly builds up and causes the needle to rapidly eject out of the cell.[74-83]

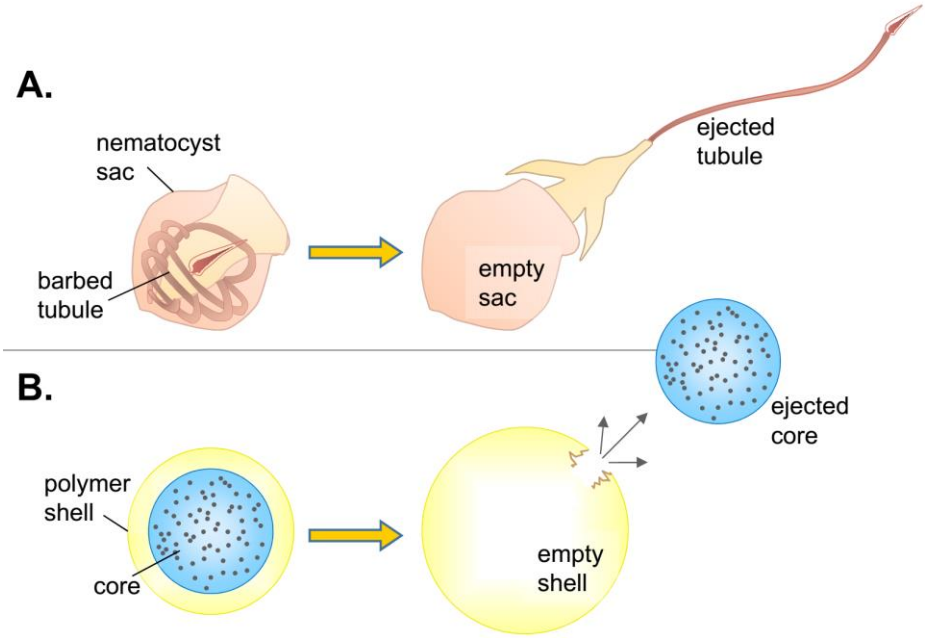

Figure 3.1. Analogy between the response of nematocysts and of the capsules in this study. A) The nematocysts are specialized cells in jellyfish that have a barbed tubule (needle) in a coiled state in their sacs. When perturbed, a high osmotic pressure rapidly builds up in the sac, and this causes the tubule to rapidly eject with force into the body of a predator. **B)** The capsules in this study have a gel core and a polymer shell. An internal reaction in the core results in the evolution of gas, and the resulting pressure stretches the shell and inflates the capsule. Ultimately, the shell bursts, and this can be a violent explosion, inducing the core to be ejected with force.

Here, we show that it is possible to control the inflation and rupture of capsules, including their extent of inflation, the time until rupture, and the intensity of rupture. In the case of violent rupture (which results in core ejection), an analogy can be made to the behavior of the nematocysts, as indicated in Figure 3.1. We believe the ability to emulate a natural phenomenon in itself makes this study interesting. In addition, such inflating capsules could prove useful in delivery applications where a large payload of drug or other chemical has to be delivered in a single, large dose or bolus.[74, 84] Future designs of soft robots may also use the core ejection strategy to defend against predators.

3.2 Experimental

Materials. The monomers N,N′-dimethylacrylamide (DMAA), acrylamide (AAm), and N-isopropylacrylamide (NIPA), and the accelerant, N,N,N′,N′-tetramethylethylene-diamine (TEMED) were from TCI America. Hydrogen peroxide (30% solution) was purchased from BDH Chemicals and glacial acetic acid from Fisher Scientific. Sodium bicarbonate powder and calcium carbonate powder (10 μm) were from J.T. Baker. All other chemicals were from Sigma-Aldrich. Two biopolymers were used: alginate, i.e., medium viscosity alginic acid, sodium salt from brown algae and xanthan gum (from Xanthomonas campestris). Other chemicals included N,N′ methylenebis(acrylamide) (BIS), calcium chloride dihydrate ($CaCl_2$) salt, ammonium persulfate (APS), and silver (Ag) microparticles (average size of 2 – 3.5 μm). Deionized (DI) water was used in all experiments.

Preparation of Ag-containing alginate gel beads. Ag microparticles of varying concentrations were suspended in a 2 wt% alginate solution in DI water; standard Ag concentration was 2 wt% unless otherwise stated. This solution was sonicated for a minute to break up any particle clumps and suspend the particles in solution. The solution was immediately loaded into a syringe while the particles where suspended and added dropwise to the reservoir solution containing 0.5 M of $CaCl_2$ in dionized water. The Ca^{2+} ions crosslink the alginate chains, thus converting the droplet into a gelled bead, as shown in Figure 3.2A. The size of the droplets, which was also the size of the beads, could be altered by changing the diameter of the nozzle at the end of the syringe. Typically, the

bead size was 4 – 5 mm using a 22G needle attached to a syringe. After 20 min of incubation in the reservoir solution, the alginate beads, with Ag particles in them, were washed and stored in DI water.

Preparation of capsules with a chemically crosslinked polymer layer. The Ag-containing alginate beads were used as the core template for the formation of capsules. The cores were soaked in a 15 mg/mL solution of the initiator APS for 2 min (see Figure 3.2B). The APS-loaded cores were transferred to a second solution containing monomer, crosslinker (BIS), the accelerant (TEMED), and xanthan gum (Figure 3.2C). The monomer concentrations were kept at 1 M and the BIS concentration was varied; unless otherwise stated, BIS concentrations were 2.2 mol% with respect to the monomer. The solution also contained 1.5 mg/mL TEMED and 0.5 – 0.75 wt% xanthan gum. TEMED is an accelerant that allows the polymerization to proceed at room temperature and the xanthan gum increases the solution viscosity so that the cores remain suspended during the process. Polymerizations were conducted at room temperature for 15 min. The result of the polymerization was a layer of chemically crosslinked polymer (DMAA, NIPA, or AAm) around the alginate cores, as shown in Figure 3.2D. The capsules thus formed were washed and stored in DI water.

Preparation of capsules with a chemically crosslinked polymer layer. To create a multiple polymer layers, the process mentioned above was repeated using the 1-layered capsule as the template. A layered capsule was placed in the APS solution for 2 min then transferred to a monomer solution. The polymerization was allowed to proceed at room

temperature for 15 min. The now 2-layered capsule was removed and washed with DI water. This 2-layered capsule can now be used a the template if another layer is desired.

Preparation of $CaCO_3$- and $NaHCO_3$-containing alginate gel beads. Two separate solutions were made of $CaCO_3$ powder and $NaHCO_3$ powder (5 wt%) in a 2 wt% alginate solution in DI water. $CaCO_3$ is insoluble in water and was stirred to create a homogeneous solution. $NaHCO_3$ is soluble in water but was added above its solubility concentration so the solution appears turbid. The solutions were loaded separately into syringes and added dropwise to a reservoir solution containing 0.5 M of $CaCl_2$ in DI water. The Ca^{2+} ions crosslink the alginate chains, thus converting the droplet into a gelled bead, as shown in Figure 3.2A. The size of the droplets, which was also the size of the beads, could be altered by changing the diameter of the nozzle at the end of the syringe. Typically, the bead size was 4 mm using a 22G needle attached to a syringe. After 20 min of incubation in the reservoir solution, the alginate beads containing $CaCO_3$ or $NaHCO_3$ were washed and used as a template for layered capsules.

Synthesis of NIPA gel control. Two solutions were made – the first being the monomer solution and the second containing our initiator. The monomer solution contained 1 mol NIPA, 2.2 mol% crosslinker (BIS) with respect to the monomer, 0.15 g TEMED, 2 wt% Ag, and 6 g DI water. In the initiator solution was 0.15g APS in 3 g water. Both solutions were cooled to 5 ºC. In a petri dish, the two solutions were mixed together and let sit. The polymerization occurred immediately. A small section of the gel was cut (~10mm) and placed in H_2O_2.

Synthesis of rheology gels. The gels used for rheology were synthesized in a petri dish and cut to size, a circle 20 mm in diameter and 4 mm thick. For each gel, two solutions were made – the first being the monomer solution and the second containing our initiator. The monomer solution contained 1 mol monomer (either NIPA, DMAA, or AAm), 2.2 mol% crosslinker (BIS) with respect to the monomer, 0.15 g TEMED, 2 wt% Ag, and 6 g DI water. In the initiator solution was 0.15g APS in 3 g water. Both solutions were cooled to 5 ºC. In a petri dish, the two solutions were mixed together and let sit. The polymerization occurred immediately. In the case of NIPA, gels with varying amounts of BIS (2.2, 4.4, and 8.8 mol%) were synthesized.

Optical microscopy. Bright field images of capsules were captured with a Zeiss Axiovert 135 TV microscope. Images were taken using a ×2.5 objective. In some cases, the microscopy was performed with slight under-focus, which helped to clearly define the outlines of the layers and/or the overall capsule.

High-speed capsule videos. To observe the dynamics of the capsule when exposed to the H_2O_2 solution, a Vision Research Phantom Miro M110 high-speed color camera was used to record videos at 600 frames per second (1666 μs exposure, $f/2.8$). Videos were limited to 30 – 45 s due to high frame rate. Lighting of the scene was supplemented with an external LED source. Images presented have been post-processed in Vision Research PCC 2.8 to correct lighting and coloring of the original videos. All other videos were taken on an iPhone 5SE and edited using MovieMaker.

Rheological studies. All rheological experiments were run on an AR 2000 rheometer (TA instruments) at 25°C and 50°C using a parallel plate geometry (20 mm in diameter). For the oscillatory shear (dynamic rheology) experiments, gel samples were cut into discs of diameter 20 mm and thickness 4 mm. The linear viscoelastic region of each sample was obtained by stress-sweep experiments, and a strain within this region (typically 1%) was used to run the frequency-sweep experiments.

3.3 Results and Discussion

3.3.1 Synthesis of Inflating Capsules

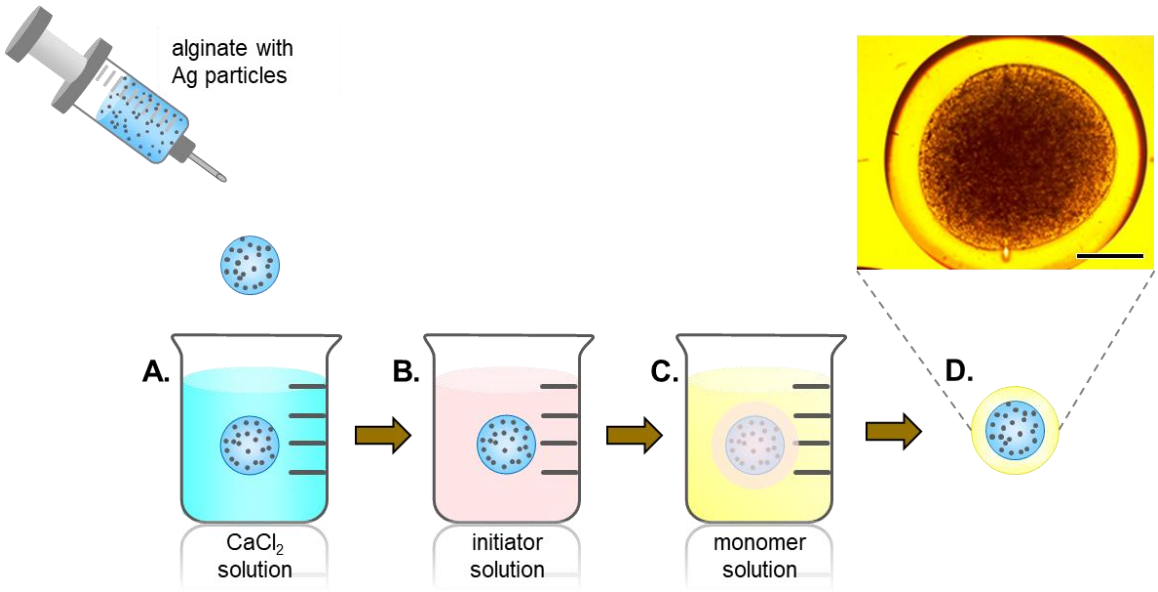

Figure 3.2. Synthesis of inflating capsules. A) An alginate solution with suspended Ag particles is dropped from a syringe into a $CaCl_2$ solution. The droplet is instantaneously converted into a gelled bead. The Ag-containing bead is used as a core template. **B)** The core is incubated in an initiator solution **C)** Then, it is placed in a solution of monomer (acrylamide derivative), crosslinker, and accelerant. **D)** Upon polymerization, a layer of chemically-crosslinked polymer gel is formed around the capsule. A microscope image of the capsule is shown in the inset. Scale bar: 1 mm.

The procedure for synthesizing capsules in this study is shown schematically in Figure 3.2. First, we create core particles by contacting the anionic biopolymer, sodium alginate, with divalent cations like Ca^{2+}. A 2 wt% alginate solution is mixed with 2 wt% of silver microparticles (~ 2 – 3.5 µm in diameter) and this slurry is added dropwise into a reservoir containing 0.5 M $CaCl_2$ (Figure 3.2A). The droplet is converted into a gelled

bead due to crosslinking of alginate chains by Ca^{2+} ions. Ag microparticles (μP) are immobilized in the bead. We chose Ag for its ability to catalyze the decomposition of H_2O_2 (see below). Next, we employ an "inside-out" technique previously devised by our lab to create a layer of chemically-crosslinked polymer gel around the alginate core. For this, the bead is loaded with a free-radical initiator (ammonium persulfate, APS) and then transferred to a solution containing monomer (NIPA or DMAA or AAm) and crosslinker (BIS). Within a few minutes, a polymer layer (chemical gel) grows outward from the core and results in a capsule with a distinct layer or shell (Figure 3.2D). To create a second polymer layer, the process is repeated using the 1-layered capsule as the core template.

3.3.2 Crosslinked Polymer Layer Required for Inflation

When the above Ag-containing aqueous capsule is placed in a solution of H_2O_2, the H_2O_2 is able to diffuse through the capsule shell and contact the Ag μPs. The Ag catalyzes the decomposition of H_2O_2 into water and oxygen (O_2) gas. The interesting result we then observe is that the capsule inflates due to the gas generated (Figure 3.3C). We will discuss the inflation in detail below. However, it is important to note that inflation is seen only for capsules that have the crosslinked polymer layer surrounding the alginate gel core. For comparison, consider the case of an alginate bead with Ag μPs in its core (Figure 3.3A). In this case, when the bead is placed in a solution of H_2O_2, the O_2 gas is released into the surrounding solution in the form of bubbles. Thus, no inflation of the bead occurs. We also made a gel of NIPA containing the same Ag μPs. When placed in H_2O_2, once again O_2 gas is produced, but it does not remain within the gel; rather it is

again released into the surrounding solution in the form of bubbles (Figure 3.3B). Thus, the scenario of inflation is seen only when there is a distinct core (alginate gel containing Ag) and a chemically crosslinked shell. We will show that in this case, the generated gas occupies a space between the core and the shell, which is why it is able to cause inflation of the shell.

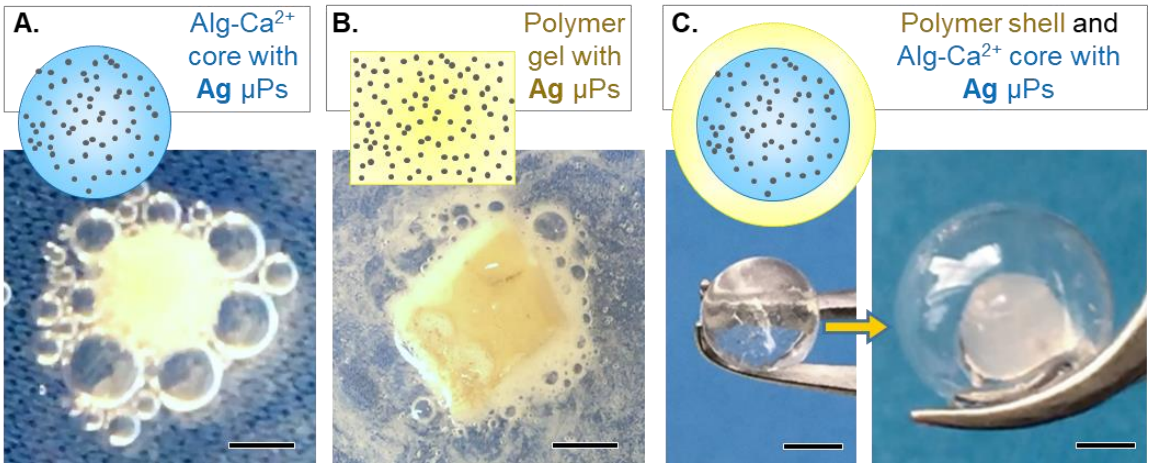

Figure 3.3. Images demonstrating that capsules inflate but beads, gels do not. In all cases, the structures have 2 wt% Ag µPs inside and are placed in a solution of 30% H_2O_2. The Ag catalyzes the decomposition of H_2O_2 into O_2 gas. **A)** Alginate gel-beads generate the O_2 in the form of bubbles, which surround the bead in the external solution. No inflation is seen. **B)** NIPA gels also produce O_2 bubbles in the surrounding solution. Again, no inflation is seen. **C)** Capsules with an alginate core and a NIPA shell inflate due to the O_2 generated in the core. Scale bars: 3 mm.

3.3.3 Capsule Inflation and Rupture: Different Modes

We have studied capsule inflation using three different polymer shells: NIPA, AAm, and DMAA. In all cases, the core was the same alginate gel containing Ag particles (2 wt%) and all capsules were placed in 30% H_2O_2 unless otherwise stated. The core size was about 4 to 5 mm and the shell thickness was about 0.5 mm. All shells were

synthesized with 1 M monomer, 2.2 mol% BIS with respect to the monomer, 1.5 mg/mL TEMED, 0.5 wt% xanthan gum, and 0.015g/mL APS. For these three cases, we find three different modes of behavior when the capsule is placed in a H_2O_2 solution, as shown in Figures 3.4 to 3.6.

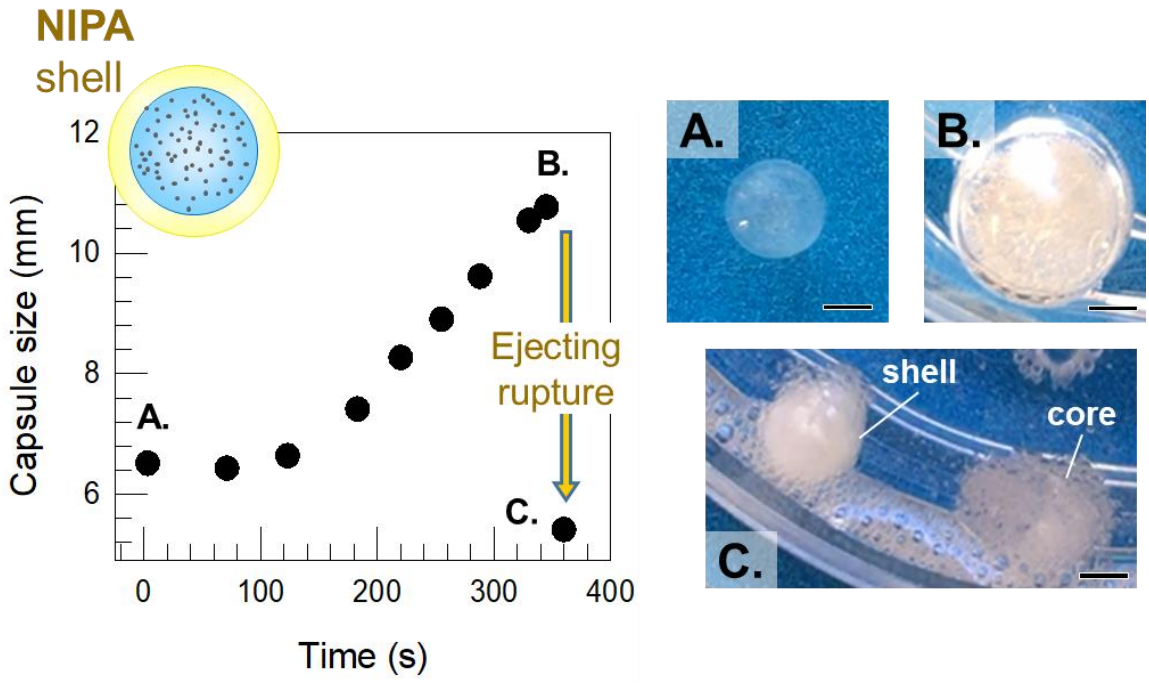

Figure 3.4. Inflation and rupture of a capsule with a NIPA shell: A) Initial capsule in 30% H_2O_2. **B)** Capsule inflates, increasing linearly in size until rupture. **C)** Capsule ruptures rapidly, and the Ag-loaded core is ejected with some force from the shell. Scale bars: 3 mm.

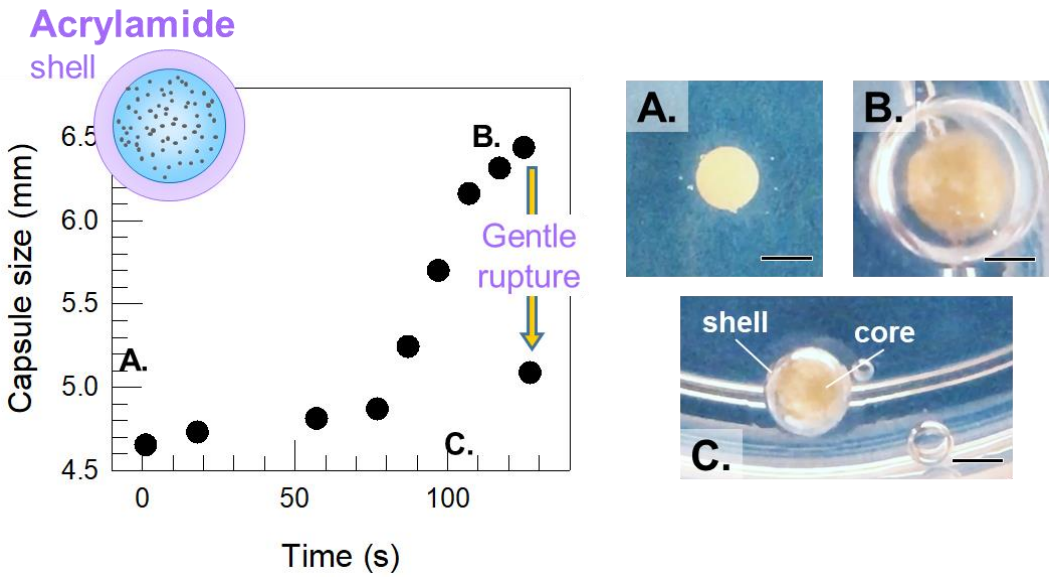

Figure 3.5. Inflation and rupture of a capsule with an AAm shell: A) Initial capsule in 30% H_2O_2. **B)** Capsule inflates, increasing in size until rupture. **C)** Capsule undergoes a gentle rupture, and the core remains inside the broken shell. Scale bars: 3 mm.

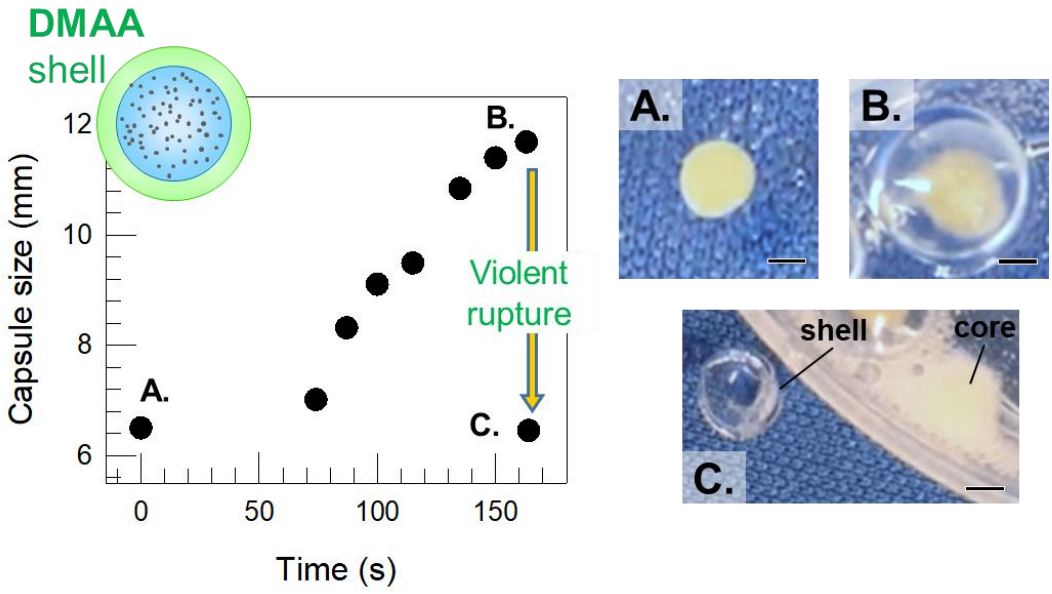

Figure 3.6. Inflation and rupture of a capsule with a DMAA shell: A) Initial capsule in 30% H_2O_2. **B)** Capsule inflates, increasing in size until rupture. **C)** Capsule ruptures violently, and the Ag-loaded core is ejected with force far from the shell. Scale bars: 3 mm.

The data presented in Figures 3.4 to 3.6 is for the capsule size [diameter] as a function of time. The capsule is placed in the H_2O_2 solution at $t = 0$. Sizes at discrete time points thereafter were extracted by analyzing still images from a recorded movie of the entire process. In all three cases, there is a lag period over the first 50 to 100 s when the capsule size is unaffected as H_2O_2 is diffusing into the capsule. Once the reaction begins, the capsule begins to inflate, i.e., increase uniformly in size in all directions. This increase is roughly linear in time, which is especially evident in the case of the NIPA shell (Figure 3.4). In all cases, the inflation for 100 to 200 s, but ultimately the shell ruptures. Once the rupture occurs, the gas escapes and the size drops to the original one. The data point for size after rupture in the above graphs is the size of the outer envelope (shell) that is left behind.

The key differences between the three shells is in the manner of rupture. The capsule with the AAm shell has the most gentle rupture (Figure 3.5). In this case, when the shell ruptures, the core remains inside the broken shell. The NIPA-shell capsule, on the other hand, ruptures rapidly with enough force that the core is ejected from the shell (Figure 3.4). The rupture of the DMAA-shell capsule is the most violent; in this case, the shell breaks into two halves and the core is ejected with force. If the experiment is done in a Petri dish, the core typically shoots into the air and out of the Petri dish.

In the above cases, the shells were made using a monomer concentration of 1 M and a crosslinker:monomer ratio of 2.2 mol%. Thus, we expect the three shells to be polymer networks with similar crosslinking densities. Nevertheless, rheological studies on the three polymer gels corresponding to the shell compositions show appreciable differences. All these gels were prepared independently as disks (see Experimental Section) and tested on a rheometer. The gels showed the expected solid-like rheology (frequency-independent elastic G' and viscous G'' moduli), and can be therefore characterized by their elastic modulus G', which is a measure of the gel stiffness. The G' of the DMAA gel was 9800 Pa, which was about 10 times that of the AAm gel (1100 Pa), and the corresponding value for the NIPA gel was intermediate at 7900 Pa. Thus, the violent-rupture mode corresponds to the stiffest polymer shell (DMAA).

3.3.4 Controlling Capsule Inflation and Rupture

We tested the effects of several variables on capsule inflation and rupture. To characterize inflation, we measured the size increase (%), i.e., the difference between the maximum size reached by the capsule upon inflation compared to its original size. To characterize rupture, we measured the rupture time, i.e., the time it takes for the capsule to rupture (with $t = 0$ being the instant when the capsule is contacted with H_2O_2).

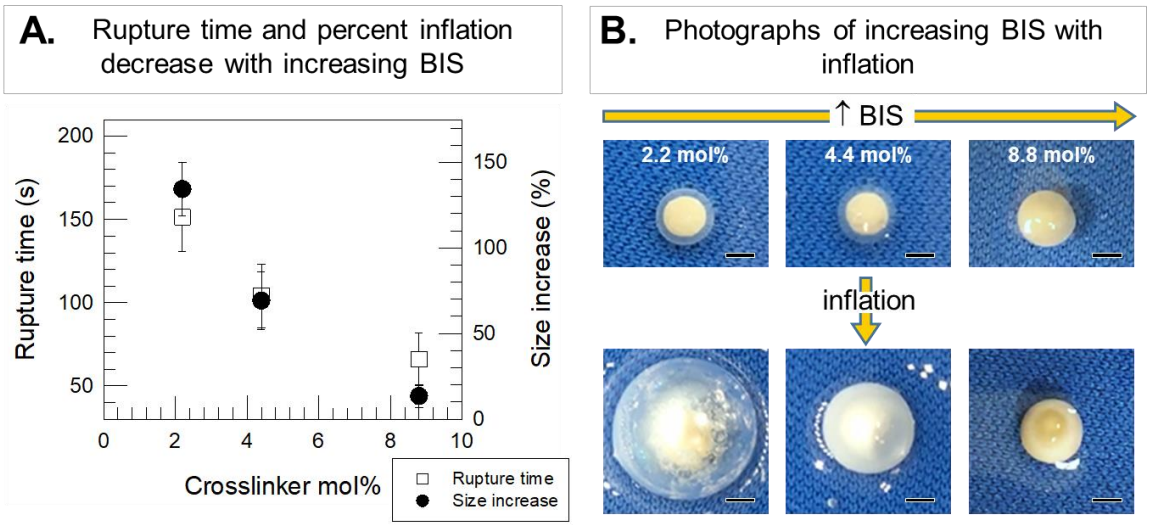

Figure 3.7. Effect of crosslinker concentration on capsule inflation and rupture. Capsules with NIPA shells and 15% Ag in the core were made with different mol% of BIS crosslinker relative to monomer. Data for rupture time and size increase (%) against BIS mol% are plotted in (**A**) (the error bars are standard deviations calculated from multiple measurements). Photos of the different capsules are provided in (**B**) (scale bars: 3 mm). The results reveal that as BIS mol% is increased, the capsules inflate less and rupture faster.

One variable that has a significant effect is the amount of crosslinker (BIS) used during synthesis. We tested this with NIPA as the monomer at a concentration of 1 M. Photos of these capsules before and after inflation, and data for the size increase (%) and rupture time are shown in Figure 3.7. All capsules had 2 wt% Ag in the core and were studied in 30 wt% H_2O_2. The capsules with the lowest BIS (2.2 mol%) inflate the most (240% size increase) and take the longest (150 s) to rupture. Increasing the BIS causes a monotonic decrease in both these parameters. We also studied the rheology of NIPA gels corresponding to the three BIS concentrations tested. As expected, the elastic modulus G' increased monotonically with increasing BIS (from 7900 Pa for 2.2 mol% BIS to 11000 Pa for 8.8 mol% BIS). This confirms that increasing BIS makes the polymer

gel stiffer, which is due to the increase in crosslink density. Thus, our finding in regard to capsule inflation is that the stiffer the shell (meaning the less it will stretch), the lower the extent of inflation. Conversely, the stiffer the shell, the easier it will rupture, i.e., the more it will be fragile or brittle.

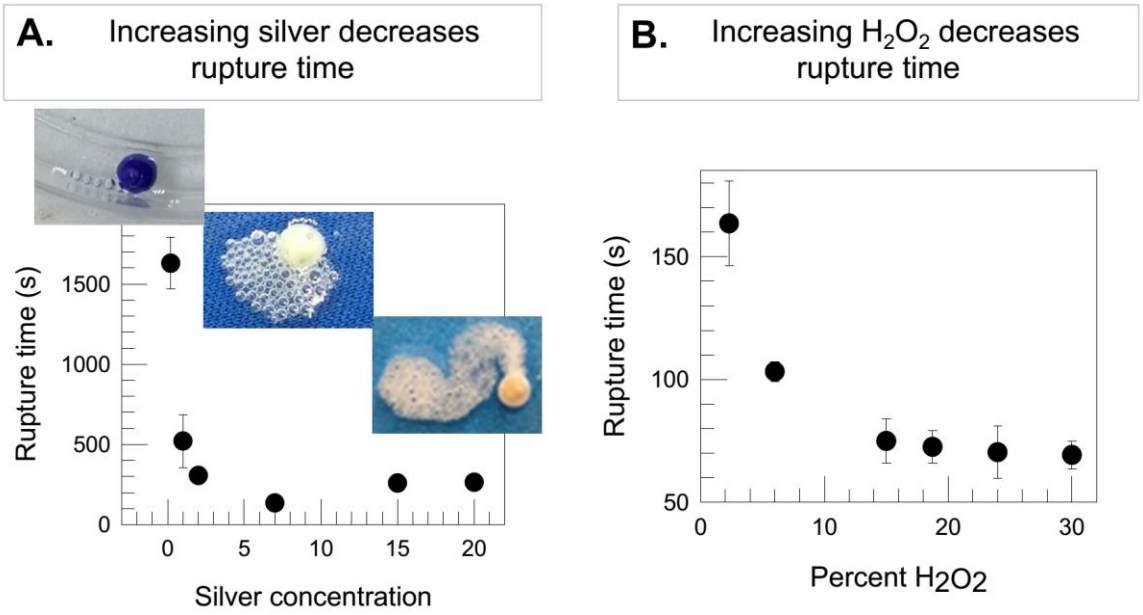

Figure 3.8. Effects of Ag concentration in the core (A) and H_2O_2 concentration in the solution (B) on capsule rupture time. Capsules with NIPA shells crosslinked with 2.2 mol% of BIS were used for these tests. For the tests in (**A**), capsules were placed in 30 wt% H_2O_2. Photos of capsules with different Ag loadings (0.2 wt% – 20 wt%) after rupture are shown in the insets to (**A**). From left to right: 1 wt%, 7 wt%, 20 wt% Ag. For the tests in (**B**), the Ag loading in the capsules was kept constant at 10 wt% and H_2O_2 concentration in the surrounding solution was varied from 2.5% – 30%. The error bars are standard deviations calculated from multiple measurements.

Other important variables are the concentration of Ag particles in the capsule core and the concentration of H_2O_2 in the solution. These were tested for capsules with a shell of NIPA (1 M) crosslinked with 2.2 mol% BIS. The Ag and H_2O_2 concentrations had no discernible effect on the extent of inflation, but both caused a

decrease in the rupture time. Both these variables increase the rate at which O_2 gas is produced and thereby the concentration of gas at any instant of time. With increased gas, the NIPA shell will be stretched to its breaking point in a shorter time.

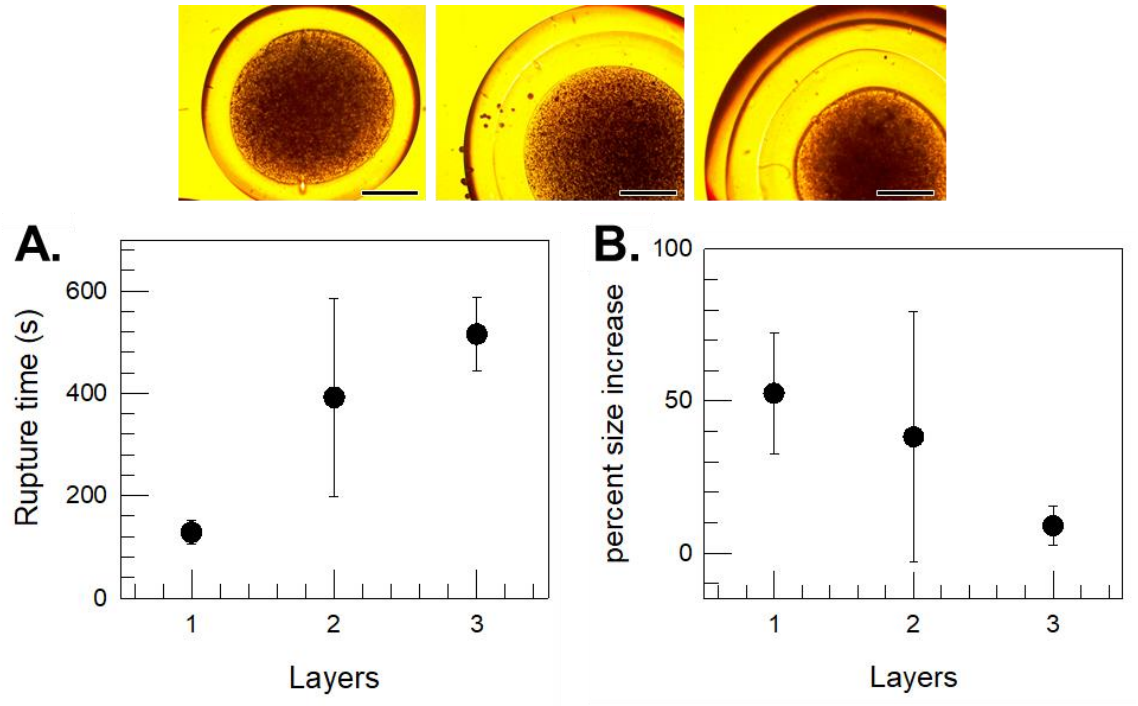

Figure 3.9. Effect of the number of layers on capsule inflation and rupture. Capsules were made with 1, 2, or 3 identical layers (see photos, scale bars 1 mm) of NIPA crosslinked with 2.2 mol% of BIS. All capsules had 2 wt% Ag in the core and were placed in 30 wt% H_2O_2 for these measurements. Plots are shown for the rupture time (**A**) and size increase (%) (**B**) vs. the number of layers. The error bars are standard deviations calculated from multiple measurements.

One other variable we have investigated is the capsule structure itself, i.e., whether the capsule has a single layer or more layers. For this case, capsules with identical NIPA-BIS layers (1, 2, or 3) were made (Figure 3.9), with each layer being about 500 μm in thickness. All capsules had identical cores loaded with 2 wt% Ag and

were placed in 30 wt% H_2O_2. The data in Figure 3.9 show that, as the number of layers increases, the capsules take longer to rupture and their inflation is slightly reduced. With regard to the rupture, this is observed in all shells of 2- and 3-layer capsules, not just the outer shell alone. But, while the 1-layer NIPA capsule ejects its core during rupture (Figure 3.4), the core of the 3-layer NIPA capsule remains together with the punctured shells.

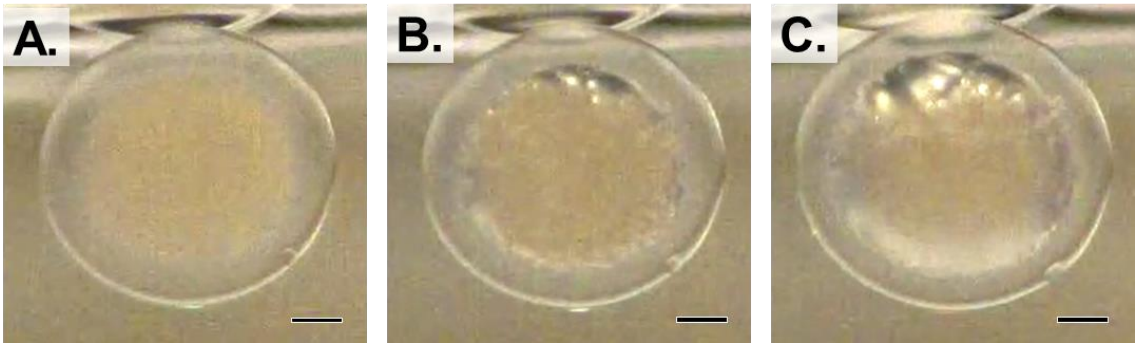

Figure 3.10. Stills from a high-speed video of capsule inflation showing the formation of a gap between the core and shell. The experiment designed for a 30-45 s time-frame due to camera limitations. Capsule was chosen for fast rupture and low inflation to keep capsule in focus during inflation. Capsule contains 7 wt% Ag in its core and a shell of DMAA. **A)** Initially, the shell and core of the capsule are in close contact. **B)** When the capsule is in 30% H_2O_2, bubbles of O_2 gas are seen to form, and these collect in a gap between the shell and the core. **C)** As more gas is produced, this gap widens, and the shell is thereby stretched. This expansion (i.e., capsule inflation) continues until the shell ruptures. Scale bars: 1 mm.

3.3.5 Why Do Capsule Inflation and Rupture Occur?

To further understand the phenomena of inflation and rupture, we examined the process using a high-speed camera. Stills from the corresponding movie at the onset of inflation are particularly revealing and are shown in Figure 3.10. The key

insight is regarding the nature of the interface between the core (alginate gel) and the shell (DMAA or other gel) during the "inside-out" polymerization used to synthesize the capsule (Figure 3.2). We infer that the core and shell are discrete layers that are only weakly adhered together by physical bonds. Consequently, as the O_2 gas is produced, the gas bubbles are able to collect between the core and the shell, creating a gap zone (Figure 3.10B). That is, the path of least resistance for the gas is to fall into the gap between two aqueous layers (rather than diffusing through the polymer shell and out into the external solution). As the gas continues to evolve, this gap widens. In the process, the pressure exerted by the gas stretches the segments of the polymer network present in the shell, i.e., inflates the capsule (Figure 3.10C).

The above aspects are shown in the schematics in Figure 3.11. Initially (Figure 3.11A), the segments between adjacent crosslinks in the shell-network are loose and unstretched. When the gas is produced due to the catalytic reaction in the core, we suggest that the gas bubbles create a gap between the core and the shell (Figure 3.11B). As this gap widens, the segments in the shell-network will become stretched significantly due to the gas pressure. This stretching cannot continue indefinitely. At some point, the stress in the shell will become so high that it will exceed the yield stress or stress-at-break of the network. When this point is reached, the shell will rupture. The retraction force when the stretching of the shell is suddenly released will be proportional to the elastic modulus of the network (much like the spring constant of a spring). This retraction force is responsible for core ejection. Thus, a stiffer

network will experience a more violent ejection, which is consistent with our findings.

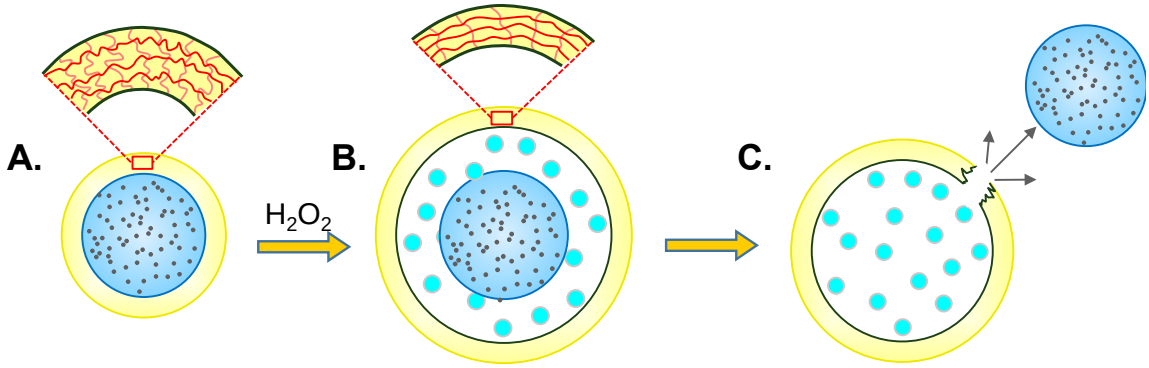

Figure 3.11. Mechanism for capsule inflation and rupture. A) Before inflation, the capsule shell is a polymer network in which the segments between crosslinks are loose and unstretched. The shell and core are weakly adhered. **B)** When gas is produced, it collects in a gap between the core and shell. The gas pressure stretches the segments in the shell-network. **C)** When the stress in the shell becomes too high, it ruptures, causing the core to be ejected out.

3.3.6 Other Ways to Inflate the Capsule

So far, we have shown capsule inflation using O_2 produced by the Ag-catalyzed decomposition of H_2O_2. We have also investigated other gas-producing reactions to utilize for capsule inflation. For example, instead of a catalyst, we can use insoluble particles of calcium carbonate ($CaCO_3$) in the core of our capsules. The particles (10 µm in diameter) were again added to the alginate solution in the first step of the capsule synthesis. When the capsule is placed in a solution of glacial acetic acid (CH_3COOH), a reaction occurs that generates carbon dioxide (CO_2) gas. Figure 3.12B shows that this is sufficient to inflate the capsule to 78% of the original capsule size. 5 wt% $CaCO_3$ was not

enough to cause the capsule to rupture but capsules with 10 wt% $CaCO_3$ produced enough CO_2 to rupture the capsule shell.

We can also use a water-soluble reagent like sodium bicarbonate ($NaHCO_3$) instead of $CaCO_3$. In this case, we added 5 wt% $NaHCO_3$ to the alginate solution in the first step of the capsule synthesis. 5 wt% is above the solubility of $NaHCO_3$ in water so the capsule appears turbid. When the corresponding capsule is placed in acetic acid (CH_3COOH), the reaction between the soluble moieties again generates CO_2 gas, which is again enough to inflate the capsule. In this case, the capsule only inflates to 24% of the original capsule size with not enough CO_2 produced to rupture the capsule. This capsule most likely inflates less due to some diffusion of the soluble catalyst out of the core during synthesis. Note that the $NaHCO_3$ and $CaCO_3$ will be used up by the reaction, unlike in the case of the catalyst.

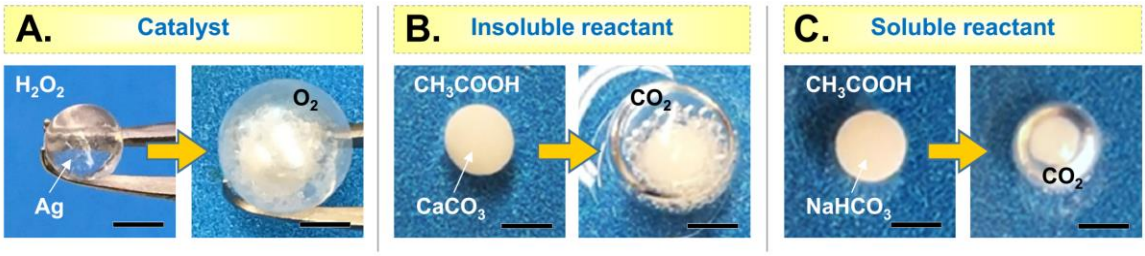

Figure 3.12. Capsule inflation by three ways. In all cases, the capsule shells were formed by NIPA crosslinked with BIS. **A)** Inflation using a catalyst: the core has 2 wt% Ag and the capsule is placed in 30 wt% H_2O_2. The capsule inflates due to O_2 gas production. **B)** Inflation using an insoluble reactant: The core has 5 wt% $CaCO_3$ particles and the capsule is placed in CH_3COOH. The capsule inflates due to the formation of CO_2. **C)** Inflation using a soluble reactant: The core has 5 wt% $NaHCO_3$ (a soluble reagent) and the capsule is again placed in CH_3COOH. Inflation is again due to CO_2. Scale bars: 3 mm.

3.4 Conclusions

We have demonstrated a design for capsules that undergo inflation to more than twice their original size when placed in a chemical fuel (H_2O_2). The capsules have a gelled core (alginate-Ca^{2+}) loaded with catalytic (Ag) nanoparticles, and a shell composed of a chemically crosslinked polymer (NIPA or DMAA or AAm). Inflation occurs because the Ag catalyzes the decomposition of H_2O_2 into O_2 gas, which collects in a zone between the core and the shell; the resulting gas pressure causes the shell to stretch. As the capsule inflates, the chain segments in the shell are stretched more until a point is reached when further stretching is not possible. At this point, the shell ruptures. Shells that are more densely crosslinked rupture in a shorter time. Three rupture modes are documented: gentle, moderate, and violent. The latter involves the core being forcefully ejected out of the shell in a manner similar to the ejection of needles out of nematocyst cells present on jellyfish. Finally, we have shown that capsule inflation is possible using other reactions that generate other gases, such as CO_2.

Chapter 4

Capsules Exhibiting Pulsed Release of Solute

4.1 Introduction

In this Chapter, we use the same capsule design as in Chapter 3, but in a different context. To briefly recap, our capsules have an alginate core containing silver (Ag) particles. The core is surrounded by a chemically-crosslinked shell of an acrylamide polymer. When this capsule is placed in hydrogen peroxide (H_2O_2), the Ag particles catalyze the decomposition of H_2O_2 into oxygen (O_2) gas, which causes the capsule to inflate and then burst.[35, 36, 43, 85-87] Here, the focus is not on inflation, but on the release of solutes contained in the capsule. Solute release is an important application for capsules, with solutes of interest ranging from small-molecule drugs to biomacromolecules (enzymes or nucleotides) to cosmetic ingredients to agrochemicals.[56, 88, 89] Typically, the release of solutes from capsules occurs by molecular diffusion. If the solute is much smaller than the mesh size of the capsule shell, the molecules will be able to readily diffuse out of the capsule. This is the case for the capsules studied here. As a model for small-molecule solutes, we use hydrophilic dyes such as basic fuchsin and rhodamine 6G (R6G).

When an aqueous capsule loaded with a hydrophilic solute is placed in a bath of water and there is no convection (stirring), then the only way for the solute to be released is by passive diffusion. This is shown in Figure 1a for our capsule loaded with basic

fuchsin dye. The capsule is placed in water at t = 0, and at a time t = 40 s, we observe a ring of pink color around the central capsule, indicating that the dye has diffused out into the solution. The outer boundary of this ring is at a distance of ~ 5 mm from the capsule surface, and this is an estimate of how far the diffusion has occurred in the time tested (i.e., of the diffusivity of the solute). As time progresses, the pink ring moves outward indicating that the dye has diffused further from the capsule.

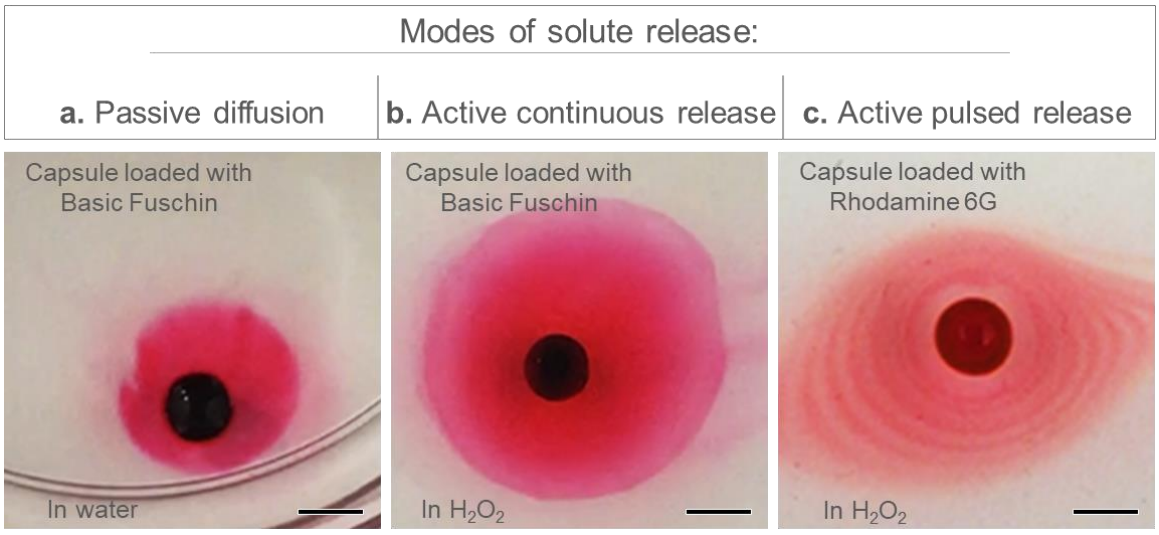

Figure 4.1. Modes of solute release: a) passive diffusion; b) active continuous release; and c) active pulsed release. All capsules have an alginate core containing 2% Ag and a shell of crosslinked N,N′-dimethylacrylamide (DMAA). In each case, the capsules are loaded with a 2.4 wt% dye solution. a) Passive diffusion: a capsule with basic fuchsin dye is placed in water at t = 0. The dye diffuses out of the capsule, forming a ring that extends to a distance of ~ 5 mm in the image taken at 40 s. b) Active continuous release: a capsule with basic fuchsin dye is placed in 30% H_2O_2 at t = 0. The dye is released at a higher rate, with the ring extending to a distance of ~ 11 mm in the image taken at 40 s. c) Active pulsed release: a capsule loaded with rhodamine 6G is placed in 30% H_2O_2 at t = 40. The dye is released in a series of periodic pulses, as shown by the image taken at 150 s. Scale bars: 6 mm.

An interesting question is whether it is possible for a capsule (or gel) to release solute at *a rate faster than diffusion* (in the absence of convection). To our knowledge, the only study that has shown such results was one conducted by Sen *et al*., which studied solute release from a gel while an enzymatic reaction was going on in the gel.[90] That is, the gel contained both an enzyme and a dye (solute) while the substrate for the enzyme was in the solution. The authors showed that the rate of solute release was faster when the enzyme was reacting with the substrate. This was interpreted to imply that the enzyme was serving as a "micropump" and actively pumping out the solute. Here, we see a similar release mode for solute in the presence of the Ag-catalyzed reaction. The capsule in this case is loaded with the same concentration of basic fuchsin dye as in Figure 4.1a and placed in a solution of 30 wt% H_2O_2 (Figure 4.1b). We find that the dye is released much faster than in Figure 4.1a, i.e., the ring of dye in Figure 4.1b at t = 40 s extends up to a distance of ~ 11 mm, which is twice as far as in the case of simple diffusion. This mode of solute release is termed "*active continuous release*" and is intriguing in its own right. It is only exhibited while the catalytic reaction is taking place in the capsule core.

An even more unusual case is observed when the dye in the capsule is R6G. When the capsule is placed in 30 wt% H_2O_2 (Figure 4.1c), we find that the dye appears to be "pumped out" of the capsule in a series of pulses. In a movie of this process, the capsule appears like a beating heart – concentric rings of dye move outward from the capsule in a periodic fashion. The periodic rings can be clearly seen in Figure 4.1c, which was taken at a time t = 40 s. We term this mode "*active pulsed release*", and it will be the focus of this study. To our knowledge, such behavior has not been reported before in the

literature. We document the conditions under which pulsed release occurs and then analyze the reasons why it occurs only with R6G.

4.2 Experimental

Materials. The monomers N,N′-dimethylacrylamide (DMAA), acrylamide (AAm), and N-isopropylacrylamide (NIPA), and the accelerant, N,N,N′,N′-tetramethylethylene-diamine (TEMED) were from TCI America. Hydrogen peroxide (30% solution) was purchased from BDH Chemicals and glacial acetic acid from Fisher Scientific. Calcium carbonate (10 μm) was from J.T. Baker. Nigrosin and Aniline Blue were purchased from Matheson, Coleman & Bell, Methyl Violet from Harleco, Safranin from Alfa Aesar, Malachite Green from Pfaltz and Bauer, Inc. and Basic Fuchsin from Allied Chemicals. All other chemicals were from Sigma-Aldrich. Two biopolymers were used: alginate, i.e., medium viscosity alginic acid, sodium salt from brown algae and xanthan gum (from Xanthomonas campestris). Dyes included: Rhodamine 6G, Rhodamine B, Sulforhodamine, Brilliant Yellow, Calcein, Methylene Blue, and Indigo Carmine. Other chemicals included N,N′ methylenebis(acrylamide) (BIS), calcium chloride dihydrate ($CaCl_2$) salt, sodium chloride, ammonium persulfate (APS), and silver (Ag) microparticles (average size of 2 – 3.5 μm). Deionized (DI) water was used in all experiments.

Preparation of Ag-containing alginate gel beads. Ag microparticles at a concentration of 2 wt% were suspended in a 2 wt% alginate solution in DI water. This solution was sonicated for a minute to break up any particle clumps and suspend the particles in solution. The solution was immediately loaded into a syringe while the particles where suspended and added dropwise to a reservoir solution containing 0.5 M of $CaCl_2$ in DI

water. The Ca^{2+} ions crosslink the alginate chains, thus converting the droplet into a gelled bead. The size of the droplets, which was also the size of the beads, could be altered by changing the diameter of the nozzle at the end of the syringe. Typically, the bead size was 4 – 5 mm. After 20 min of incubation in the reservoir solution, the Ag-loaded alginate beads were washed and stored in DI water.

Preparation of capsules with a chemically crosslinked polymer layer. The Ag-containing alginate beads were used as the core template for the formation of capsules. The cores were soaked in a 15 mg/mL solution of the initiator APS for 2 min. The APS-loaded cores were transferred to a second solution containing monomer, crosslinker (BIS), the accelerant (TEMED), and xanthan gum. The monomer concentrations were kept at 1 M and the BIS concentration was varied; standard BIS concentrations were 2.2 mol% with respect to the monomer. The solution also contained 1.5 mg/mL TEMED and 0.5 – 0.75 wt% xanthan gum. TEMED is an accelerant that allows the polymerization to proceed at room temperature and the xanthan gum increases the solution viscosity so that the cores remain suspended during the process. Polymerizations were conducted at room temperature for 15 min. The result of the polymerization was a layer of chemically crosslinked polymer (DMAA, NIPA, or AAm) around the alginate cores. The capsules thus formed were washed and stored in DI water.

Solute-release experiments. The above capsules were loaded with solute (dye) by placing in a solution at 2.4 wt% dye in DI water for 12 h. The capsules were then rinsed with DI water before placing in 30% H_2O_2. The entire experiment was captured on video

using an iPhone 5SE or a Samsung Galaxy Note 5. Ambient sunlight was used as the lighting source for the video.

Video analysis. Videos involving pulsed release were analyzed using a computer program written in the Python programming language. First, the video was uploaded to the program and resized to make the video smaller and faster to analyze. Next, the video was denoised using the Open Source Computer Vision Library (OpenCV). The denoising removes any background noise or camera flicker in the video. The parameter controlling filter strength, h, was set to 5 to minimize background noise while still tracking small pulses from the capsule. Next, the program isolated the part of the video where change is taking place by monitoring the pixels. Each pixel is stored as a set of RGB values representing the color seen in the video. As the video progresses, the pixels are tracked frame by frame (30 frames per second) to see if the pixel changes color value. Initially, the pixels should be white since our background is white. As the capsule pulses, some of the pixels become pink or red due to the dye released during the pulse. The program was set to only recognize changes with a 2% or greater change in pixel color value, which struck a good balance of filtering out background noise while still tracking the pulsing. The program records how much each frame differs from the previous frame in terms of total RGB values. Tracking the pixel change gives insight into how far the pulse spans, how rapidly the pulse occurs, and how frequently the pulses happen. Using this data, a graph was generated plotting time versus the change in pixel color values. The graph shows a visual representation of the capsule pulsing.

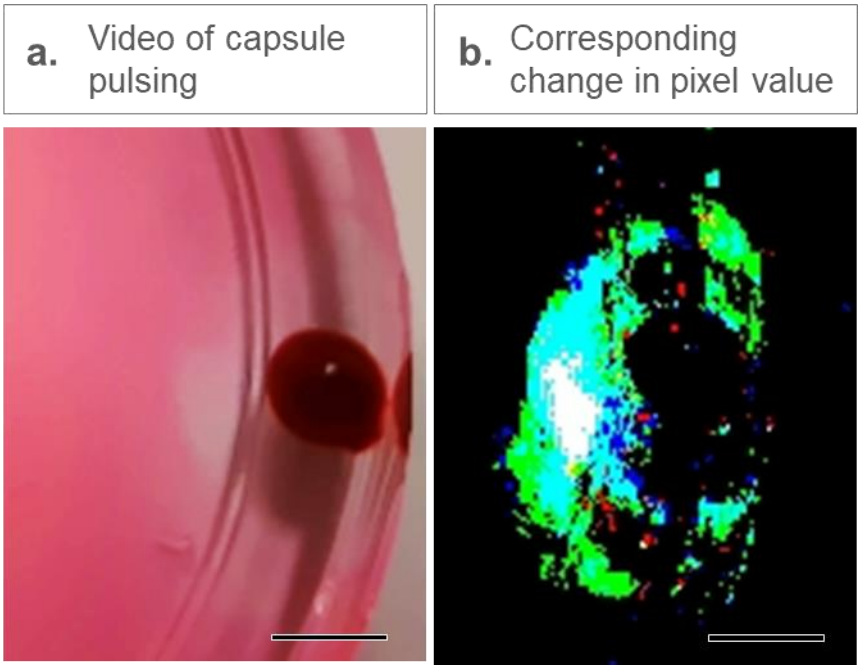

Figure 4.2. Video analysis of capsule pulsing: This example shows a capsule having an alginate core with 10% Ag and a shell of DMAA loaded with R6G and placed in H_2O_2. As the capsule pulses, the program monitors the pixel change frame by frame (30 frames per second). Each pixel is stored as an RGB value and if that value increases more than 2% in the following frame, we count it as a pixel change. Here we are showing side by side images of what we see during the pulsing process **(a)** and a visualization of what the program is seeing **(b)** If the pixel color changes more than 2% from previous frame, the pixel is illuminated to visualize where the pulsing is happening. Scale bar: 6 mm.

Optical microscopy. Bright field images of capsules were captured with a Zeiss Axiovert 135 TV microscope. Images were taken using a ×2.5 objective. In some cases, the microscopy was performed with slight under-focus, which helped to clearly define the outlines of the layers and/or the overall capsule.

4.3 Results and Discussion

4.3.1 Synthesis of Capsules for Solute-Release Experiments

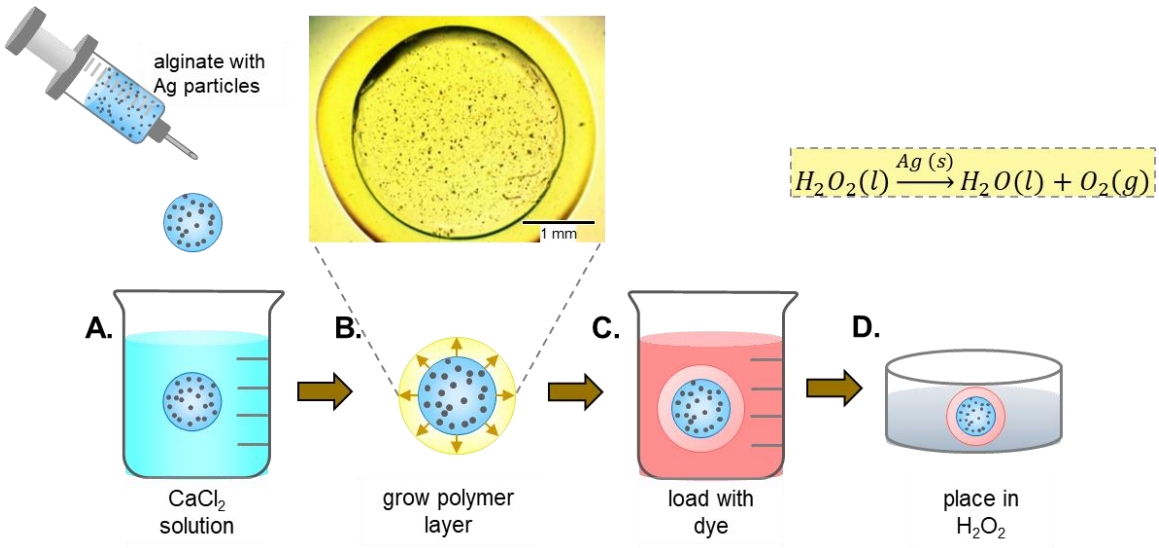

Figure 4.3. Synthesis of capsules loaded with solute (dye). A) A 2 wt% alginate solution with suspended Ag particles is dropped into a 0.5 M $CaCl_2$ solution. The droplet is instantaneously converted into a gelled bead. The Ag-containing bead is used as a core template. **B)** A shell of crosslinked acrylamide polymer (NIPA or DMAA or AAm) is grown around the gelled core to form a capsule. **C)** The capsule is then placed in a 2.4 wt% dye solution for 12 h to load it with dye. **D)** The dye-loaded capsule is placed in a 30% H_2O_2 solution at t = 0, and dye release is monitored. During the release process, the Ag particles in the capsule core catalyze the decomposition of H_2O_2 to create O_2 and H_2O. Scale bar: 1 mm.

The procedure for synthesizing capsules in this study is largely identical to that in Chapter 3 and is shown schematically in Figure 4.2. First, we create core particles by contacting the anionic biopolymer, sodium alginate, with divalent Ca^{2+}. A 2 wt% alginate solution is mixed with 2 wt% of Ag particles and this slurry is added dropwise into a reservoir containing 0.5 M $CaCl_2$ (Figure 4.2A). The droplet is converted into a gelled

bead due to crosslinking of alginate chains by Ca^{2+} ions. Ag particles are immobilized in the bead. We chose Ag for its ability to catalyze the decomposition of H_2O_2. Next, we employ an "inside-out" technique previously devised by our lab to create a layer of chemically-crosslinked polymer gel around the alginate core. For this, the bead is loaded with a free-radical initiator (ammonium persulfate, APS) and then transferred to a solution containing monomer (NIPA or DMAA or AAm) and crosslinker (BIS). Within 20 min, a polymer layer (chemical gel) grows outward from the core and results in a capsule with a distinct layer or shell (Figure 4.2B). The capsule is then loaded with solute (dye) by soaking in a solution of 2.4 wt% dye for 12 h (Figure 4.2C). Thereafter, the solute-loaded capsules are introduced into a Petri dish containing 30 wt% H_2O_2 (Figure 4.2D) The Ag particles in the capsule catalyze the decomposition of H_2O_2 into oxygen (O_2). As the reaction goes on, solute release from the capsules is monitored.

4.3.2 Active Release: Continuous vs. Pulsed

Figure 4.3 compares the release of dye (basic fuchsin) from typical capsules (with a DMAA shell and 2% Ag particles in the core) in water and in H_2O_2.. In water, dye is released by passive diffusion (Figure 4.3A). As the dye diffuses radially outward, a ring of dye is seen around the capsule, which reflects the distance the dye has diffused over a given time. As time progresses (Panel 1 to 3), the ring becomes larger. For comparison, the same experiment is repeated in H_2O_2 (Figure 4.3B). In this case, there are two simultaneous processes: dye diffuses outward, while H_2O_2 diffuses into the capsule and gets decomposed into O_2. The panels in Figure 4.3B show that the rings of dye at 7 s and

41 s are considerably larger than the corresponding rings in Figure 4.3A. This means that the release of dye out of the capsule occurs at a much higher rate when the reaction is going on in the capsule core. This phenemenon is termed *active continuous release*.

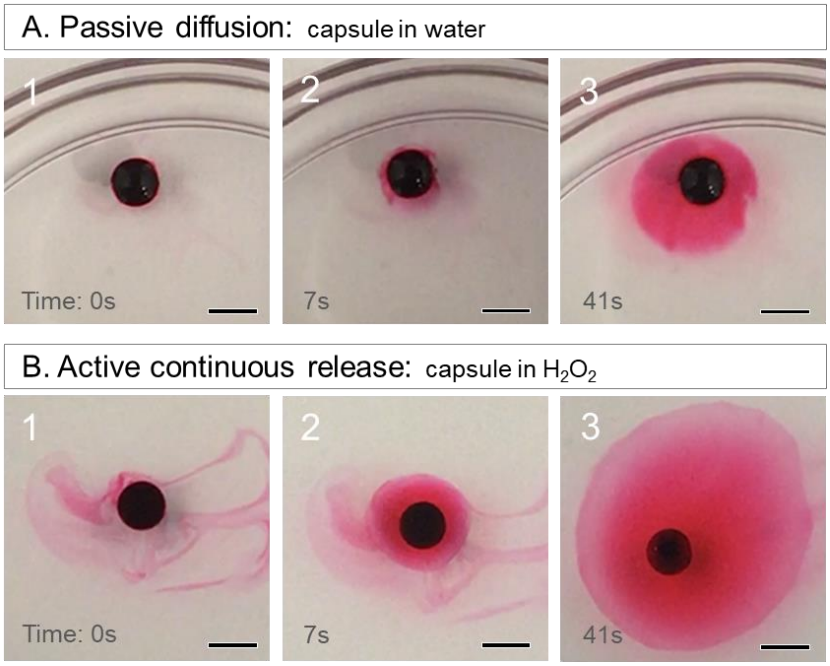

Figure 4.4. Kinetics of passive diffusion vs. active continuous release from capsules. The tests are done with capsules having an alginate core with 2% Ag and a shell of DMAA. They are both loaded with 2.4 wt% basic fuchsin dye. A) Passive diffusion: the capsule is placed in water at t = 0 (Panel 1). The dye diffuses out, forming a ring that extends outward (Panels 2, 3) B) Active continuous release: the capsule is placed in 30% H_2O_2 at t = 0. The dye is released at a higher rate, with the ring (Panels 2, 3) extending further than in (A). Scale bars: 6 mm.

We can postulate two reasons for the higher rate of active release. First, it is possible that the gas-generation inside the capsule produces convective currents in the external solution, which is known to increase the transport rate. However, the outer solution remains fairly still during this time frame. Also, any bubbles generated by the

reaction are confined within the capsule, and none can be seen outside in the solution. Thus, convection is not evident, but it cannot be ruled out. The second possibility is that the internal reaction causes an active "pumping" of internal solute, much like that postulated by Sen *et al*. in their study of solute transport from a gel coupled with an internal enzymatic reaction. In our case, the internal reaction is not enzymatic, but involves production of gas. The movement of gas outward from the core may add to the pumping action. Regardless of the precise reason, such active continuous release is observed for all tested dyes with the exception of one – rhodamine 6G (R6G).

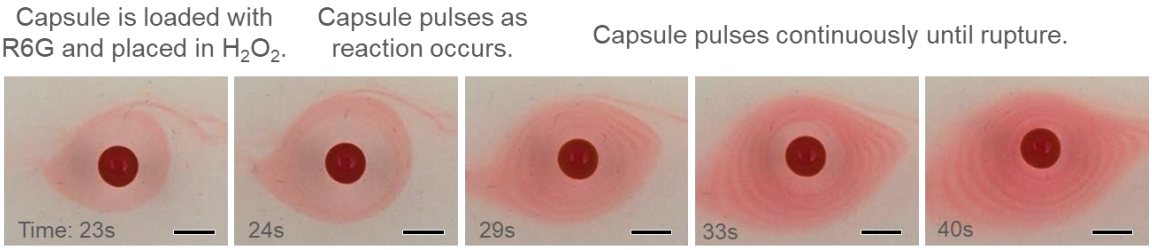

Figure 4.5. Pulsed release of Rhodamine 6G (R6G) from capsules. A capsule with an alginate core (with 2% Ag) and a shell of DMAA is loaded with 2.4 wt% R6G. When placed in 30% H_2O_2, capsule pulses, the dye is released in a series of periodic pulses. Scale bars: 6 mm.

The release of R6G dye over time from a typical capsule (with a DMAA shell and 2% Ag particles in the core) is shown in Figure 4.4. Here, we see unusual behavior: the dye is released in a series of pulses or bursts. When the first significant pulse occurs, a ring of dye is seen up to a distance of ~ 5 mm away from the capsule surface (Panel 1). The region between the ring periphery and the capsule has a lighter color (Panels 1 and 2). Subsequent pulses are seen as additional rings (Panels 3 to 5). The rings thus form a

regular, periodic pattern. We term the phenomenon as *active pulsed release*. As this is occurring, O_2 gas is being generated inside the capsule, but the capsule does not inflate appreciably. After a couple of minutes, the pulsing stops, and then the capsule inflates further before finally rupturing.

4.3.3 Pulsed-Release Kinetics and its Modulation

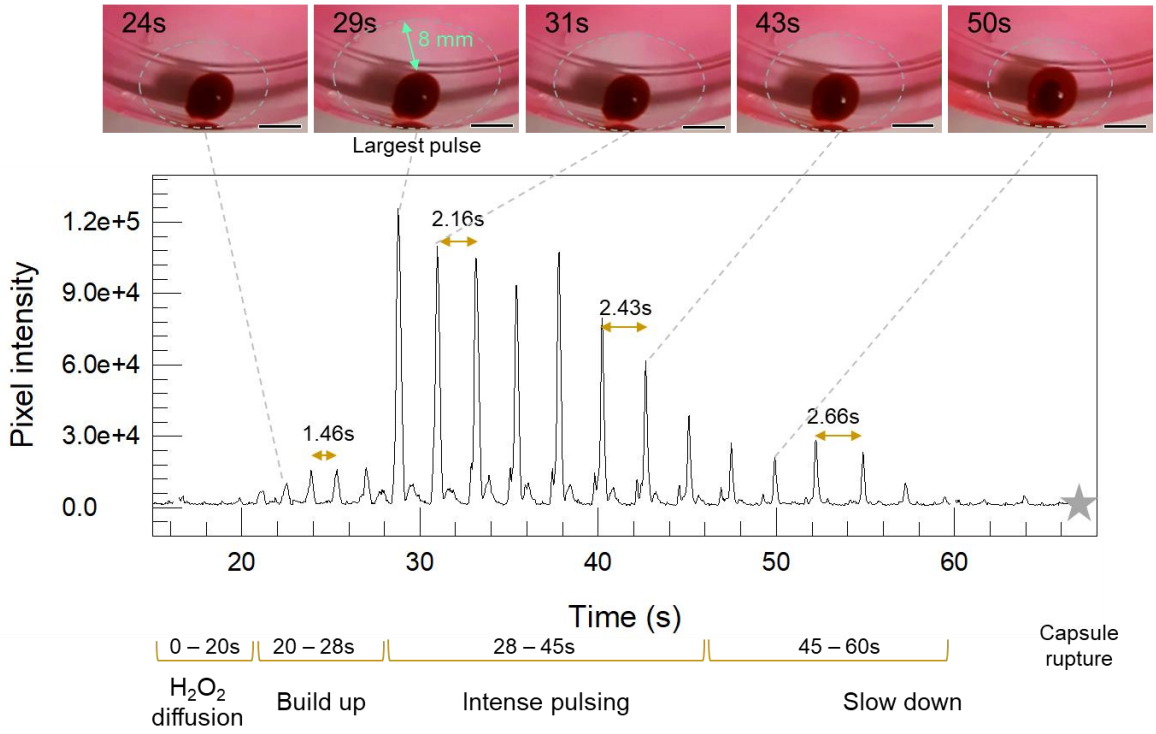

Figure 4.6. Detailed kinetics of pulsed dye release. A capsule with an alginate core (with 10% Ag) and a shell of DMAA (crosslinked with 2.2 mol% BIS) is loaded with 2.4 wt% R6G and placed in 30% H_2O_2 at t = 0. A video of the dye release is analyzed to obtain a plot of pixel intensity vs. time. Various stages during this process are marked, and still images at discrete points are shown (scale bars: 6 mm). In total, the graph shows 22 pulses over 40 s.

To analyze the observed pulsing, videos were analyzed (see Experimental Section for details) and converted into plots, as shown in Figure 4.5. This data is for a capsule with a DMAA shell crosslinked with 2.2 mol% BIS and with 10 wt% Ag particles in the core. At t = 0, the capsule is placed in 30% H_2O_2. Pulsing begins around the 20s mark, with there being a few weak pulses first. Then an intense pulse is observed at 29 s, and this traces a ring that extends 8 mm from the capsule surface (see image). Intense pulsing at regular intervals then occurs up to the 45 s mark; thereafter, from 45 to 60 s, the pulses become weaker and more widely spaced. The pulsing then stops, and the capsule then inflates and ruptures at the 67 s mark. Altogether, pulsing occurs for 40 s (starting at 20s and ending at 60 s) and there are a total of 22 pulses.

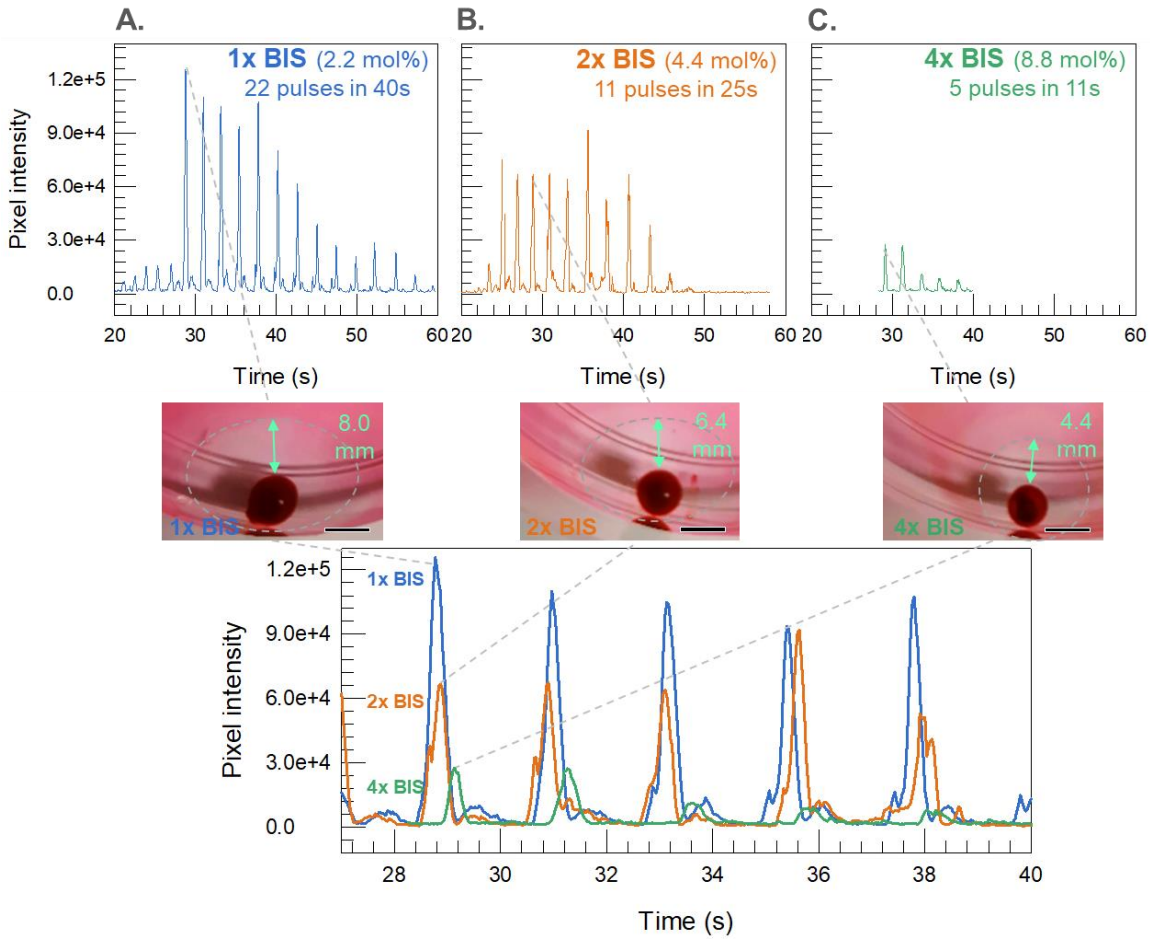

Figure 4.7. Pulsing of capsules with differently crosslinked shells. All capsules had 10% Ag in the alginate core. Their shells were DMAA crosslinked by BIS with the BIS:DMAA molar ratio at 2.2 mol% (1x) (A), 4.4 mol% (2x) (B) or 8.8 mol% (4x) (C). All capsules were loaded with 2.4 wt% R6G and were placed in 30% H_2O_2 at t = 0. Plots of pixel intensity vs. time are shown for the three cases individually, and the three plots are compared over a portion of the time frame in (D). Images of the capsules showing the most intense pulses are also provided (scale bars: 6 mm).

Next, we consider the effect of crosslink density on pulsing of R6G (Figure 4.6). This data is for capsules with a DMAA shell crosslinked with varying concentrations of BIS. As the crosslinker is increased, the pulsing reduces in intensity and in extent. For example, doubling the BIS from 2.2 to 4.4 mol% reduces the number of pulses (22 to 11), the duration of pulsing (40 to 25 s), and the intensity of the pulses (peak height). Further

doubling the BIS to 8.8 mol% makes the pulsing nearly disappear. This shows that the pulsing is magnified when the shells are flexible and elastic (lightly crosslinked) and damped when the shells are more rigid. In other words, pulsing must be associated with some transverse motion of the shell. Another variable that affects pulsing is the amount of Ag in the core. If the Ag is reduced from 10 wt% to 2 wt%, we find all the same trends seen with 10 wt% but at a lower pulsing intensity.

We have also switched up the polymer shell in the capsule from DMAA to AAm or NIPA, and in these cases also, we see pulsing of R6G (Figures 4.7 and 4.8). The AAm and NIPA shells were crosslinked with 2.2 mol% BIS, as with the DMAA shell in Figure 4.5. The capsules were otherwise identical (10 wt% Ag particles in the core), and were studied in 30% H_2O_2. The pulsing response for AAm (Figure 4.7) is similar to DMAA: pulses start small, increase, and then decrease until rupture. An interesting, but subtle, point is that we observe a consistent double pulse where one side of the capsule pulses, then the other (i.e., the pulses do not radiate outward in a symmetric manner). In the case of the NIPA shell also (Figure 4.8), we observed non-symmetric pulsing. Another quirk in this case is that the gap between pulses increases to over 10s before ceasing completely as the capsule inflates. Finally, with NIPA, once the pulsing stops, there is a large gap in time before the capsule ruptures.

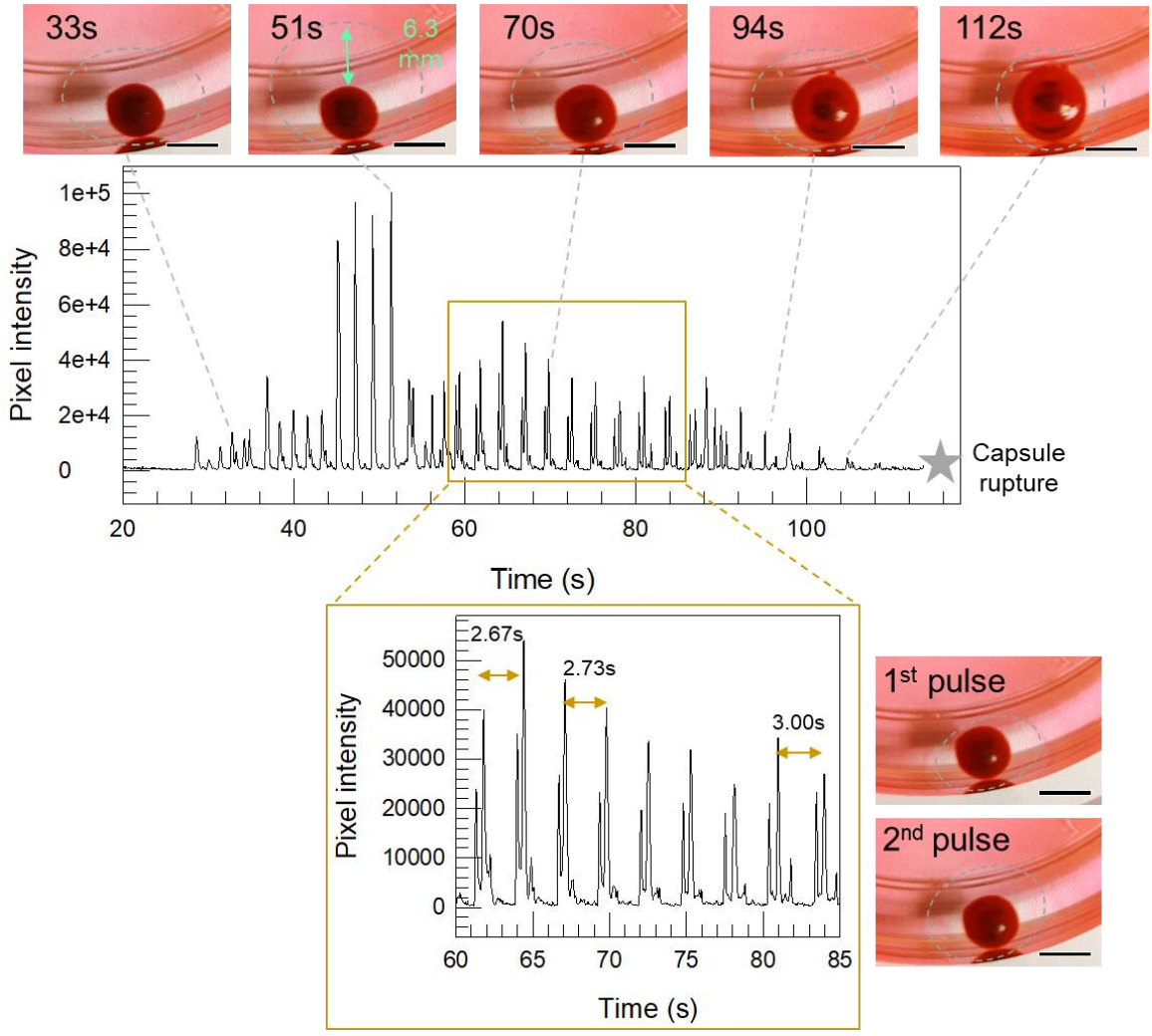

Figure 4.8. Pulsing of capsules with AAm shells. A capsule with an alginate core (with 10% Ag) and a shell of AAm (crosslinked with 2.2 mol% BIS) is loaded with 2.4 wt% R6G and placed in 30% H_2O_2 at t = 0. A video of the dye release is analyzed to obtain a plot of pixel intensity vs. time, and a zoomed-in version of this plot between 60-85s is shown to indicate the distinct double pulses. Still images at discrete points are also shown (scale bars: 6 mm).

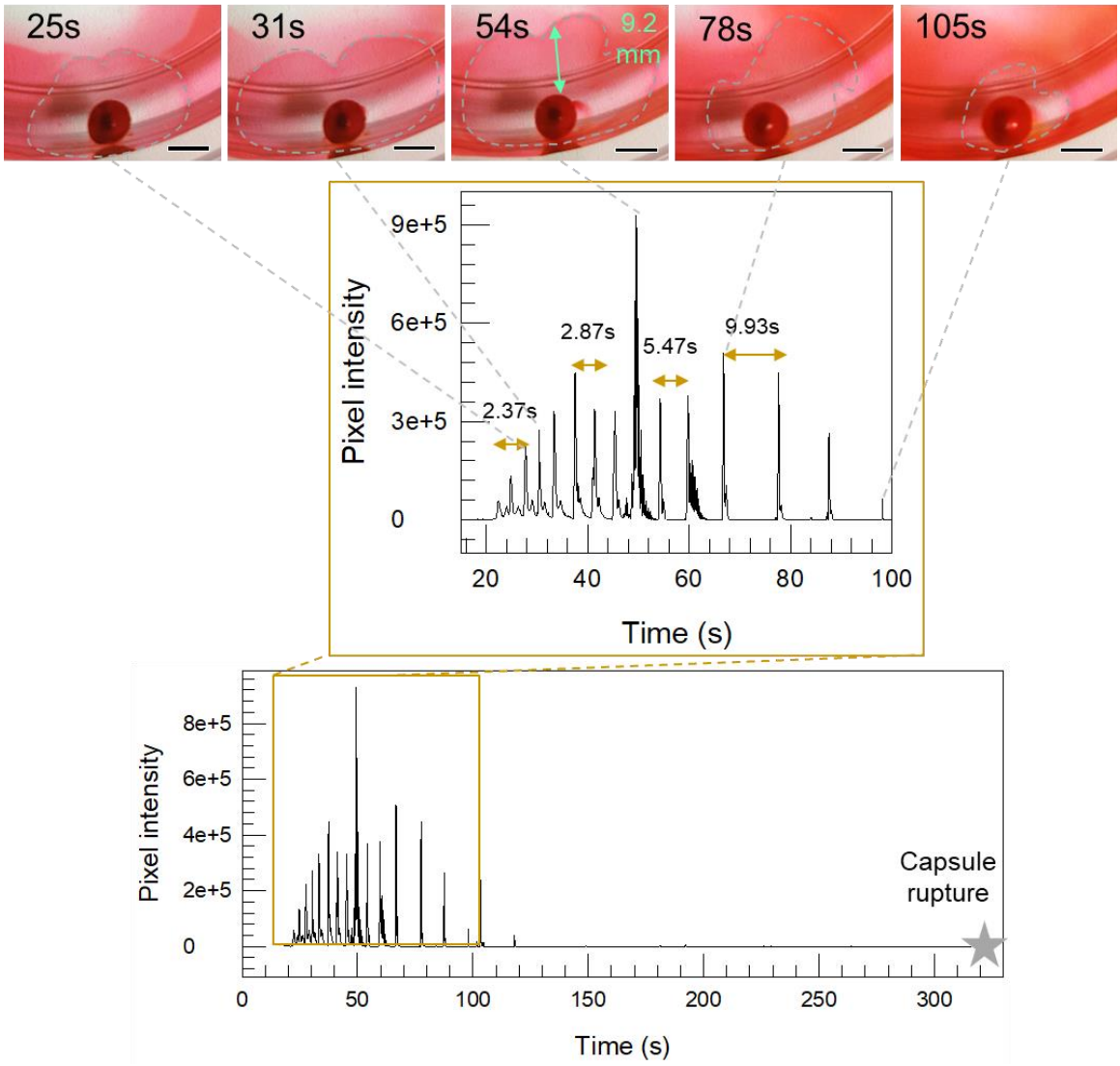

Figure 4.9. Pulsing of capsules with NIPA shells. A capsule with an alginate core (with 10% Ag) and a shell of NIPA (crosslinked with 2.2 mol% BIS) is loaded with 2.4 wt% R6G and placed in 30% H_2O_2 at t = 0. A video of the dye release is analyzed to obtain a plot of pixel intensity vs. time, and a zoomed-in version of this plot between 20-100 s is shown. The capsule stops pulsing after 100 s and continues inflating until it bursts after 300 s. Still images at discrete points are also shown (scale bars: 6 mm).

4.3.4 Why Does Pulsing Occur?

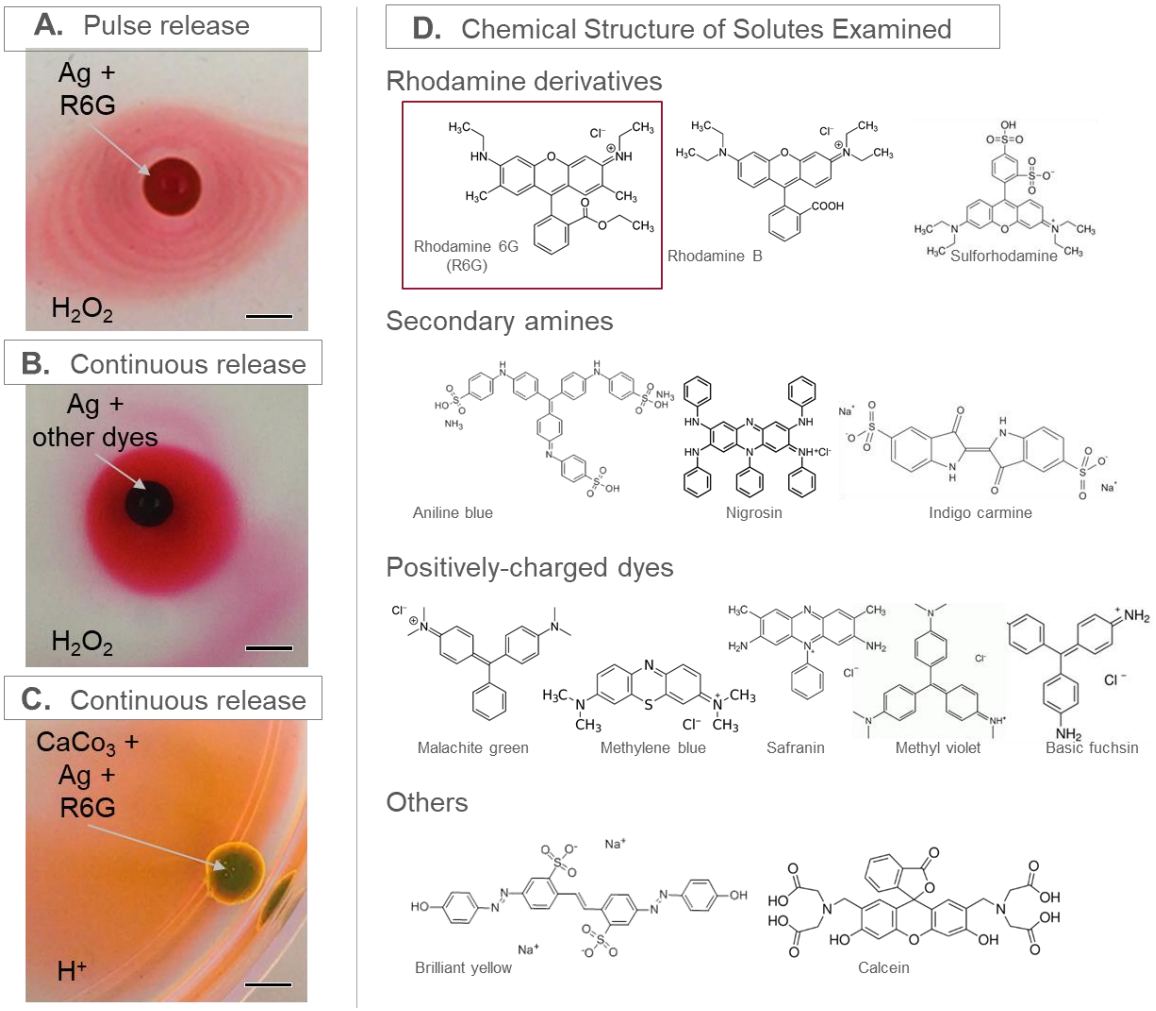

Figure 4.10. Pulsing only occurs with Ag in the core, R6G dye, and H_2O_2 as the chemical fuel. A variety of scenarios are tested with capsules having an alginate core with 2% Ag and a shell of DMAA crosslinked with 2.2 mol% BIS. The capsules are loaded with 2.4 wt% of the dyes shown in **D)**. **A)** Capsules with Ag and R6G show pulsed release in 30% H_2O_2. **B)** Capsules with Ag and other dyes exhibit active continuous release in 30% H_2O_2 – no pulsing occurs. **C)** Capsules with 10 wt% $CaCO_3$ as well as Ag and R6G are placed in glacial CH_3COOH. Here, the reaction of $CaCO_3$ and CH_3COOH produces CO_2 gas. The R6G is released continuously with no pulsing. Scale bars in the images: 6 mm.

We have tested capsules loaded with a variety of different dyes whose chemical structures are indicated in Figure 4.9D. A key conclusion from these tests is that pulsed release occurs only for the specific case of R6G with capsules containing Ag particles and only when these capsules are placed in H_2O_2. Other dyes with the Ag-H_2O_2 combination show active continuous release, as mentioned before and shown again in Figure 4.9B. Another important control experiment is shown in Figure 4.9C. Here, we use a different way to generate gas in the capsule. The capsule contains 10 wt% of calcium carbonate ($CaCO_3$) particles as well as 2 wt% Ag. It is placed in a solution of glacial acetic acid (CH_3COOH). The reaction between the two generates carbon dioxide (CO_2) gas and these capsules still inflate and rupture similarly to the Ag-loaded capsules. When loaded with R6G, however, these capsules exhibit active continuous release, and not pulsed release. Thus, even though R6G and Ag are present, the pulsing requires the catalytic reaction of Ag with H_2O_2.

We also tested dyes that are both similar and different to R6G in chemical structure. R6G is a fluorescent dye with a positive charge on the secondary amine. We tried other positively charged dyes (methylene blue, malachite green, methyl violet), dyes containing secondary amines (nigrosin, aniline blue), dyes containing primary amines (safranin, basic fuchsin), and other rhodamine derivatives (rhodamine B, sulforhodamine). We also tested a few others: Brilliant Yellow, Calcein, and Indigo Carmine. All these capsules resulted in active continuous release and did not pulse. The capsule pulsing is attributed to the interaction between R6G and the Ag particles in the core. Several studied have commented on this unique interaction and have taken action to

further understand the binding mechanism.[91, 92] It has been theorized that the dye molecules form dimers at high concentrations, which then adhere to the surface of silver nanoparticles. Two orientations are possible, head-to-tail (J-type) or parallel (H-type) dimers, and both are suggested to be present on the Ag surface.[91, 92] There is also evidence to suggest that R6G particles form large micelles around the silver particles.[91]

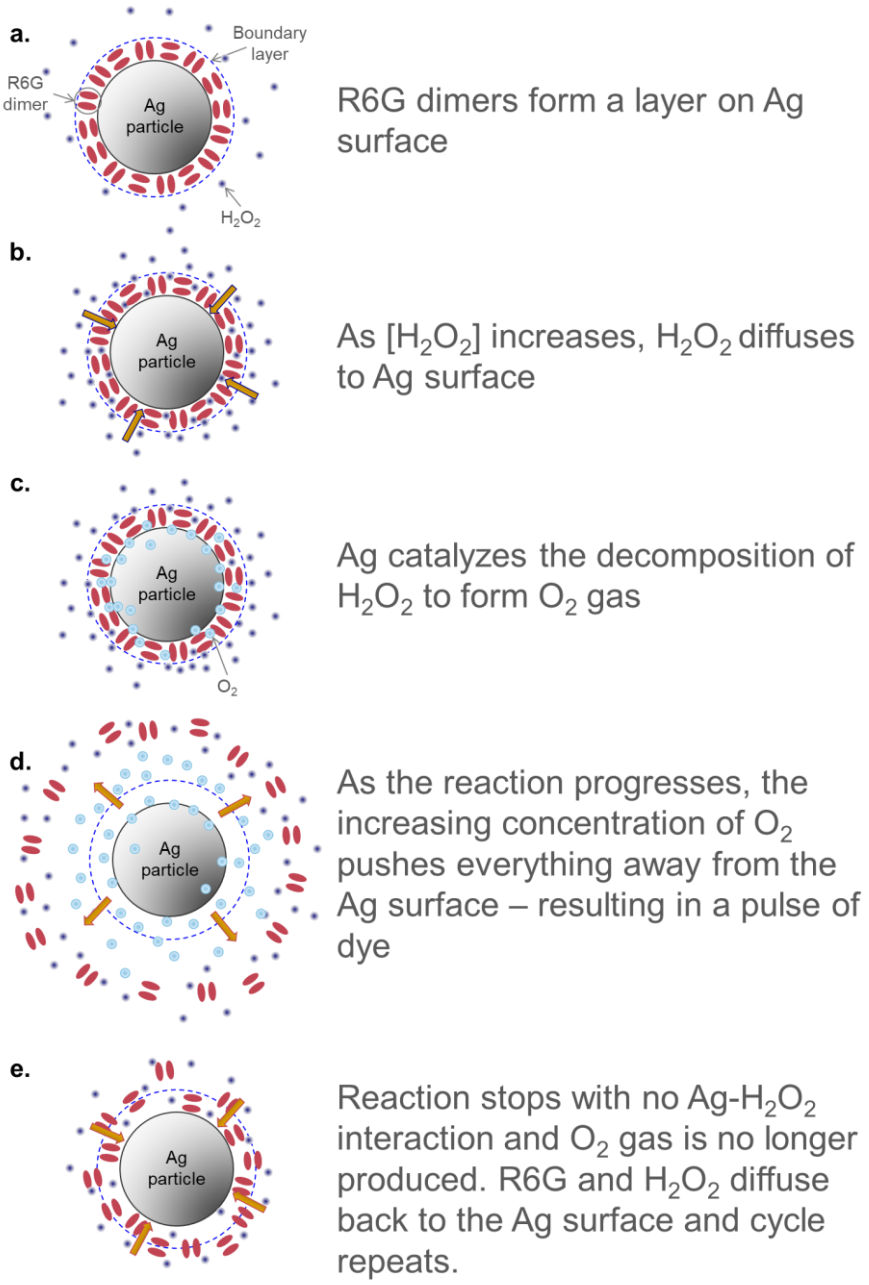

Figure 4.11. Schematic of the pulsing mechanism Pulsing capsules are synthesized with Ag in the core and are loaded with R6G. When placed in H_2O_2, the capsules produce O_2 and begin to pulse. **a)** When initially synthesized, R6G forms dimers and interacts with the surface of the Ag particles. **b)** When placed in H_2O_2, the H_2O_2 diffuses into the capsules and to the Ag surface. **c)** The decomposition of H_2O_2 begins and O_2 gas is produced. **d)** As the reaction progresses, the increased concentration of O_2 pushes away everything from the Ag surface. **e)** With no H_2O_2 near Ag, the reaction is hindered and no more O_2 is produced. During this lull, R6G and H_2O_2 navigate back to the surface of Ag and the cycle begins again.

We hypothesize that the R6G-Ag particle interaction inhibits the H_2O_2 from accessing the Ag. To reach the Ag, R6G must be displaced. This pulsing could be due to the forceful displacement of dye from the surface of the particles. Further understanding interaction between these molecules might allow us to replicate this pulsing process with other molecules for controlled release.

4.4 Conclusions

We have demonstrated the unusual phenomenon of solute being released in a series of periodic pulses out of an aqueous capsule. The capsules have a gelled core (alginate-Ca^{2+}) loaded with catalytic (Ag) particles, and a shell composed of a chemically crosslinked polymer (NIPA or DMAA or AAm). Pulsed release is only observed for capsules loaded with the dye R6G and when placed in H_2O_2. We hypothesize that a binding reaction between R6G and the Ag particles is the key to explaining these results. This implies a competition between H_2O_2 and R6G for the Ag surfaces, and we have postulated that this competition leads to a cyclical pattern of adsorption, which coincides with the periodicity of the pulse. Pulsing also requires that the polymer shell not be too rigid, which suggests that the transverse motion of the shell also accompanies the pulse. Further studies in this area of research may lead to applications for pulsed release in the delivery of therapeutics or other chemicals.

Chapter 5

Capsules Showing Thermally-Triggered Emergent Behavior

5.1 Introduction

In previous Chapters, we have discussed aqueous capsules that had a biopolymer (alginate) gel as its core and a crosslinked polymer hydrogel as its shell. The capsule shell was readily permeable to small molecules such as hydrogen peroxide (H_2O_2) as well as to a range of dyes. This means that such capsules cannot store small-molecules for a long time while ensuring no leakage. But what if one could design a capsule with an impermeable shell – one that kept its core contents perfectly sealed for long times (days or even months)? This design would be even more useful if the shell could be switched on-demand from impermeable to permeable.[93, 94] If such capsules were available, they could be combined in creative ways so as to enable new "emergent" properties.

In this Chapter, we will present a design for a capsule that perfectly encapsulates contents at room temperature but releases the contents upon heating. The key to this design is to make the capsule shell out of *wax*. We have devised a new way to rapidly create a thin wax shell around a preformed aqueous gel. This method is considerably simpler than previous approaches in the literature. It can be implemented with simple paraffin wax, which is a mixture of C_{20}–C_{40} hydrocarbons having a broad melting transition around 53°C. Alternately, we can use purified long-chain hydrocarbon waxes with sharper melting transitions. In either case, the property conferred by the wax shell is

shown schematically in Figure 5.1A, where a wax-shelled capsule with a gelled core is shown in water. At temperatures $T < T_m$, which is the melting temperature of the wax, the solute in the core remains perfectly sealed. However, when heated to $T > T_m$, the wax shell melts and the solute can then diffuse out of the gelled core into the water.

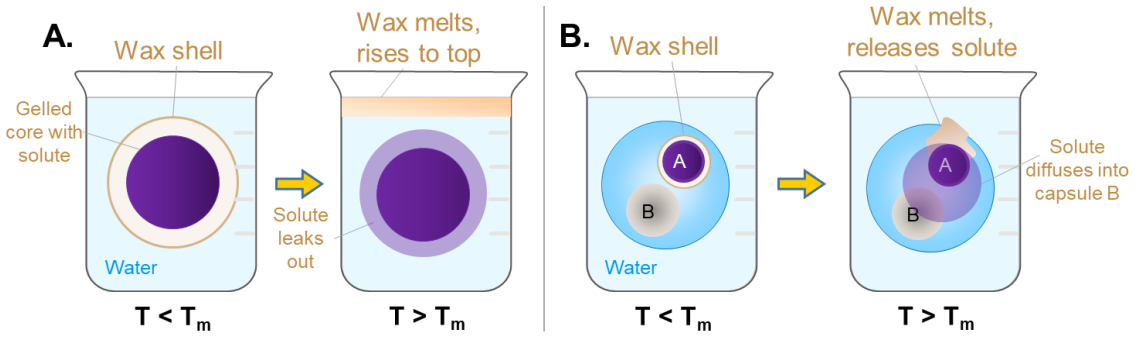

Figure 5.1. Properties conferred by a wax shell to aqueous capsules. A) Single capsule with a wax shell that has a melting temperature T_m. The solute is perfectly sealed below T_m and released above T_m. **B)** Multicompartment capsule (MCC) with two internal compartments, A and B, with A having a wax shell. Below T_m, the contents of A are prevented from contacting B. Raising the temperature above T_m allows the solute in A to diffuse to the adjacent B. This enables multi-step and cascade reactions with the MCC.

We will also exploit the wax-shelled capsules within a construct developed in our lab called multicompartment capsules (MCCs) (Figure 5.1B). The motivation behind making MCCs was to mimic the compartmentalized architecture of eukaryotic cells, which have discrete compartments called organelles in the cell. Organelles are covered by lipid membranes and have the ability to regulate the entry and exit of small molecules through their membranes. For example, lysosomes are organelles having an acidic pH that is much lower than the rest of the cell. In MCCs created so far, the internal compartments were semi-permeable, allowing small molecules to diffuse in and out while

entrapping large macromolecules and enzymes. These compartments could not maintain an acidic pH because the acid would leak away into the lumen of the MCC.

Here, the wax-shelled capsules will be used to impart new functionalities to MCCs. For example, in the schematic of Figure 5.1B, we have sketched an MCC with two inner compartments, one of which (A) has small molecules in its core and a wax shell. The other (B) may have enzymes or nanoparticles that are large enough to remain entrapped in the compartment. When the MCC is heated above the T_m of the wax, the shell of A will melt, and thereby the small molecules in A will be able to diffuse out and contact the contents of B. Thus, multi-step and cascade processes will be possible using wax-shelled inner compartments in MCCs.

5.2 Experimental

Materials. The monomer N,N′-dimethylacrylamide (DMAA), the accelerant N,N,N′,N′-tetramethylethylenediamine (TEMED), and methyl red were from TCI America. Hydrogen peroxide (30% solution) was purchased from BDH Chemicals and glacial acetic acid and sodium thiosulfate from Fisher Scientific. Palmitic acid (95% purity, T_m 62 – 65 ºC) and *n*-eicosane (99% purity, T_m 35 – 37 ºC) were purchased from Alfa Aesar. All other chemicals were from Sigma-Aldrich. Three biopolymers were used: alginate, i.e., medium viscosity alginic acid, sodium salt from brown algae, xanthan gum from Xanthomonas campestris), and starch from potato. Several dyes and indicators were also used, including brilliant yellow, methylene blue, and phenolphthalein. Other chemicals included ethanol, N,N′ methylenebis(acrylamide) (BIS), calcium chloride dihydrate ($CaCl_2$) salt, sodium chloride, ammonium persulfate (APS), silver (Ag) microparticles (average size of 2 – 3.5 μm), sodium hydroxide, phenolphthalein, potassium iodide, octadecane (99% purity, T_m 26 – 28 ºC) and paraffin wax (ASTN D 87, T_m 53 – 57 ºC). Deionized (DI) water was used in all experiments. Fiberglass mesh with 3 mm mesh size was manufactured from Adfors Saint-Gobain.

Preparation of alginate gel beads. A 2 wt% alginate solution in DI water was loaded into a syringe and added dropwise to a reservoir solution containing 0.5 M of $CaCl_2$ in DI water. The Ca^{2+} ions crosslink the alginate chains, thus converting the droplet into a gelled bead. The size of the droplets, which was also the size of the beads, could be altered by changing the diameter of the nozzle at the end of the syringe. Typically, using

a 22G needle, the bead size was 4-5 mm. After 20 min of incubation in the reservoir solution, the alginate beads were washed and stored in DI water. Ag-containing alginate beads were prepared by including 2 wt% Ag microparticles in the alginate solution, and then sonicating for a minute to break up any particle clumps and suspend the particles. This slurry was then immediately used in the dropwise addition step.

Preparation of paraffin wax-shelled capsules. The alginate beads from the above step were cooled to 5 ºC and subsequently dropped using tweezers into a reservoir of molten paraffin wax (T_m ~57 ºC) heated to 65 ºC. A thin wax layer forms around the cold bead within seconds, whereupon the wax-shelled capsule was removed with tweezers. Instead of an alginate bead, the same procedure was also done with liquids, such as a 2 wt% alginate solution.

Preparation of palmitic acid wax-shelled capsules. Alginate beads were cooled to 5 ºC and subsequently dropped using tweezers into a reservoir of molten palmitic acid (T_m ~65 ºC) heated to 70 ºC. A thin wax layer forms around the cold bead within seconds, whereupon the wax-shelled capsule was removed with tweezers. Instead of an alginate bead, the same procedure was also done with liquids, such as a 2 wt% alginate solution.

Preparation of *n*-eicosane wax-shelled capsules. Alginate beads were cooled to 5 ºC and subsequently dropped using tweezers into a reservoir of molten *n*-eicosane (T_m ~38 ºC) heated to 45 ºC. A thin wax layer forms around the cold bead within seconds,

whereupon the wax-shelled capsule was removed with tweezers. The resulting shell is patchy and leaks. To seal the capsule, *n*-octadecane is used.

Preparation of *n*-eicosane + *n*-octadecane wax-shelled capsules. The capsules with *n*-eicosane wax shells were sealed with *n*-octadecane. *n*-octadecane (T_m ~28 ºC) was melted at 30 ºC and the wax-shelled capsules were dipped in the heated solution for 5 – 10 s. A thin wax layer forms around the cold bead within seconds, whereupon the wax-shelled capsule was removed with tweezers.

Preparation of wax-shelled capsules using filter. A fiberglass mesh sheet was cut in a circle to fit in the bottom of a beaker. Thin wires were attached to the sides for easy removal. A wax solution was heated ~5 ºC above its T_m and the fiberglass mesh was placed at the bottom of the heated solution. The alginate beads were cooled to 5 °C and subsequently dropped using tweezers into the reservoir, landing on the mesh. A thin wax layer forms around the cold bead within seconds. The mesh was lifted out of the solution and the wax-shelled capsules were removed with tweezers.

Preparation of capsules with a chemically crosslinked polymer layer. Ag-containing alginate beads were soaked in a 15 mg/mL solution of the initiator APS for 2 min. The APS-loaded beads were transferred to a second solution containing the monomer DMAA (1 M), crosslinker BIS (2.2 mol% with respect to monomer), TEMED (1.5 mg/mL), and xanthan gum (0.5 to 0.75 wt%). TEMED is an accelerant that allows the polymerization to proceed at room temperature and the xanthan gum increases the solution viscosity so

that the cores remain suspended during the process. Polymerizations were conducted at room temperature for 15 min. The result of the polymerization was a layer of chemically crosslinked DMAA around the alginate cores. The capsules thus formed were washed and stored in DI water.

Preparation of multicompartment capsules (MCCs). First, the internal compartments were prepared as above (these could be alginate beads, wax-shelled capsules or polymer-shelled capsules). These structures were then suspended in an alginate solution (2 wt%) which was then added dropwise through a larger nozzle (typically a transfer pipette with the tip cut off ~5 mm diameter) to a reservoir solution containing 0.5 M of $CaCl_2$ and incubated for 10-20 min. The droplets were thereby converted to MCCs with a typical size being 9 mm.

Optical microscopy. Bright field images of capsules were captured with a Zeiss Axiovert 135 TV microscope. Images were taken using a ×2.5 objective. In some cases, the microscopy was performed with slight under-focus, which helped to clearly define the outlines of the layers and/or the overall capsule.

5.3 Results and Discussion

5.3.1 Synthesis of Wax-Shelled Capsules

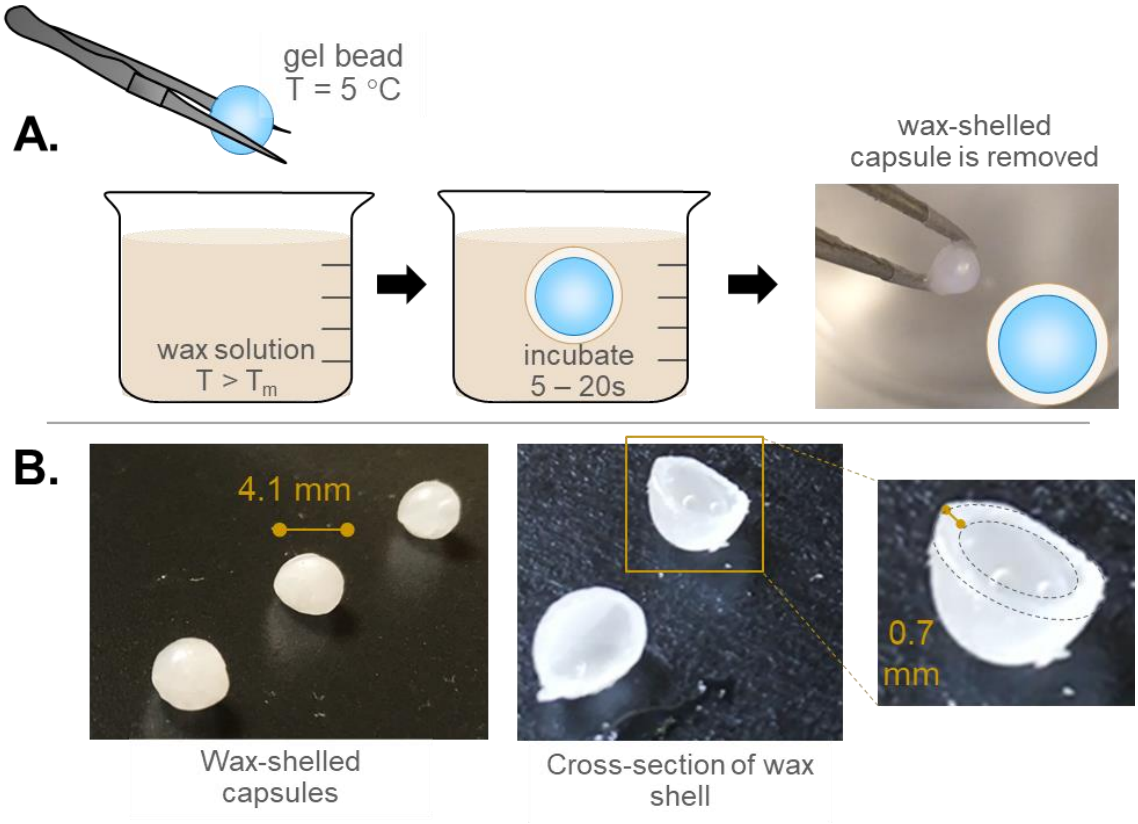

Figure 5.2. Synthesis of wax-shelled capsules. A) A cold gel-bead or liquid droplet (at 5°C) is dropped into molten wax (at a temperature $T > T_m$ of the wax). A wax shell forms within 5 to 20 s. The capsule is then removed using tweezers. **B)** Cross-sections of cut capsules showing their average diameter (4.1 ± 0.1 mm) and shell thickness (0.7 ± 0.2 mm).

The procedure for synthesizing wax-shelled capsules is shown schematically in Figure 5.2A. We begin with spherical gels (~ 4 mm diameter) formed by combining the anionic biopolymer, sodium alginate with divalent Ca^{2+}. The gels are cooled to 5°C and then dropped into molten wax maintained at a temperature above its melting temperature T_m. For example, in the case of paraffin wax (T_m ~ 57°C), it was heated to 65°C. The

temperature difference between the wax and the cold capsule is key to forming the wax shell. The shell forms within 5 to 20 s, and after 20 s, the wax-shelled capsule is removed from solution with tweezers. Cross-sections of these capsules (cut in half) are shown in Figure 5.2B. The wax shell is about 0.7 mm in thickness.

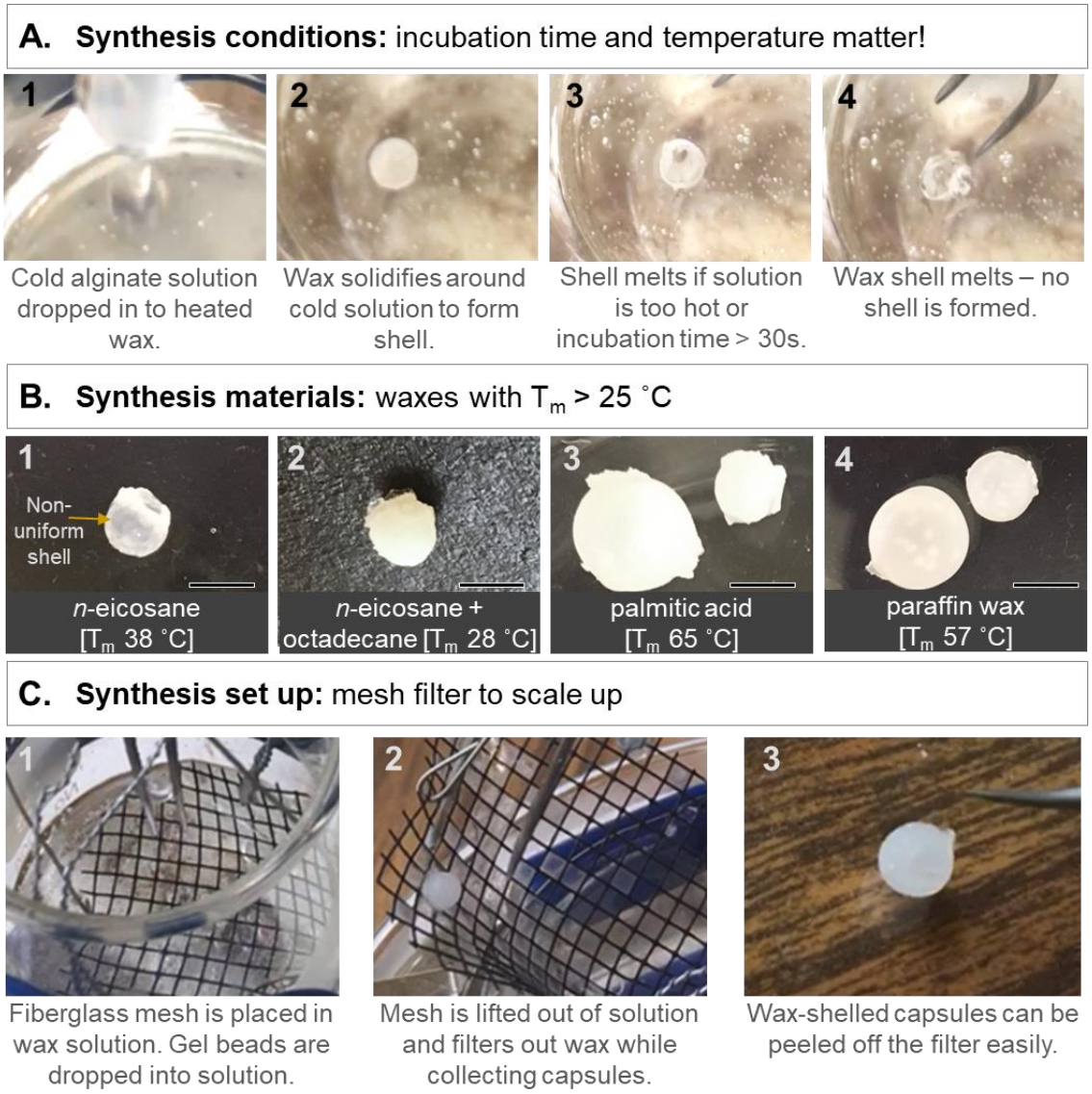

Figure 5.3. Considerations during synthesis of wax-shelled capsules. A) The temperature of the molten (liquid) wax must be above its T_m, but not too high. If the liquid is too hot or if the gel core is incubated in the liquid for too long (> 30 s), the wax shell formed initially will melt and disintegrate. **B)** Shells can be formed with several waxy materials with varying T_m, as shown in the images (scale bars: 4 mm). For short-chain hydrocarbons like *n*-eicosane, a second sealing step with octadecane is necessary. **C)** Several capsules can be coated at once, using a fiberglass mesh to lift out the wax-shelled capsules after incubation.

Figure 5.3 indicates some key considerations during the above synthesis. First, is the concurrent importance of temperature and incubation time. The temperature T of the molten (liquid) wax has to, of course, be higher than the T_m of the wax, but it is better if it was not too much higher. Similarly, it is important to keep the incubation time of the cold gel core in the liquid wax to be 5 to 20 s, but not much more. This point is shown by Figure 5.3A: if $T >> T_m$ or if the incubation time was > 30 s, then the wax shell that was formed initially (Panel 2) melts and disintegrates (Panels 3 and 4).

In addition to paraffin wax, other waxy materials can be used to form the shell, including *n*-eicosane (saturated C_{20} alkane with a T_m of 38 °C) and palmitic acid (acid with a saturated C_{16} tail and a T_m of 65 °C). The shell formed by palmitic acid is uniform and very similar to that formed by paraffin wax. However, the shell of *n*-eicosane (formed at 45°C) is thinner and less uniform. To obtain a leak-proof shell, we subsequently immersed the capsule in octadecane (saturated C_{18} alkane and has a T_m of 28 °C) for 5 s. This second step ensured a leak-proof shell.

We have devised a variation of the technique to enable synthesis of numerous wax-shelled capsules at one time (see Figure 5.3C). For this, a fiberglass mesh with square holes of dimensions 3 mm x 3 mm is placed below the hot molten wax. We drop several cold gel-beads into the liquid wax, thus converting the beads into wax-shelled capsules within a few seconds of incubation. The capsules collect on the mesh, which is then lifted out of the wax, and the capsules are gently removed from the mesh.

Another consideration is regarding the types of core materials that can be encapsulated within a wax-shelled capsule. In addition to alginate gel beads, we can also encapsulate liquids. For example, if a 2 wt% alginate solution cooled to 5 °C is dropped into paraffin wax at 65 °C, a wax shell readily forms around the droplet. When the capsule is cut open, the liquid spills out, indicating that it is indeed unaffected by the shell. One aspect here is the liquid viscosity. If the liquid is slightly viscous, like the above alginate solution, the final capsule is spherical. If the liquid has low viscosity like 0.5 wt% alginate or similar to water, the final capsule is pancake-like.

5.3.2 Properties of Wax-Shelled Capsules

Figure 5.4 shows that the wax shell of the capsules is indeed impermeable to aqueous solutes, both from the outside-in and the inside-out. The capsules in this figure have an alginate core and a shell of paraffin wax. In Figure 5.4A, the capsule is placed in a solution of 10 mM methylene blue (MB) dye for 3 days (Panel 1). When removed and rinsed with DI water, we find that the capsule is colorless, both outside and inside (Panel 3), indicating that no dye molecules are able to diffuse through the wax shell. In Figure 5.4B, the alginate gel-bead is loaded with 10 mM of MB dye prior to encasing the gel with the wax shell. The dye-filled capsule is placed in DI water for 3 days (Panel 1). The surrounding water remains uncolored, indicating that the shell is impermeable and leak-proof. Upon heating the water to 65 °C, the wax shell melts and floats to the water

surface (Panels 2, 3). With the shell removed, the dye in the core gel is now able to diffuse into the solution (Panel 4).

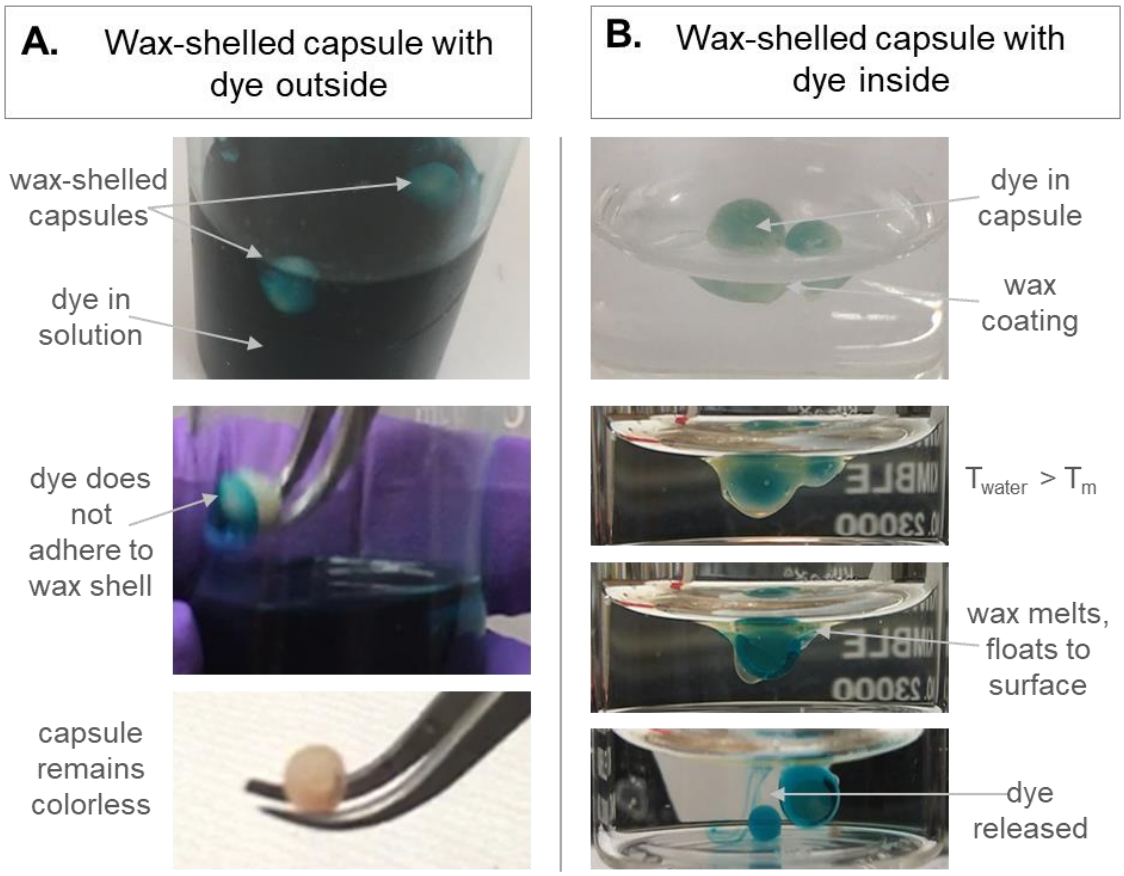

Figure 5.4. Impermeability of the wax shell in the capsules. The capsules have an alginate core and a shell of paraffin wax. **A)** Capsules are left in a solution of 10 mM MB dye for 3 days (Panel 1). When the capsule is removed and rinsed, no dye is found to have penetrated or irreversibly adsorbed to the shell (Panels 2, 3). **B)** Here, 10 mM MB was loaded into the core before creating a wax shell. The dye-loaded capsules are left in water for 3 days. No dye has leaked into the water (Panel 1). When the water is heated to 65 °C, the wax melts and rises to the surface (Panels 2, 3). Dye is then released from the core into the water (Panel 4).

In addition to dyes, hazardous and caustic reagents can also be safely encapsulated in wax-shelled capsules. This includes strong bases and strong acids (Figure

5.5). For the experiments in Figure 5.5A, the alginate gel-beads were soaked in a 2 M NaOH solution for 20 min at 5 °C, and then dropped into paraffin wax to form a shell. The wax-shelled capsule is placed in a solution of 10 mM phenolphthalein in water-ethanol solution (70/30 v/v). Phenolphthalein is an acid/base indicator that turns bright pink at basic pH. Panel 1 shows that there is no leakage of base from the capsule at room temperature. However, when heated above T_m, the wax shell melts and the base diffuses into solution, resulting in a bright pink color (Panels 2, 3). Figure 5.5B shows a similar capsule containing glacial acetic acid in its core and placed in a solution of 10 mM methyl red in ethanol. Again, there is no release at room temperature (Panel 1), but there is release when heated above T_m (Panels 2, 3).

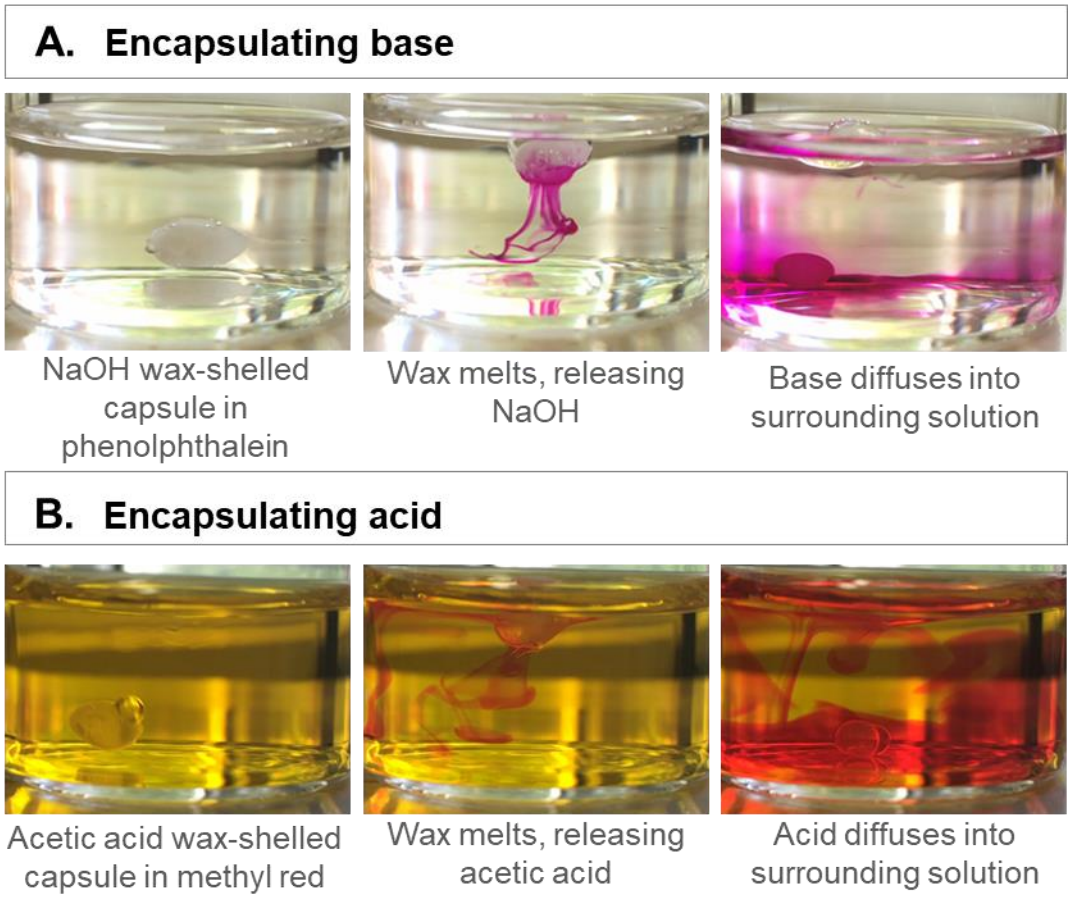

Figure 5.5. Encapsulating acids and bases in wax-shelled capsules. The capsules have an alginate core and a shell of paraffin wax. **A)** Capsule with 2 M NaOH is placed in a solution of 10 mM phenolphthalein. The base remains encapsulated at room temperature (Panel 1), but leaks out (Panels 2, 3) when heated to $T > T_m$ of the wax shell (as evident from the bright pink color). **B)** Capsule with 10 glacial acetic acid is placed in a solution of 10 mM methyl red. The acid remains encapsulated at room temperature (Panel 1), but leaks out (Panels 2, 3) when heated to $T > T_m$ of the wax shell (as evident from the color change from yellow to red).

5.3.3 MCCs with Wax-Shelled Compartments

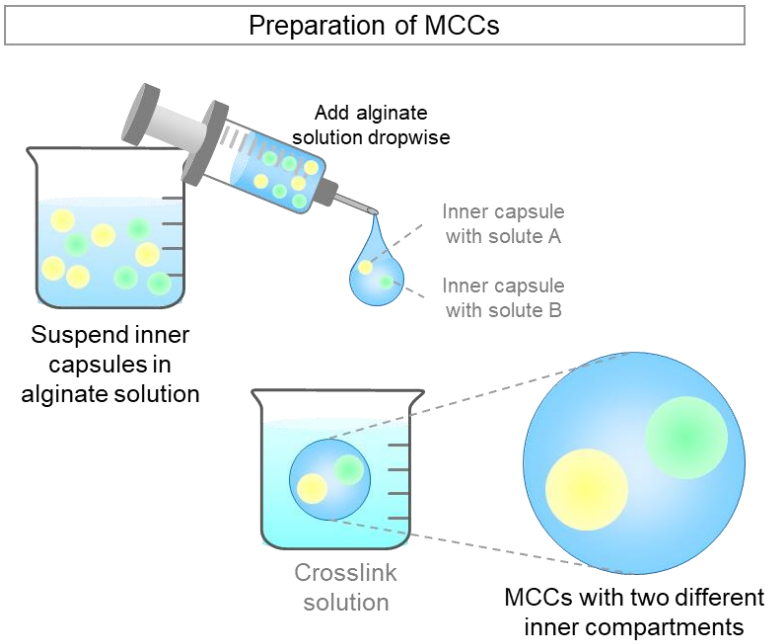

Figure 5.6. Preparation of multicompartment capsules (MCCs). Inner capsules are suspended in an alginate solution, which is added dropwise to a reservoir containing a solution of 0.5 M $CaCl_2$. Upon contact, the droplets are converted into MCCs.

Next, wax-shelled capsules were incorporated into multicompartment capsules (MCCs), as depicted in Figure 5.6. MCCs can have a variety of inner compartments, some or all of which could have wax shells. To make MCCs, the previously synthesized inner capsules are dispersed in a 2 wt% alginate solution. Droplets from this solution are then added to a reservoir solution of 0.5 M $CaCl_2$. This results in the final MCCs, which typically had diameters around 10 mm (the diameters of the inner compartments were typically 3-5 mm).

An initial experiment to illustrate the utility of this approach is shown in Figure 5.7. Here, the MCC has two inner capsules with different wax shells, having a wide

disparity in T_m (Figure 5.7A). Capsule 1 has an alginate gel-core loaded with base (2 M NaOH) and then sealed with *n*-eicosane [T_m ~ 38 °C), followed by a second sealing with octadecane. Capsule 2 is loaded with 10 mM of MB dye and then sealed with paraffin wax (T_m ~ 57 °C). The MCC is placed in a solution of 10 mM phenolphthalein. At 25 °C, both inner capsules are intact, and we see no release of any solute (Figure 5.7A). When the system is heated to 40 °C, the *n*-eicosane shell of Capsule 1 melts and NaOH from Capsule 1 is released into solution (Figure 5.7B). This release is visually indicated by the bright pink color in the solution. At this stage, Capsule 2 remains intact and leak-proof. Next, the temperature is further raised to 65 °C, whereupon the shell of Capsule 2 also melts, and the dye is released into solution. Overall, the MCC in Figure 5.7 is used to demonstrate a step-wise release of encapsulated reagents using two shell materials.

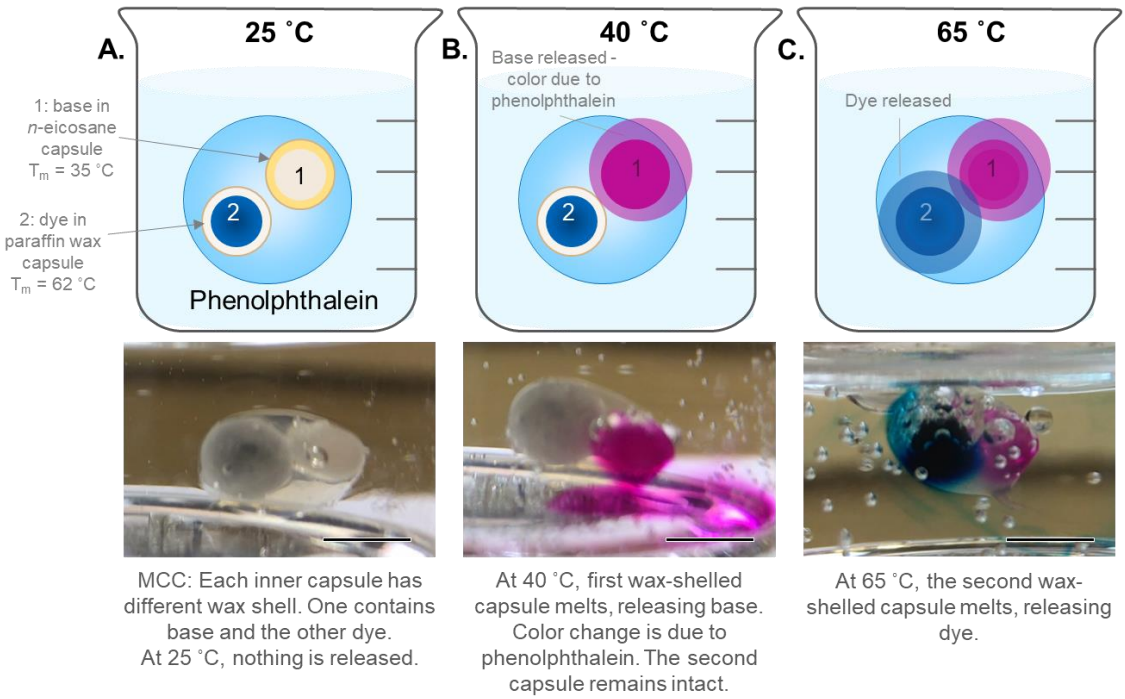

Figure 5.7. Two-step release of solutes from MCCs. The MCC has inner capsules 1 and 2, which have different solutes in their cores and different shell materials. **A)** The MCC is placed in a 10 mM phenolphthalein solution at 25 °C. Both capsules 1 and 2 are intact at this stage. B) At 40 °C, the shell of Capsule 1 melts, releasing NaOH and changing the color of the solution. Capsule 2 remains intact. C) At 65 °C, the shell of Capsule 2 also melts and releases MB dye into solution. Scale bars: 4 mm.

5.3.4 Cascade Processes Using MCCs

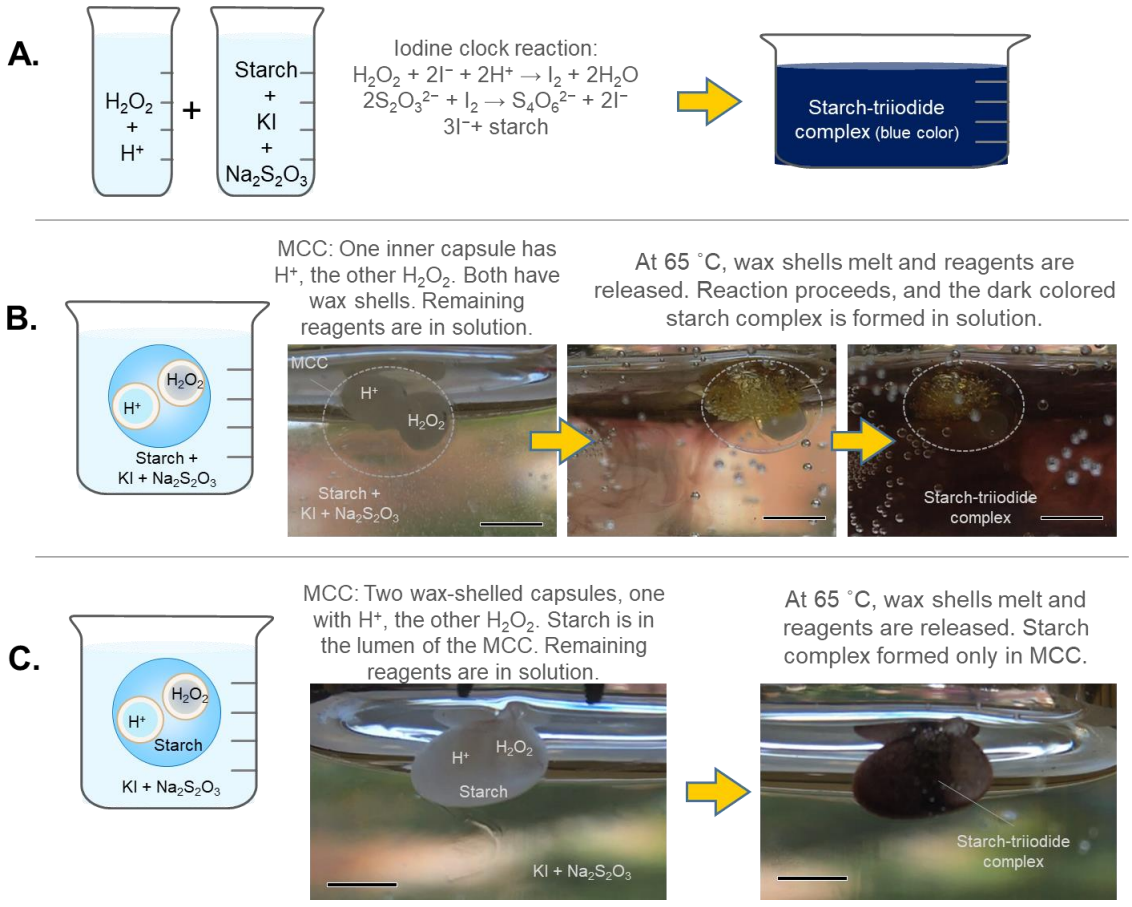

Figure 5.8. Iodine clock reaction implemented in MCCs and triggered by heat. A) The iodine clock reaction used here involves combining two solutions, one with H_2O_2 (30%) + H^+ (glacial acetic acid) and the other containing starch (1 wt%) + KI (1 M) + $Na_2S_2O_3$ (1 M). A starch-triiodide complex forms, resulting in a dark blue color. **B)** This reaction is implemented in an MCC. Inside the MCC are two wax-shelled capsules, one with H_2O_2 and the other with acetic acid. The MCC is placed in a solution of the remaining reagents. At room temperature, no reaction occurs. When the shells melt at 65°C, the reagents are released and the starch complex is formed in the surrounding solution. **C)** A second implementation using a different MCC. The MCC still contains the same inner capsules, but in addition, starch is present in the lumen. When the shells melt at 65°C, the starch complex forms only in the lumen of the MCC. Scale bars: 4 mm.

Next, we demonstrate the use of MCCs to conduct the *iodine clock reaction*, which involves multiple reagents. In the iodine clock reaction, hydrogen peroxide (H_2O_2) reacts with potassium iodide (KI) and acid (H^+) to form iodine (I_2) and water. The iodine then reacts with sodium thiosulfate ($Na_2S_2O_3$) to form a triiodide (I_3^-) ion, which forms a complex with starch resulting in a dark blue color in the solution (Figure 5.8A). We monitor this reaction by observing the color change. The reactions corresponding to this process are shown in Figure 5.8A.

For the first implementation in an MCC (Figure 5.8B), we initially create two paraffin-wax-shelled capsules. In one case, an alginate gel-bead is loaded with 30% H_2O_2 and then covered with the wax shell. In a second case, an alginate gel is loaded with glacial acetic acid and then covered by the wax shell. These were then incorporated into an MCC as shown in Figure 5.6. The MCC was placed in a solution containing KI (1 M), $Na_2S_2O_3$ (1 M) and starch (1 wt%). At room temperature, no reaction occurs. When heated to 65 °C, the wax shells melt, releasing H_2O_2 and H^+, thus starting the reaction. The surrounding solution changes color within 5 min as the starch complex is formed.

A variation of this experiment is shown with a second MCC (Figure 5.8C). In this case, the MCC contains the same inner capsules as in Figure 5.8B. In addition, we incorporate starch into the lumen of the MCC. To do this, we dissolved starch (1 wt%) along with the 2 wt% alginate in the feed solution of Figure 5.6 before dropping into the Ca^{2+}. The MCC now contains three reagents, H_2O_2, H^+, and starch. Note that the starch is a polysaccharide of molecular weight 100,000 Da, and due to its large size, it will not

diffuse out through the MCC even though there is no wax shell. The MCC is then placed in a solution containing the other reagents, i.e., KI (1 M) and $Na_2S_2O_3$ (1 M). When heated to 65 °C, the wax shells melt, starting the reaction, but we observe the color change due to the starch-triiodide complex only within the MCC.

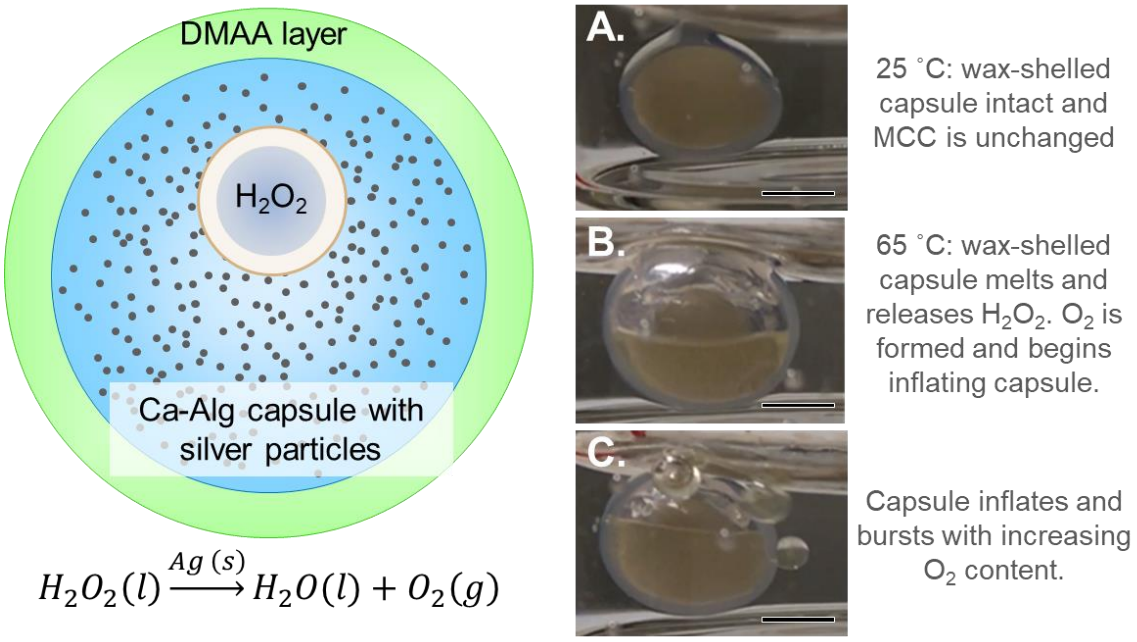

Figure 5.9. Emergent properties of an MCC (inflation and rupture) triggered by heat. The MCC design is shown on the left. It contains a wax-shelled compartment loaded with 30% H_2O_2, 10 wt% Ag particles suspended in the capsule lumen, and an elastic layer of crosslinked polymer (DMAA) around the MCC. **A)** The MCC is placed in water at 25°C and there is no reaction. **B)** When heated to 65 °C, the wax shell melts and H_2O_2 is released. The decomposition of H_2O_2 into O_2 gas is catalyzed by the Ag particles. In turn, the released gas causes the capsule to inflate. **C)** The inflation continues until the shell ruptures, as seen from the release of gas bubbles into solution. Scale bars in the images are 4 mm.

Finally, we design an MCC that shows the emergent properties described in Chapter 3 (inflation and rupture), but only when triggered by heat. The design of the

MCC is shown in Figure 5.9. The inner compartment is an alginate gel-bead loaded with 30% H_2O_2 and then covered with a shell of paraffin wax. The H_2O_2 will serve as the chemical fuel for the inflation process. Next, we introduce 10 wt% of silver (Ag) microparticles into the lumen of the MCC, as was done previously in Figure 5.8C. The Ag will act to catalyze the decompostion of H_2O_2 to water and oxygen (O_2) gas. Lastly, to get the capsule to inflate, we must further modify this MCC to add an elastic layer of chemically-crosslinked polymer around it. This is done using the "inside-out" method previously described in Chapters 3 and 4. Here, the layer is a hydrogel of the acrylamide derivative DMAA (1 M), crosslinked with 2.2 mol% BIS.

The behavior of the above MCC is illustrated by the images in Figure 5.9. First, at room temperature, the MCC placed in water is inactive and its inner compartment is intact (Figure 5.9A). Next, the system is heated to 65 °C. This melts the wax shell and releases the H_2O_2 into the lumen. The Ag-catalyzed reaction produces O_2 gas, which in turn causes the capsule to inflate (Figure 5.9B). As shown in Chapter 3, the gas gets trapped in between the MCC lumen and the DMAA layer, thereby stretching the outer polymer network and leading to inflation. Utimately, the stress in the polymer layer becomes too great and this leads to the shell being ruptured (Figure 5.9C). Bubbles of O_2 then escape into the surrounding solution. Thus, we have shown that it is possible to trigger inflation of the MCC in water using heat. The chemical fuel needed for inflation is included in the MCC; thus, inflation will occur regardless of the composition of the external solution.

5.4 Conclusions

The focus of this Chapter was on imparting new "emergent" properties to capsules upon the application of a thermal trigger. To achieve this, we have shown a way to perfectly encapsulate solutes in a capsule core until the capsule is heated. The key to this property was to create a wax shell around a liquid or gel core, and we have shown a simple method for doing this. A thin wax shell reliably formed within seconds when there was a sufficient temperature differential between a cold core and the surrounding molten wax. Using this method, we have successfully encapsulated a variety of solutes in the capsule cores, including strong acids, bases, and dyes. There was no release of encapsulated materials at room temperature, but when heat was applied and the wax shell melted, the solutes were able to diffuse out of the cores. Wax-shelled capsules were then used as inner compartments in MCCs. This enabled us to carry out multi-step reactions such as the iodine clock reaction upon a temperature trigger. Finally, we encapsulated a chemical fuel, H_2O_2 in a wax-shelled capsule, and used this as an inner compartment in an MCC with Ag particles in the lumen and a crosslinked polymer as the outer shell. Under a thermal trigger, the fuel was released into the lumen, and the Ag-catalyzed decomposition of H_2O_2 produced O_2 gas, which caused the MCC to inflate and rupture.

Chapter 6

Conclusions and Recommendations

6.1 Project Summary and Principal Contributions

In this dissertation, we have presented various types of polymer capsules that utilize internal chemical reactions to produce emergent capsule properties. Specifically, we created inflating and ejecting capsules, solute-release capsules, and wax coated capsules. These capsules are synthesized simply with inexpensive, easily accessible materials. Additionally, we can precisely tune the properties of these capsules by altering the materials utilized during synthesis.

In Chapter 3, we present our bioinspired inflating and ejecting capsules, mimicking the behavior of the nematocyst. We utilize our "inside-out" technique to create an elastic polymer layer around our core capsule that contains our silver (Ag) catalyst. When placed in the presence of a chemical fuel H_2O_2, our capsules produce oxygen gas, which causes the overall capsule to inflate and eventually eject the capsule core. By changing the polymer layer around the capsules, we experience different rupture properties from violent, core-ejecting rupture to a gentler deflation. Altering other synthesis parameters like increasing the amount of crosslinker in the polymer shell or varying the concentration of our reagents, allows us the control the inflation size and rupture times of the capsules. We also demonstrate how these capsules are effective using

different chemical reactions (sodium bicarbonate or sodium carbonate and acid) to produce gas.

In Chapter 4, we focus on two new types of solute-release from our layered capsules: active continuous release and active pulse release. Here, we synthesize layered capsules and subsequently load them with dye before introducing them to the chemical fuel. When the dye-loaded capsules are not introduced to the chemical fuel and are instead placed in water, we observe a diffusive release of the dye into solution. However, when the capsules are placed in the chemical fuel, active continuous release is observed as the chemical reaction pumps the dye out of the capsule interior. This is observed with all tested dyes apart from one. When our Ag-cored capsules are loaded with Rhoadmine 6G (R6G) dye, they exhibit pulsed release of solute. Using video analysis, we were able to track quantify the pulsing length, intensity, and frequency from various types of capsules. Altering our capsule synthesis once again allows us to tune the pulsing properties of these capsules. Interestingly, this pulsing only happens when both silver and R6G are present, indicating interaction between the two substances.

In Chapter 5, we introduce a technique to synthesize wax-coated capsules and the utility of these capsules for multi-reagent reactions. To create these capsules, we drop cold alginate cores or solution into a warm wax solution to coat and create wax capsules. These capsules can be synthesized with several wax materials including paraffin wax, n-

eicosane, and palmitic acid. The wax capsules are impermeable and do not release internal contents until the wax coating melts. Hazardous materials can also be encapsulated with no leakage and released upon demand. To show the utility of this easy encapsulation, we incorporated the wax capsules in MCCs. Using the MCCs, we show a two-step release with one internal capsule coated with a low T_m and the other with a slightly higher T_m. Slowly increasing the temperature of the solution shows how one internal container melts and releases contents before the other container. We then demonstrate a multi-reagent reaction, the iodine clock reaction, using wax capsules in the MCC. In one case, we produce our final product in the surrounding solution and in the other, we demonstrate isolation of the product in the lumen of the MCC. Finally, we use these MCCs for our inflating capsules from Chapter 3, showing how this model can be used to induce emergent behaviors.

6.2 Recommendations for Future Work

6.2.1 Ejecting Barbs from Inflating and Ejecting Capsules

Chapter 3 describes the design and creation of nematocyst-like capsules, in the sense that our capsules eject the internal contents of the capsule by increasing pressure. However, nematocysts expel a barded tubule what has the capability of penetrating skin. Can we alter our ejecting capsules to shoot out barbs? If so, this could be a potential use for transdermal drug delivery. To do this, our internal core would contain a barded or sharp particle. This is possible however, our current system does not allow for the control over directionality. Control over directionality can be achieved several different ways. We can create a weakness in our capsule shell. As pressure builds in the capsule, a weak point give way first, allowing the capsule to rupture and eject from that point. We can also adjust the shape of our capsules to add directionality. Synthesizing a teardrop or cylindrical core might allow us to localize the Ag catalyst in one spot and rupture in one direction. Investigating these different capsules could lead to a direct application for these nematocyst-like capsules.

6.2.2 Inflation and Ejection via Other Stimuli

Along the same lines, we would also like to extend the inflation and ejection to reactions other than the production of gas. The nematocyst builds pressure in the organelle by increasing the osmotic pressure. The gel network in the organelle is composed of poly-y-glutamate and cations. Upon activation of an external trigger, water

rushes into the sac and frees the ions in solution. This causes a drastic osmotic pressure increase, which results in evacuation of a barbed tubule. Are we able to replicate this pressure increase using a decomposition reaction triggered by light or pH? A positively charged surfactant, p-octyloxydiphenyliodonium hexafluoroantimonate (ODPI), is able to interact with negatively charged alginate chains to create stable polymer capsules. Upon exposure to UV light, ODPI degrades to uncharged, hydrophobic byproducts and the capsules fall apart. This increase in molecules could lead to a large enough osmotic pressure gradient to eject a core in layered polymer capsules.

6.2.3 Extend Active Pulsing Release to Other Systems

In Chapter 4, we discuss the synthesis of solute-release capsules that exhibit pulsing and have analyzed this pulsing using video analysis. We deduced that this pulsing only occurs when our capsules are synthesized with silver in the core and are loaded with Rhodamine 6G. Here, we propose to further investigate this mechanism so we can extend the system using other solutes. We believe the pulsing is a direct result of the coordination of the Rhodamine 6G molecules on the silver microparticles, which has been studied previously. To test this theory, we propose loading our capsules with other materials that adhere to the surface of silver. It has been documented that dopamine, melamine, and pyronin Y also coordinate on the silver surface. We can load our silver-cored capsules with these materials and place them in H_2O_2. If they also pulse, it supports our pulsing theory. We can extend our reaction to platinum core capsules also, still using H_2O_2 as a chemical fuel, and utilize molecules that coordinate to the platinum surface.

Understanding this pulsing mechanism could be advantageous to expanding the applications of this discovery.

References

[1] Bonabeau, E.; Dessalles, J.-L.; Grumbach, A., *Characterizing emergent phenomena (2): a conceptual framework*. 1995.

[2] Hillis, W. D. C. F. p. d. W., Intelligence as an Emergent Behavior; Or, the Songs of Eden. *Daedalus* **1988,** *117* (1), 175-189.

[3] Gibb, B. C., Reaching out to complexity. *Nature Chemistry* **2009,** *1*, 252.

[4] Groff, R., *Revitalizing Causality: Realism about Causality in Philosophy and Social Science*. Taylor & Francis: 2007.

[5] Benner, S. A.; Sismour, A. M., Synthetic biology. *Nature Reviews Genetics* **2005,** *6*, 533.

[6] Oliveira, P. S.; Rico-Gray, V.; Castillo-Guevara, C. D.-C. a. C., Interaction between ants, extrafloral nectaries and insect herbivores in Neotropical coastal sand dunes: herbivore deterrence by visiting ants increases fruit set in Opuntia stricta (Cactaceae). *Functional Ecology* **1999,** *13* (5), 623-631.

[7] Werner, B. T., Complexity in Natural Landform Patterns. *Science* **1999,** *284* (5411), 102.

[8] Lloyd, S.; Coveney, P.; Highfield, R.; Holland, J. H.; Kauffman, S.; Johnson, G. C. F. p. d. M. A. Y., Complexity Simplified. *Scientific American* **1996,** *274* (5), 104-108.

[9] Altschuler, S. J.; Angenent, S. B.; Wang, Y.; Wu, L. F., On the spontaneous emergence of cell polarity. *Nature* **2008,** *454*, 886.

[10] Nadell, C. D.; Foster, K. R.; Xavier, J. B., Emergence of Spatial Structure in Cell Groups and the Evolution of Cooperation. *PLOS Computational Biology* **2010,** *6* (3), e1000716.

[11] Chaffey, N., Alberts, B., Johnson, A., Lewis, J., Raff, M., Roberts, K. and Walter, P. Molecular biology of the cell. 4th edn. *Annals of Botany* **2003,** *91* (3), 401-401.

[12] de Hoog, H.-P. M.; Nallani, M.; Tomczak, N., Self-assembled architectures with multiple aqueous compartments. *Soft Matter* **2012,** *8* (17), 4552-4561.

[13] Deng, N.-N.; Yelleswarapu, M.; Huck, W. T. S., Monodisperse Uni- and Multicompartment Liposomes. *Journal of the American Chemical Society* **2016,** *138* (24), 7584-7591.

[14] Hosta-Rigau, L.; Chung, S. F.; Postma, A.; Chandrawati, R.; Städler, B.; Caruso, F., Capsosomes with "Free-Floating" Liposomal Subcompartments. *Advanced Materials* **2011,** *23* (35), 4082-4087.

[15] Kim, J.; Arifin, D. R.; Muja, N.; Kim, T.; Gilad, A. A.; Kim, H.; Arepally, A.; Hyeon, T.; Bulte, J. W. M., Multifunctional Capsule-in-Capsules for Immunoprotection and Trimodal Imaging. *Angewandte Chemie International Edition* **2011,** *50* (10), 2317-2321.

[16] Kisak, E. T.; Coldren, B.; Zasadzinski, J. A., Nanocompartments Enclosing Vesicles, Colloids, and Macromolecules via Interdigitated Lipid Bilayers. *Langmuir* **2002,** *18* (1), 284-288.

[17] Perro, A.; Nicolet C Fau - Angly, J.; Angly J Fau - Lecommandoux, S.; Lecommandoux S Fau - Le Meins, J.-F.; Le Meins Jf Fau - Colin, A.; Colin, A., Mastering a double emulsion in a simple co-flow microfluidic to generate complex polymersomes. (1520-5827 (Electronic)).

[18] Chandrawati, R.; van Koeverden, M. P.; Lomas, H.; Caruso, F., Multicompartment Particle Assemblies for Bioinspired Encapsulated Reactions. *The Journal of Physical Chemistry Letters* **2011,** *2* (20), 2639-2649.

[19] Delcea, M.; Yashchenok, A.; Videnova, K.; Kreft, O.; Möhwald, H.; Skirtach, A. G., Multicompartmental Micro- and Nanocapsules: Hierarchy and Applications in Biosciences. *Macromolecular Bioscience* **2010,** *10* (5), 465-474.

[20] Fu, Z.; Ochsner Ma Fau - de Hoog, H.-P. M.; de Hoog Hp Fau - Tomczak, N.; Tomczak N Fau - Nallani, M.; Nallani, M., Multicompartmentalized polymersomes for selective encapsulation of biomacromolecules. (1364-548X (Electronic)).

[21] Gaitzsch, J.; Huang, X.; Voit, B., Engineering Functional Polymer Capsules toward Smart Nanoreactors. *Chemical Reviews* **2016,** *116* (3), 1053-1093.

[22] Hammer, D. A.; Kamat, N. P., Towards an artificial cell. *FEBS Lett* **2012,** *586* (18), 2882-90.

[23] Hosta-Rigau, L.; Shimoni, O.; Städler, B.; Caruso, F., Advanced Subcompartmentalized Microreactors: Polymer Hydrogel Carriers Encapsulating Polymer Capsules and Liposomes. *Small* **2013,** *9* (21), 3573-3583.

[24] Kreft, O.; Skirtach, A. G.; Sukhorukov, G. B.; Möhwald, H., Remote Control of Bioreactions in Multicompartment Capsules. *Advanced Materials* **2007,** *19* (20), 3142-3145.

[25] LoPresti, C.; Lomas, H.; Massignani, M.; Smart, T.; Battaglia, G., Polymersomes: nature inspired nanometer sized compartments. *Journal of Materials Chemistry* **2009,** *19* (22), 3576-3590.

[26] Lu, A. X.; Oh, H.; Terrell, J. L.; Bentley, W. E.; Raghavan, S. R., A new design for an artificial cell: polymer microcapsules with addressable inner compartments that can harbor biomolecules, colloids or microbial species. *Chemical Science* **2017,** *8* (10), 6893-6903.

[27] Marguet, M.; Bonduelle, C.; Lecommandoux, S., Multicompartmentalized polymeric systems: towards biomimetic cellular structure and function. *Chemical Society Reviews* **2013,** *42* (2), 512-529.

[28] Peters, R. J. R. W.; Louzao, I.; van Hest, J. C. M., From polymeric nanoreactors to artificial organelles. *Chemical Science* **2012,** *3* (2), 335-342.

[29] Stadler, B.; Price, A. D.; Chandrawati, R.; Hosta-Rigau, L.; Zelikin, A. N.; Caruso, F., Polymer hydrogel capsules: en route toward synthetic cellular systems. *Nanoscale* **2009,** *1* (1), 68-73.

[30] Städler, B.; Price, A. D.; Zelikin, A. N., A Critical Look at Multilayered Polymer Capsules in Biomedicine: Drug Carriers, Artificial Organelles, and Cell Mimics. *Advanced Functional Materials* **2011,** *21* (1), 14-28.

[31] Tanner, P.; Egli, S.; Balasubramanian, V.; Onaca, O.; Palivan, C. G.; Meier, W., Can polymeric vesicles that confine enzymatic reactions act as simplified organelles? *FEBS Lett* **2011,** *585* (11), 1699-706.

[32] van Dongen, S. F.; Nallani M Fau - Cornelissen, J. J. L. M.; Cornelissen Jj Fau - Nolte, R. J. M.; Nolte Rj Fau - van Hest, J. C. M.; van Hest, J. C., A three-enzyme cascade reaction through positional assembly of enzymes in a polymersome nanoreactor. (1521-3765 (Electronic)).

[33] Zelikin, A. N.; Price, A. D.; Städler, B., Poly (Methacrylic Acid) Polymer Hydrogel Capsules: Drug Carriers, Sub-compartmentalized Microreactors, Artificial Organelles. *Small* **2010,** *6* (20), 2201-2207.

[34] Peters, R. J.; Marguet, M.; Marais, S.; Fraaije, M. W.; van Hest, J. C.; Lecommandoux, S., Cascade reactions in multicompartmentalized polymersomes. *Angew Chem Int Ed Engl* **2014,** *53* (1), 146-50.

[35] Lu, A. X.; Liu, Y.; Oh, H.; Gargava, A.; Kendall, E.; Nie, Z.; DeVoe, D. L.; Raghavan, S. R., Catalytic Propulsion and Magnetic Steering of Soft, Patchy Microcapsules: Ability to Pick-Up and Drop-Off Microscale Cargo. *ACS Applied Materials & Interfaces* **2016,** *8* (24), 15676-15683.

[36] Li, L.; Wang, J.; Li, T.; Song, W.; Zhang, G., Hydrodynamics and propulsion mechanism of self-propelled catalytic micromotors: model and experiment. *Soft Matter* **2014,** *10* (38), 7511-7518.

[37] Manjare, M.; Yang, B.; Zhao, Y. P., Bubble Driven Quasioscillatory Translational Motion of Catalytic Micromotors. *Physical Review Letters* **2012,** *109* (12), 128305.

[38] Orozco, J.; Cortés, A.; Cheng, G.; Sattayasamitsathit, S.; Gao, W.; Feng, X.; Shen, Y.; Wang, J., Molecularly Imprinted Polymer-Based Catalytic Micromotors for Selective Protein Transport. *Journal of the American Chemical Society* **2013,** *135* (14), 5336-5339.

[39] Zhao, G.; Sanchez, S.; Schmidt, O. G.; Pumera, M., Poisoning of bubble propelled catalytic micromotors: the chemical environment matters. *Nanoscale* **2013,** *5* (7), 2909-2914.

[40] Rohen, J. W.; Yokochi, C.; Lütjen-Drecoll, E., *Color Atlas of Anatomy: A Photographic Study of the Human Body*. Lippincott Williams & Wilkins: 2006.

[41] Akbarzadeh, A.; Rezaei-Sadabady, R.; Davaran, S.; Joo, S. W.; Zarghami, N.; Hanifehpour, Y.; Samiei, M.; Kouhi, M.; Nejati-Koshki, K., Liposome: classification, preparation, and applications. *Nanoscale Res Lett* **2013,** *8* (1), 102.

[42] Al-Jamal, W. T.; Kostarelos, K., Construction of nanoscale multicompartment liposomes for combinatory drug delivery. *International Journal of Pharmaceutics* **2007,** *331* (2), 182-185.

[43] Solovev, A. A.; Sanchez, S.; Schmidt, O. G., Collective behaviour of self-propelled catalytic micromotors. *Nanoscale* **2013,** *5* (4), 1284-1293.

[44] Mori, K.; Yoshioka, N.; Kondo, Y.; Takeuchi, T.; Yamashita, H., Catalytically active, magnetically separable, and water-soluble FePt nanoparticles modified with cyclodextrin for aqueous hydrogenation reactions. *Green Chemistry* **2009,** *11* (9), 1337-1342.

[45] Kikuchi, A.; Okano, T., Pulsatile drug release control using hydrogels. *Advanced Drug Delivery Reviews* **2002,** *54* (1), 53-77.

[46] Sriamornsak, P.; Kennedy, R. A., Effect of sodium fluorescein on release characteristics of a macromolecule from calcium alginate gel beads. *Carbohydrate Polymers* **2011,** *84* (3), 1208-1212.

[47] Javvaji, V.; Baradwaj, A. G.; Payne, G. F.; Raghavan, S. R., Light-Activated Ionic Gelation of Common Biopolymers. *Langmuir* **2011,** *27* (20), 12591-12596.

[48] Arya, C.; Oh, H.; Raghavan, S. R., "Killer" Microcapsules That Can Selectively Destroy Target Microparticles in Their Vicinity. *ACS Applied Materials & Interfaces* **2016,** *8* (43), 29688-29695.

[49] Bartkowiak, A.; Hunkeler, D., Alginate−Oligochitosan Microcapsules: A Mechanistic Study Relating Membrane and Capsule Properties to Reaction Conditions. *Chemistry of Materials* **1999,** *11* (9), 2486-2492.

[50] Ghaffarian, R.; Pérez-Herrero, E.; Oh, H.; Raghavan, S. R.; Muro, S., Chitosan–Alginate Microcapsules Provide Gastric Protection and Intestinal Release of ICAM-1-Targeting Nanocarriers, Enabling GI Targeting In Vivo. *Advanced Functional Materials* **2016,** *26* (20), 3382-3393.

[51] Gupta, A.; Terrell, J. L.; Fernandes, R.; Dowling, M. B.; Payne, G. F.; Raghavan, S. R.; Bentley, W. E., Encapsulated fusion protein confers "sense and respond" activity to chitosan–alginate capsules to manipulate bacterial quorum sensing. *Biotechnology and Bioengineering* **2013,** *110* (2), 552-562.

[52] Sundaramurthy, A.; Sundramoorthy, A. K., Polyelectrolyte capsules preloaded with interconnected alginate matrix: An effective capsule system for encapsulation and release of macromolecules. *International Journal of Biological Macromolecules* **2017**.

[53] Zargar, A.; Quan, D. N.; Abutaleb, N.; Choi, E.; Terrell, J. L.; Payne, G. F.; Bentley, W. E., Constructing 'quantized quorums' to guide emergent

phenotypes through quorum quenching capsules. LID - 10.1002/bit.26080 [doi]. (1097-0290 (Electronic)).

[54] Dowling, M. B.; Bagal, A. S.; Raghavan, S. R., Self-Destructing "Mothership" Capsules for Timed Release of Encapsulated Contents. *Langmuir* **2013,** *29* (25), 7993-7998.

[55] Jiang, K.; Lu, A. X.; Dimitrakopoulos, P.; DeVoe, D. L.; Raghavan, S. R., Microfluidic generation of uniform water droplets using gas as the continuous phase. *Journal of Colloid and Interface Science* **2015,** *448*, 275-279.

[56] Zarket, B. C.; Raghavan, S. R., Onion-like multilayered polymer capsules synthesized by a bioinspired inside-out technique. *Nature Communications* **2017,** *8* (1), 193.

[57] Kisak, E. T.; Coldren, B.; Evans, C. A.; Zasadzinski, C. B. a. J. A., The Vesosome - A Multicompartment Drug Delivery Vehicle. *Current Medicinal Chemistry* **2004,** *11* (2), 199-219.

[58] Bordi, F.; Cametti, C.; Sennato, S.; Diociaiuti, M., Direct Evidence of Multicompartment Aggregates in Polyelectrolyte-Charged Liposome Complexes. *Biophysical Journal* **2006,** *91* (4), 1513-1520.

[59] Paleos, C. M.; Tsiourvas, D., Interaction between complementary liposomes: a process leading to multicompartment systems formation. *Journal of Molecular Recognition* **2006,** *19* (1), 60-67.

[60] Chandrawati, R.; Caruso, F., Biomimetic Liposome- and Polymersome-Based Multicompartmentalized Assemblies. *Langmuir* **2012,** *28* (39), 13798-13807.

[61] Sorrell, I.; Shipley, R. J.; Hearnden, V.; Colley, H. E.; Thornhill, M. H.; Murdoch, C.; Webb, S. D., Combined mathematical modelling and experimentation to predict polymersome uptake by oral cancer cells. *Nanomedicine: Nanotechnology, Biology and Medicine* **2014,** *10* (2), 339-348.

[62] Marchenko, I.; Yashchenok, A.; Borodina, T.; Bukreeva, T.; Konrad, M.; Möhwald, H.; Skirtach, A., Controlled enzyme-catalyzed degradation of polymeric capsules templated on CaCO3: Influence of the number of LbL layers, conditions of degradation, and disassembly of multicompartments. *Journal of Controlled Release* **2012,** *162* (3), 599-605.

[63] Blandino, A.; Macías, M.; Cantero, D., Formation of calcium alginate gel capsules: Influence of sodium alginate and CaCl2 concentration on gelation kinetics. *Journal of Bioscience and Bioengineering* **1999,** *88* (6), 686-689.

[64] De Geest, B. G.; Stubbe, B. G.; Jonas, A. M.; Van Thienen, T.; Hinrichs, W. L. J.; Demeester, J.; De Smedt, S. C., Self-Exploding Lipid-Coated Microgels. *Biomacromolecules* **2006,** *7* (1), 373-379.

[65] De Geest, B. G.; Skirtach, A. G.; De Beer, T. R. M.; Sukhorukov, G. B.; Bracke, L.; Baeyens, W. R. G.; Demeester, J.; De Smedt, S. C., Stimuli-Responsive Multilayered Hybrid Nanoparticle/Polyelectrolyte Capsules. *Macromolecular Rapid Communications* **2007,** *28* (1), 88-95.

[66] De Geest, B. G.; De Koker, S.; Immesoete, K.; Demeester, J.; De Smedt, S. C.; Hennink, W. E., Self-Exploding Beads Releasing Microcarriers. *Advanced Materials* **2008,** *20* (19), 3687-3691.

[67] De Geest, B. G.; De Koker, S.; Demeester, J.; De Smedt, S. C.; Hennink, W. E., Pulsed in vitro release and in vivo behavior of exploding microcapsules. *Journal of Controlled Release* **2009,** *135* (3), 268-273.

[68] De Geest, B. G.; De Koker, S.; Demeester, J.; De Smedt, S. C.; Hennink, W. E., Self-exploding capsules. *Polymer Chemistry* **2010,** *1* (2), 137-148.

[69] De Koker, S.; Lambrecht, B. N.; Willart, M. A.; van Kooyk, Y.; Grooten, J.; Vervaet, C.; Remon, J. P.; De Geest, B. G., Designing polymeric particles for antigen delivery. *Chemical Society Reviews* **2011,** *40* (1), 320-339.

[70] De Koker, S.; Hoogenboom, R.; De Geest, B. G., Polymeric multilayer capsules for drug delivery. *Chemical Society Reviews* **2012,** *41* (7), 2867-2884.

[71] G., D. G. B.; Stefaan, D. K.; Kristof, I.; Jo, D.; C., D. S. S.; E., H. W., Self-Exploding Beads Releasing Microcarriers. *Advanced Materials* **2008,** *20* (19), 3687-3691.

[72] De Cock, L. J.; De Koker, S.; De Geest, B. G.; Grooten, J.; Vervaet, C.; Remon, J. P.; Sukhorukov, G. B.; Antipina, M. N., Polymeric Multilayer Capsules in Drug Delivery. *Angewandte Chemie International Edition* **2010,** *49* (39), 6954-6973.

[73] Wainwright, P.; Turingan, R., *Evolution of Pufferfish Inflation Behavior*. 1997; p 506.

[74] Ayalon, A.; Shichor, I.; Tal, Y.; Lotan, T., Immediate topical drug delivery by natural submicron injectors. *International Journal of Pharmaceutics* **2011,** *419* (1), 147-153.

[75] Nüchter, T.; Benoit, M.; Engel, U.; Özbek, S.; Holstein, T. W., Nanosecond-scale kinetics of nematocyst discharge. *Current Biology* **2006,** *16* (9), R316-R318.

[76] Özbek, S.; Balasubramanian, P. G.; Holstein, T. W., Cnidocyst structure and the biomechanics of discharge. *Toxicon* **2009,** *54* (8), 1038-1045.

[77] Özbek, S., The cnidarian nematocyst: a miniature extracellular matrix within a secretory vesicle. *Protoplasma* **2011,** *248* (4), 635-640.

[78] Park, S.; Capelin, D.; Piriatinskiy, G.; Lotan, T.; Yossifon, G., Dielectrophoretic characterization and isolation of jellyfish stinging capsules. *ELECTROPHORESIS* **2017,** *38* (16), 1996-2003.

[79] Park, S.; Piriatinskiy, G.; Zeevi, D.; Ben-David, J.; Yossifon, G.; Shavit, U.; Lotan, T., The nematocyst's sting is driven by the tubule moving front. *Journal of The Royal Society Interface* **2017,** *14* (128).

[80] Szczepanek, S.; Cikala, M.; David, C. N., Poly-γ-glutamate synthesis during formation of nematocyst capsules in Hydra. *Journal of Cell Science* **2002,** *115* (4), 745.

[81] Weber, J., Nematocysts (stinging capsules of Cnidaria) as Donnan-potential-dominated osmotic systems. (0014-2956 (Print)).

[82] Weber, J., Poly(gamma-glutamic acid)s are the major constituents of nematocysts in Hydra (Hydrozoa, Cnidaria). (0021-9258 (Print)).

[83] Yue, Y.; Yu, H.; Li, R.; Xing, R.; Liu, S.; Li, K.; Wang, X.; Chen, X.; Li, P., Biochemical and kinetic evaluation of the enzymatic toxins from two stinging scyphozoans Nemopilema nomurai and Cyanea nozakii. *Toxicon* **2017,** *125*, 1-12.

[84] Tal, Y.; Ayalon, A.; Sharaev, A.; Kazir, Z.; Brekhman, V.; Lotan, T., Continuous Drug Release by Sea Anemone Nematostella vectensis Stinging Microcapsules. *Marine Drugs* **2014,** *12* (2), 734-745.

[85] Ibele, M. E.; Wang, Y.; Kline, T. R.; Mallouk, T. E.; Sen, A., Hydrazine Fuels for Bimetallic Catalytic Microfluidic Pumping. *Journal of the American Chemical Society* **2007,** *129* (25), 7762-7763.

[86] Kline, T. R.; Paxton, W. F.; Wang, Y.; Velegol, D.; Mallouk, T. E.; Sen, A., Catalytic Micropumps: Microscopic Convective Fluid Flow and Pattern Formation. *Journal of the American Chemical Society* **2005,** *127* (49), 17150-17151.

[87] Solovev, A. A.; Sanchez, S.; Mei, Y.; Schmidt, O. G., Tunable catalytic tubular micro-pumps operating at low concentrations of hydrogen peroxide. *Physical Chemistry Chemical Physics* **2011,** *13* (21), 10131-10135.

[88] Bhalla, A. S.; Siegel, R. A., Mechanistic studies of an autonomously pulsing hydrogel/enzyme system for rhythmic hormone delivery. *Journal of Controlled Release* **2014,** *196*, 261-271.

[89] Dinarvand, R.; D'Emanuele, A., The use of thermoresponsive hydrogels for on-off release of molecules. *Journal of Controlled Release* **1995,** *36* (3), 221-227.

[90] Sengupta, S.; Patra, D.; Ortiz-Rivera, I.; Agrawal, A.; Shklyaev, S.; Dey, K. K.; Córdova-Figueroa, U.; Mallouk, T. E.; Sen, A., Self-powered enzyme micropumps. *Nature Chemistry* **2014,** *6*, 415.

[91] Deng, H.; Yu, H., Self-assembly of rhodamine 6G on silver nanoparticles. *Chemical Physics Letters* **2018,** *692*, 75-80.

[92] Zhao, J.; Jensen, L.; Sung, J.; Zou, S.; Schatz, G. C.; Van Duyne, R. P., Interaction of Plasmon and Molecular Resonances for Rhodamine 6G Adsorbed on Silver Nanoparticles. *Journal of the American Chemical Society* **2007,** *129* (24), 7647-7656.

[93] Cai, J.; Huang, S.; He, R.; Chen, L.; Chen, D.; Jiang, S.; Li, B.; Li, Y., Access to functionalized thienopyridines via a reagent-capsule-assisted coupling, thiolation and cyclization cascade sequence. *Organic & Biomolecular Chemistry* **2017,** *15* (2), 333-337.

[94] Chaoren, S.; Anke, S.; Xiao-Feng, W., Palladium-Catalyzed Carbonylative Four-Component Synthesis of Thiochromenones: The Advantages of a Reagent Capsule. *Angewandte Chemie International Edition* **2016,** *55* (16), 5067-5070.